THE PROCEEDINGS OF
THE PHYSICAL SOCIETY

Section A

VOL. 64, PART 9 1 September 1951 No. 381 A

The Absorption of Light by Alkali Metals

BY P. N. BUTCHER
Department of Mathematics, Imperial College, London

Communicated by H. Jones; MS. received 6th April 1951

ABSTRACT. The theory of the absorption of light by photo-excitation of the valency electrons in cubic metals is developed. The matrix elements vanish when calculated with respect to the Wigner–Seitz approximate wave functions for the occupied states in the first band, and free electron wave functions for the states in the higher bands. Calculations of the contribution to the absorbing powers of the alkali metals due to photo-excitation are made, using the approximation of nearly free electrons to obtain all the unperturbed wave functions. The calculated values for sodium, potassium and rubidium agree quite well with those observed if the first non-vanishing Fourier coefficient of the self-consistent potential field has the values 0·323, 0·305 and 0·350 ev. respectively.

§1. INTRODUCTION

ABSORPTION of visible and ultra-violet light by metals is due to two processes, firstly scattering of the oscillating electrons by the vibrating lattice, and secondly photo-excitation of the valency electrons. The former process has been treated by considering the damped oscillations of free electrons (see, for instance, Seitz 1940). This theory predicts for the alkali metals absorbing powers which are only about one-tenth of the observed values. Hence in these metals it appears that the absorption is primarily due to photo-excitation. We shall, therefore, make a detailed investigation of this effect. In previous treatments (Wilson 1935, Fan 1945) it has been assumed that the metal is isotropic with regard to absorption. We shall present the theory so as to verify this assumption. We shall show that the matrix elements vanish when calculated with respect to the Wigner–Seitz approximate wave functions for all the occupied states in the first band, and free electron wave functions for the states in the higher bands. The contribution to the absorbing powers of the alkali metals due to photo-excitation will be calculated, using the approximation of nearly free electrons to obtain all the unperturbed wave functions.

§2. THE UNPERTURBED ELECTRONIC STATES

The self-consistent field $V(\mathbf{r})$ of a cubic lattice has the periodicity and symmetry of the lattice. The unperturbed wave functions are the solutions of the equation

$$-\frac{\hbar^2}{2m}\nabla^2\Psi + V(\mathbf{r})\Psi + \frac{\hbar}{i}\frac{\partial}{\partial t}\Psi = 0, \qquad \ldots\ldots(1)$$

having the usual time dependence, which are triply periodic with period L, where $L^3 = V$ is the volume of the metal. We shall normalize these wave functions, so

that they form an orthonormal set in the cube of side L. It is convenient to use the reduced zone scheme to identify the electronic states. The energy levels fall into a series of bands which are distinguished by associating with each a positive integer l. The states within each band are distinguished by the wave vector $\mathbf{k}$ of the corresponding wave function. This wave vector may be restricted to take all values $2\pi\mathbf{n}/L$, where $\mathbf{n}$ is any triple of integers, which lie within the first Brillouin zone. Thus we may speak of the state $(l, \mathbf{k})$ with energy $E_l(\mathbf{k})$ and wave function $\Psi_l(\mathbf{k}, \mathbf{r}, t) = \psi_l(\mathbf{k}, \mathbf{r}) \exp\{-i\omega_l(\mathbf{k})t\}$, where $E_l(\mathbf{k}) = \hbar\omega_l(\mathbf{k})$. The space part of the wave function has the Bloch form $\psi_l(\mathbf{k}, \mathbf{r}) = e^{i\mathbf{k}\cdot\mathbf{r}} u_l(\mathbf{k}, \mathbf{r})$, where $u_l(\mathbf{k}, \mathbf{r})$ has the periodicity of the lattice. As an immediate consequence of the symmetry of $V(\mathbf{r})$, we find that $u_l(\mathbf{k}, \mathbf{r})$ and $E_l(\mathbf{k})$ have the respective symmetries expressed by the relations

$$u_l(\mathbf{k}, R^{-1}\mathbf{r}) = u_l(R\mathbf{k}, \mathbf{r}), \quad \ldots\ldots(2) \qquad \text{and} \qquad E_l(\mathbf{k}) = E_l(R\mathbf{k}), \quad \ldots\ldots(3)$$

where R is any one of the operations of the cubic group.

We shall be concerned ultimately with the alkali metals which have one valency electron per atom. At the absolute zero these electrons fill completely the lower half of the energy levels in the first band. Hence the number of electrons per unit volume of the metal per unit volume of the occupied region of $\mathbf{k}$ space is $1/4\pi^3$. The modifications necessary in the following theory, when the metal is not monovalent, are trivial. When the frequency of the light is not near the absorption limit, it is sufficient to consider the metal at the absolute zero. This is because the electrons in the tail of the Fermi distribution, which exists at ordinary temperatures, absorb only a small fraction of the total light energy absorbed.

§3. THEORY OF THE RATE OF EXCITATION

We will suppose that an electron in the state $(1, \mathbf{k})$ is perturbed by a wave of visible or ultra-violet light, which has scalar potential zero and vector potential $\mathbf{A} = \frac{1}{2}(\mathbf{a}e^{-i\omega t} + \mathbf{a}^* e^{i\omega t})$. The vector $\mathbf{a}$ can be taken as constant throughout the metal, because we can always choose the fundamental cube sufficiently small to justify this assumption, while still sufficiently large to contain a large number of electrons.

It is well known that the electron can only make transitions to states in the higher bands with the same wave vector $\mathbf{k}$, i.e. to states $(l, \mathbf{k})$. We will suppose that the perturbation is switched on at time $t = 0$, and denote the probability of transition to the state $(l, \mathbf{k})$ in time t by $P(l, \mathbf{k}, t)$. $P(l, \mathbf{k}, t)$ may be calculated by applying Dirac's method of the variation of constants to the perturbed wave equation. Using the periodicity of the functions $u_l(\mathbf{k}, \mathbf{r})$, the result may be expressed in the form

$$P(l, \mathbf{k}, t) = \frac{1}{2}\left(\frac{e}{mc}\right)^2 |\mathbf{a} \cdot \langle l, \mathbf{k}| \nabla |1, \mathbf{k}\rangle|^2 \frac{1 - \cos[\omega_l(\mathbf{k}) - \omega_1(\mathbf{k}) - \omega]t}{[\omega_l(\mathbf{k}) - \omega_1(\mathbf{k}) - \omega]^2},$$

where

$$\langle l, \mathbf{k}| \nabla |1, \mathbf{k}\rangle = \int_V u_l^*(\mathbf{k}, \mathbf{r}) \nabla u_1(\mathbf{k}, \mathbf{r})\, dV. \quad \ldots\ldots(4)$$

We have neglected the terms of $P(l, \mathbf{k}, t)$, which involve $\omega_l(\mathbf{k}) - \omega_1(\mathbf{k}) + \omega$, because they contribute nothing to the integrals in §4.

The symmetry property (2) of the functions $u_l(\mathbf{k}, \mathbf{r})$ leads to the useful result

$$\langle l, R\mathbf{k}| \nabla |1, R\mathbf{k}\rangle = \langle l, \mathbf{k}| R \nabla |1, \mathbf{k}\rangle. \quad \ldots\ldots(5)$$

The isotropy of a metal with a cubic lattice with regard to absorption depends on this relation, which allows us to simplify considerably the final expression for the absorbing power.

The probable rate of excitation at time t to the state $(l, \mathbf{k})$ is $d[P(l, \mathbf{k}, t)]/dt$. This can be written in a very convenient form by putting $\omega_l(\mathbf{k}) - \omega_1(\mathbf{k}) - \omega = \Omega_l(\mathbf{k})$. Thus we find

$$\frac{d}{dt} P(l, \mathbf{k}, t) = \frac{\pi}{2}\left(\frac{e}{mc}\right)^2 |\mathbf{a} \cdot \langle l, \mathbf{k}| \nabla |1, \mathbf{k}\rangle|^2 \left[\frac{\sin \Omega_l(\mathbf{k}) t}{\pi \Omega_l(\mathbf{k})}\right].$$

Since the perturbation is due to radiation, it is possible to choose t large enough to make the last factor of $d[P(l, \mathbf{k}, t)]/dt$ approximately a δ function, without invalidating the variation of constants method by making the transition probabilities too large. Hence for large t we have approximately

$$\frac{d}{dt} P(l, \mathbf{k}, t) = \frac{\pi}{2}\left(\frac{e}{mc}\right)^2 |\mathbf{a} \cdot \langle l, \mathbf{k}| \nabla |1, \mathbf{k}\rangle|^2 \delta[\Omega_l(\mathbf{k})]. \quad \ldots\ldots(6)$$

§4. THE INTRINSIC ABSORBING POWER

Summing (6) over all the occupied states in the first band, and then over all $l \neq 1$, we find that the total rate of excitation of photo-electrons per unit volume of the metal is

$$n = \frac{1}{2}\left(\frac{e}{2\pi mc}\right)^2 \Sigma_l \int |\mathbf{a} \cdot \langle l, \mathbf{k}| \nabla |1, \mathbf{k}\rangle|^2 \delta[\Omega_l(\mathbf{k})]\, d\mathbf{k}. \quad \ldots\ldots(7)$$

We choose $d\mathbf{k}$ to be a cylindrical volume element between two adjacent surfaces of the family $\Omega_l(\mathbf{k}) = \text{constant}$, with base dS_l on $\Omega_l(\mathbf{k}) = \text{constant}$ and length $ds = d\Omega_l / |\nabla_{\mathbf{k}} \Omega_l(\mathbf{k})|_{\mathbf{k}}$ where $\nabla_{\mathbf{k}} \equiv (\partial/\partial k_x, \partial/\partial k_y, \partial/\partial k_z)$. We can then carry out immediately the integration with respect to Ω_l and obtain

$$n = \frac{1}{2}\left(\frac{e}{2\pi mc}\right)^2 \Sigma_l \int_{S_l} \frac{|\mathbf{a} \cdot \langle l, \mathbf{k}| \nabla |1, \mathbf{k}\rangle|^2}{|\nabla_{\mathbf{k}} \Omega_l(\mathbf{k})|_{\mathbf{k}}} dS_l. \quad \ldots\ldots(8)$$

The summation is over those bands, except the first, for which the surface $\Omega_l(\mathbf{k}) = 0$ passes through the occupied region of $\mathbf{k}$ space. The integration is over the part of the surface $\Omega_l(\mathbf{k}) = 0$ within the occupied region, which we denote by S_l. Using (3) we see that this surface can be divided into 48 regions, each of which can be obtained from a single fundamental region, by means of one of the 48 operations of the cubic group. Let I_l denote the integral over the whole surface, S_{lf} the fundamental region of S_l and RS_{lf} the region generated from it by the operation R. We have

$$I_l = \int_{S_l} \frac{|\mathbf{a} \cdot \langle l, \mathbf{k}| \nabla |1, \mathbf{k}\rangle|^2}{|\nabla_{\mathbf{k}} \Omega_l(\mathbf{k})|_{\mathbf{k}}} dS_l = \Sigma_R \int_{RS_{lf}} \frac{|\mathbf{a} \cdot \langle l, \mathbf{k}| \nabla |1, \mathbf{k}\rangle|^2}{|\nabla_{\mathbf{k}} \Omega_l(\mathbf{k})|_{\mathbf{k}}} d(RS_{lf})$$

$$= \int_{S_{lf}} \Sigma_R \frac{|\mathbf{a} \cdot \langle l, R\mathbf{k}| \nabla |1, R\mathbf{k}\rangle|^2}{|\nabla_{\mathbf{k}} \Omega_l(\mathbf{k})|_{R\mathbf{k}}} dS_{lf}.$$

Using (3) and (5) this becomes

$$I_l = \int_{S_{lf}} \frac{1}{|\nabla_{\mathbf{k}} \Omega_l(\mathbf{k})|_{\mathbf{k}}} \Sigma_R |\mathbf{a} \cdot \langle l, \mathbf{k}| R\nabla |1, \mathbf{k}\rangle|^2 dS_{lf}.$$

Writing out the summation explicitly, we find that all the cross products between different components of $\mathbf{a}$ cancel, leaving

$$I_l = 16 |\mathbf{a}|^2 \int_{S_{lf}} \frac{|\langle l, \mathbf{k}| \nabla |1, \mathbf{k}\rangle|^2}{|\nabla_{\mathbf{k}} \Omega_l(\mathbf{k})|_{\mathbf{k}}} dS_{lf}. \quad \ldots\ldots(9)$$

Finally, substituting (9) in (8) we have

$$n=2\left(\frac{e}{\pi mc}\right)^2|\mathbf{a}|^2\Sigma_l\int_{S_{lf}}\frac{|\langle l,\mathbf{k}|\nabla|1,\mathbf{k}\rangle|^2}{|\nabla_{\mathbf{k}}\Omega_l(\mathbf{k})|_{\mathbf{k}}}\,dS_{lf}. \qquad \ldots\ldots(10)$$

One quantum of light energy is absorbed for each electron excited. Hence the mean rate of absorption of electromagnetic energy per unit volume of the metal is

$$\overline{R}_p=n\hbar\omega=2\hbar\omega\left(\frac{e}{\pi mc}\right)^2|\mathbf{a}|^2\Sigma_l\int_{S_{lf}}\frac{|\langle l,\mathbf{k}|\nabla|1,\mathbf{k}\rangle|^2}{|\nabla_{\mathbf{k}}\Omega_l(\mathbf{k})|_{\mathbf{k}}}\,dS_{lf}. \qquad \ldots\ldots(11)$$

Since the scalar potential of the light wave is zero, the electric field is $\mathbf{E}=-\dot{\mathbf{A}}/c$. Hence the mean square electric vector is

$$\overline{\mathbf{E}^2}=\omega^2|\mathbf{a}|^2/2c^2. \qquad \ldots\ldots(12)$$

Eliminating $|\mathbf{a}|^2$ between (11) and (12) we have

$$\overline{R}_p=\frac{\hbar}{\omega}\left(\frac{2e}{\pi m}\right)^2\overline{\mathbf{E}^2}\Sigma_l\int_{S_{lf}}\frac{|\langle l,\mathbf{k}|\nabla|1,\mathbf{k}\rangle|^2}{|\nabla_{\mathbf{k}}\Omega_l(\mathbf{k})|_{\mathbf{k}}}\,dS_{lf}. \qquad \ldots\ldots(13)$$

We now see that $\overline{R}_p$ is proportional to $\overline{\mathbf{E}^2}$, i.e. the metal is isotropic with regard to absorption due to photo-excitation.

If the frequency of the light is sufficiently small, none of the surfaces $\Omega_l(\mathbf{k})=0$ will pass through the occupied region of $\mathbf{k}$ space, and there will be no absorption. The frequency at which absorption begins, i.e. when $\Omega_2(\mathbf{k})=0$ touches the surface of the occupied region and transitions to the second band commence, is called the absorption limit, and denoted by ν_0.

In classical electromagnetic theory the intrinsic absorbing power of a homogeneous isotropic medium $\sigma(\omega)$ is defined by $\overline{R}=\sigma(\omega)\overline{\mathbf{E}^2}$, where $\overline{R}$ is the mean rate of absorption of electromagnetic energy per unit volume. $\overline{R}$ may be separated into a small part $\overline{R}_s$ due to scattering by the vibrating lattice, and the part $\overline{R}_p$ due to photo-excitation. We define an intrinsic absorbing power for each of these by the relations

$$\overline{R}_s=\sigma_s(\omega)\overline{\mathbf{E}^2}, \quad \ldots\ldots(14) \qquad \text{and} \qquad \overline{R}_p=\sigma_p(\omega)\overline{\mathbf{E}^2}, \quad \ldots\ldots(15)$$

so that $\sigma(\omega)=\sigma_s(\omega)+\sigma_p(\omega)$. Comparing (13) and (15) we obtain the final expression for the absorbing power due to photo-excitation

$$\sigma_p(\omega)=\frac{\hbar}{\omega}\left(\frac{2e}{\pi m}\right)^2\Sigma_l\int_{S_{lf}}\frac{|\langle l,\mathbf{k}|\nabla|1,\mathbf{k}\rangle|^2}{|\nabla_{\mathbf{k}}\Omega_l(\mathbf{k})|_{\mathbf{k}}}\,dS_{lf}. \qquad \ldots\ldots(16)$$

§ 5. APPROXIMATIONS TO $u_l(\mathbf{k},\mathbf{r})$ AND $E_l(\mathbf{k})$

Henceforth we shall be concerned only with the alkali metals sodium, potassium, rubidium and caesium. The Wigner–Seitz treatment would provide approximations to $u_1(\mathbf{k},\mathbf{r})$ and $E_1(\mathbf{k})$ for all the occupied states of these metals. In this treatment $u_1(\mathbf{k},\mathbf{r})$ is expanded as a power series in $\mathbf{k}$ within each atomic sphere. Wigner and Seitz obtained the approximation

$$u_1(\mathbf{k},\mathbf{r})=f_s(|\mathbf{r}|)+\mathbf{k}.\mathbf{r}f_p(|\mathbf{r}|), \quad |\mathbf{r}|<r_0,$$

where r_0 is the radius of the atomic sphere. Since $u_1(\mathbf{k},\mathbf{r})$ must have the periodicity of the lattice, we find $f_s'(r_0)=0$, $f_p(r_0)=0$. Accurate approximations to the wave functions of the states in the higher bands are difficult to obtain. It is reasonable to suppose that these wave functions are those of free electrons, so that $u_l(\mathbf{k},\mathbf{r})$ is independent of $\mathbf{r}$ for $l>1$. The integral in (4) is $3V/4\pi r_0^3$ times the

integral (of the same periodic integrand) over an atomic sphere. It is easily seen that the latter integral vanishes when the above approximations to $u_l(\mathbf{k}, \mathbf{r})$ are used. Thus, in this case, there is no absorption due to photo-excitation.

These considerations suggest that the relevant properties of the wave functions of the occupied states are their nearly free electron characteristics. We shall therefore obtain all the unperturbed wave functions by using the approximation of nearly free electrons. It is simpler to use the extended zone scheme, instead of the reduced one, to distinguish the electronic states in this approximation. The various bands of the reduced zone scheme are each allotted to a separate zone of $\mathbf{k}$ space, by adding appropriate vectors of the form $2\pi\mathbf{n}/a$ to the wave vectors associated with the states in the band. The electronic states are then completely distinguished by the associated wave vector $\mathbf{k}$ and the band number l becomes unnecessary. Thus we may speak of the state $(\mathbf{k})$ with energy $E(\mathbf{k})$. It is convenient to adjust the wave vector which distinguishes the electronic states so that $E(\mathbf{k})$ tends to the free electron value $(\hbar\mathbf{k})^2/2m$ when $V(\mathbf{r})$ tends to zero.

The periodicity of $V(\mathbf{r})$ allows us to expand it as a triple Fourier series $V(\mathbf{r}) = \Sigma_{\mathbf{n}} V_{\mathbf{n}} \exp\{-i(2\pi/a)\mathbf{n}.\mathbf{r}\}$, where a is the lattice constant. As a consequence of the cubic symmetry of $V(\mathbf{r})$ we find that $V_{R\mathbf{n}} = V_{\mathbf{n}}$ for all R. It is therefore convenient to denote every one of the equal coefficients $V_{R\mathbf{n}}$ by the single symbol V_n. Moreover, the structure factor for body-centred cubic lattices is $1 + \cos\pi(n_x + n_y + n_z)$, so that V_n is zero if $n_x + n_y + n_z$ is an odd integer (Mott and Jones 1936). Provided $\mathbf{k}$ does not approach any zone boundary, the corresponding normalized wave function has the space part

$$\psi(\mathbf{k}, \mathbf{r}) \equiv e^{i\mathbf{k}.\mathbf{r}} u(\mathbf{k}, \mathbf{r})$$
$$= \frac{e^{i\mathbf{k}.\mathbf{r}}}{\sqrt{V}}\left[1 + \Sigma_n \frac{2\pi m a^2}{h^2} \frac{V_n}{a\mathbf{n}.\mathbf{k} - \pi n^2} \exp\{-i(2\pi/a)\mathbf{n}.\mathbf{r}\}\right], \quad \ldots\ldots(17)$$

to the first order of V_n (Wilson 1936).

We still have to consider $E(\mathbf{k})$. It is well known that for sodium this has very nearly the free electron value with only small energy gaps. There is little satisfactory information about $E(\mathbf{k})$ for potassium, rubidium and caesium. We will therefore assume that $E(\mathbf{k})$ is given approximately by the free electron formula, with only small energy gaps, for these metals as well as for sodium. Thus, neglecting the energy gaps, we have

$$E(\mathbf{k}) \equiv \hbar\omega(\mathbf{k}) = (\hbar\mathbf{k})^2/2m. \quad \ldots\ldots(18)$$

As the alkali metals are monovalent and have body-centred cubic lattices, if $E(\mathbf{k})$ is given by (18), the occupied region of $\mathbf{k}$ space is the Fermi sphere with radius $k_m = (6\pi^2)^{1/3}/a$.

In order to calculate $\sigma_p(\omega)$ we shall neglect the effects of the zone boundaries, and use (17) and (18) for all $\mathbf{k}$.

§ 6. CALCULATION OF $\sigma_p(\omega)$

The selection rule for body-centred cubic lattices in the notation of the extended zone scheme is

$$\mathbf{k}' = \mathbf{k} + (2\pi/a)\mathbf{n}, \qquad n_x + n_y + n_z = \text{even integer}, \quad \ldots\ldots(19)$$

where $\mathbf{k}$ and $\mathbf{k}'$ are the wave vectors of the initial and final states respectively. Writing (16) in the notation of the extended zone scheme we have

$$\sigma_p(\omega) = \frac{\hbar}{\omega}\left(\frac{2e}{\pi m}\right)^2 \Sigma_n \int_{S_{nf}} \frac{|\langle \mathbf{k} + (2\pi/a)\mathbf{n}|\nabla|\mathbf{k}\rangle|^2}{|\nabla_{\mathbf{k}}\Omega_{\mathbf{n}}(\mathbf{k})|_{\mathbf{k}}} dS_{nf}, \quad \ldots\ldots(20)$$

where

$$\langle \mathbf{k}+(2\pi/a)\mathbf{n}|\ \nabla|\mathbf{k}\rangle = \int_V e^{-i(2\pi/a)\,\mathbf{n}\,.\,\mathbf{r}}\, u^*[\mathbf{k}+(2\pi/a)\mathbf{n},\mathbf{r}]\,\nabla u(\mathbf{k},\mathbf{r})\,dV, \qquad \ldots\ldots(21)$$

and

$$\Omega_{\mathbf{n}}(k) = \omega[\mathbf{k}+(2\pi/a)\mathbf{n}] - \omega(\mathbf{k}) - \omega. \qquad \ldots\ldots(22)$$

Consider the totality of the surfaces of $\Omega_{\mathbf{n}}(\mathbf{k})=0$, for which $n_x+n_y+n_z$ is an even integer and $|\mathbf{n}|$ has the same value n. The summation in (20) is over all values of n for which this composite surface passes through the occupied region of $\mathbf{k}$ space. The integration is over the fundamental region S_{nf} of the part of the composite surface within the occupied region.

Substituting (18) in (22) we find

$$\Omega_{\mathbf{n}}(\mathbf{k}) = (h/ma^2)(a\mathbf{n}\,.\,\mathbf{k}+\pi n^2) - \omega, \qquad \ldots\ldots(23)$$

which gives after differentiating

$$\nabla_{\mathbf{k}}\Omega_{\mathbf{n}}(\mathbf{k}) = (h/ma)\mathbf{n}. \qquad \ldots\ldots(24)$$

Substituting (17) in (21) we find, to the first order of V_n,

$$\langle \mathbf{k}+(2\pi/a)\mathbf{n}|\ \nabla|\mathbf{k}\rangle = \frac{-imaV_n}{\hbar^2(a\mathbf{n}\,.\,\mathbf{k}+\pi n^2)}\,\mathbf{n}. \qquad \ldots\ldots(25)$$

For the alkali metals and light frequencies in the visible and ultra-violet, the only planes of the set $\Omega_n(\mathbf{k})=0$ which pass through the Fermi sphere are those for which $n=\sqrt{2}$. Hence the sum in (20) reduces to the single term with $n=\sqrt{2}$. Let ω_0 and ω_1 be the angular frequencies of the light at which $S_{\sqrt{2}f}$ enters and leaves the Fermi sphere respectively. We find immediately

$$\omega_0 = (\sqrt{2}h/ma^2)(\sqrt{2}\pi - ak_m) \quad \text{and} \quad \omega_1 = (\sqrt{2}h/ma^2)(\sqrt{2}\pi + ak_m).$$

The absorption limit is $\nu_0=\omega_0/2\pi$. Inserting the values $a=4{\cdot}24$, $5{\cdot}25$, $5{\cdot}62$ and $6{\cdot}05\times10^{-8}$ cm. for sodium, potassium, rubidium and caesium respectively, we find the absorption limits $\nu_0=5{\cdot}11$, $3{\cdot}23$, $2{\cdot}94$ and $2{\cdot}37\times10^{14}\,\mathrm{sec}^{-1}$ respectively. It appears that the absorption limits of sodium and potassium given by Fan (1945) in his Table 1 should be interchanged. If $\omega_0<\omega<\omega_1$, the fundamental region $S_{\sqrt{2}f}$ is a quadrant of a circle with radius

$$r = [k_m{}^2 - (\omega ma/\sqrt{2}h - \sqrt{2}\pi/a)^2]^{1/2} = (ma/\sqrt{2}h)[(\omega-\omega_0)(\omega_1-\omega)]^{1/2}.$$

Substituting (24) and (25) in (20) we find that the integrand is constant over $S_{\sqrt{2}f}$ so that the integral can be immediately evaluated. The final result may be written in the form (Wilson 1936, equation (197))

$$\sigma_p(\omega) = \frac{4\sqrt{2}mae^2\pi^2}{\hbar^4}\,|V_{\sqrt{2}}|^2\,\frac{(\omega-\omega_0)(\omega_1-\omega)}{\omega^3}. \qquad \ldots\ldots(26)$$

In the Figure we show $\sigma_p(\omega)$ calculated from (26) for sodium, potassium, rubidium and caesium by assuming the values $|V_{\sqrt{2}}|=0{\cdot}323$, $0{\cdot}305$, $0{\cdot}350$ and $0{\cdot}522$ ev. respectively. According to the approximation of nearly free electrons $2|V_{\sqrt{2}}|$ is the energy gap across the surface of the first Brillouin zone. This interpretation is perhaps not relevant here because $|V_{\sqrt{2}}|$ arises in (26) from the wave functions of states which are not near the planes bounding the first zone. The circles are the observed values of the absorbing power less the contribution due to scattering by the vibrating lattice. The former was calculated from the observed values of the refractive index n and the extinction coefficient K_0, obtained by Ives and Briggs (1936, 1937), by using the well known expression

$$\sigma(\omega) = nK_0\omega/2\pi. \qquad \ldots\ldots(27)$$

$\sigma_s(\omega)$ was calculated from the classical formula (Seitz 1940)

$$\sigma_s(\omega) = \frac{e^4 n_0^2 \rho}{e^4 n_0^2 \rho^2 + m^2 \omega^2}, \qquad \ldots\ldots (28)$$

where ρ is the ordinary resistivity and $n_0 = 2/a^3$ is the number of electrons per unit volume of the metal. ρ was given the empirical values for the bulk material, i.e. 4·35, 6·62, 12·0 and $19{\cdot}0 \times 10^{-6}$ ohm cm. for sodium, potassium, rubidium and caesium respectively (Seitz 1940, Table III). The magnitude of $\sigma_p(\omega)$ is determined by $|V_{\sqrt{2}}|$ and the above values of the latter were chosen so as to obtain the best fit between the theoretical curves and the points which were determined from experimental data.

The question arises as to whether (27) will give the intrinsic absorbing power of the perfect metal, with which we are concerned, or that of a distorted and

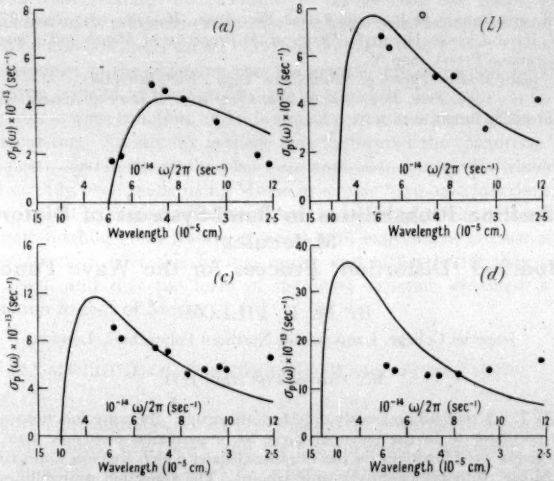

Absorbing powers of the alkali metals due to photo-excitation. (*a*) Sodium. (*b*) Potassium. (*c*) Rubidium. (*d*) Caesium.

contaminated surface layer. We shall suppose that the former is the case for two reasons. Firstly, Ives and Briggs took great care to obtain uncontaminated specular surfaces without polishing or cutting. Secondly, in the case of sodium, we may verify from (28) and the Figure that $\sigma_s(\omega)$ would be greater than the observed value of $\sigma(\omega)$ for low frequencies if ρ were increased by more than $3{\cdot}63 \times 10^{-6}$ ohm cm. Such an increase would not alter the position of the points which were determined from the experimental data for higher frequencies sufficiently to affect the appropriate value of $|V_{\sqrt{2}}|$ very much. Further, in the case of potassium, rubidium and caesium, such an increase of ρ would not seriously alter the position of the points which were determined from experimental data.

The predicted absorption edge of sodium coincides with that observed as indicated by the circles. Unfortunately, the optical constants of the other alkali metals have not been observed for sufficiently long wavelengths to indicate the

position of their inner photoelectric absorption limits. The agreement between the theoretical curves and the points determined from experimental data is fair for sodium, potassium and rubidium, but there is little agreement for caesium. Since the assumed value of $|V_{\sqrt{2}}|$ is about the same for each of the former three metals, it appears that the differences between their absorbing powers are due largely to the differences between their lattice constants. Further, it appears that the nearly free electron model is inadequate for the discussion of the absorption of light by caesium.

ACKNOWLEDGMENT

The author would like to thank Professor H. Jones for many helpful discussions during the course of this work.

REFERENCES

FAN, H. Y., 1945, *Phys. Rev.*, **68**, 43.
IVES, H. E., and BRIGGS, H. B., 1936, *J. Opt. Soc. Amer.*, **26**, 238; 1937, *Ibid.*, **27**, 181, 395.
MOTT, N. F., and JONES, H., 1936, *Theory of the Properties of Metals and Alloys* (Oxford: Clarendon Press), chap. V.
SEITZ, F., 1940, *Modern Theory of Solids* (New York: McGraw-Hill).
WILSON, A. H., 1935, *Proc. Roy. Soc.* A, **151**, 274; 1936, *Theory of Metals* (Cambridge: University Press), sect. 2.6.

Transition Probabilities in Band-Systems of Diatomic Molecules: A Modified 'Distortion' Process for the Wave Functions

BY M. E. PILLOW
Imperial College, London, and Northern Polytechnic, London

MS. received 19*th April* 1951

ABSTRACT. A method previously used for 'distorting' the wave functions of a simple harmonic oscillator to fit the potential curve for a particular electronic state has been modified, giving wave functions for the vibrational states which are close approximations to those of Morse, with comparatively little labour. The transition probabilities obtained from these functions are compared with experimental values for the first negative bands of N_2^+, the Swan bands of C_2, the CN violet bands, and the α-system of BO.

§ 1. INTRODUCTION

A NUMBER of attempts have been made to compare the relative intensities of the bands in a band-system, or the transition probabilities deduced from these, with the corresponding values predicted theoretically, making various assumptions as to the form of the vibrational wave functions ψ_1, ψ_2, and taking the transition probability as proportional to $[\int \psi_1 \psi_2 \, dr]^2$. Since many diatomic molecules have vibrational energy terms of a form approximating closely to $\omega_e(v+\frac{1}{2}) - x\omega_e(v+\frac{1}{2})^2$, with the usual notation, the Morse potential function and the corresponding wave functions are likely to give values for the transition probabilities in good agreement with those obtained from intensity measurements, and this has been found to be so where the test has been made.

But the length of the calculations involved, which must be made independently for every electronic state considered, prevents extensive use of this method, limiting it to a few bands of low vibrational quantum numbers. In some cases the probabilities have been calculated assuming simple harmonic vibrations. For molecules which are symmetrical, or nearly so, this can be done by the method of Hutchisson (1930), and for any molecule the wave functions for such motion can be plotted from the tables given by Gaydon and Pearse (1939) and by Pillow (1949, 1950), and the integration carried out numerically. Here, as might be expected, there is fair agreement with experiment where intense bands occur at low vibrational levels for both states, that is, where the equilibrium internuclear distance is nearly the same for the two electronic states; but the departures from agreement become rapidly more marked as the quantum numbers increase above 1 or 2.

Between these methods lie various ways of distorting the simple harmonic wave functions to fit potential curves derived from band measurements, such as those used by Gaydon and Pearse (1939) and Pillow (1949, 1950). Both of these methods are open to the objection that the central zero or turning point of each wave function is fixed at the equilibrium internuclear distance r_e. This is not so for the Morse wave function, and it is almost certainly not true of the vibrations actually occurring. An attempt is made here to improve the 'distortion' process in this respect. So far, the method has been applied to systems for which calculations had already been made using Morse or simple harmonic functions, so that comparison could be made with these as well as with experiment. It will be seen that the new method gives results agreeing with experiment at least as well as the Morse function over this limited range, and rather better than the other methods used, and that the form of the wave function obtained is a close approximation to that of Morse.

§ 2. METHOD OF DISTORTING WAVE FUNCTIONS

Method A.

In Figure 1 the dotted curve APE represents the potential function for simple harmonic vibrations, $U=Da^2\xi^2$, and the full curve BPF represents the Morse potential function $U=D(1-e^{-a\xi})^2$, where $D=\omega_e{}^2/4x\omega_e$, $a^2=8\pi^2\mu\boldsymbol{c}x\omega_e/\boldsymbol{h}$, $\xi=r-r_e$. For any chosen value of U, write $\xi_0=\mathrm{AC}=\mathrm{CE}$, $\xi_1=\mathrm{CF}$, $\xi_2=\mathrm{BC}$, taking the numerical value of each length, without regard to the direction in which it is measured. The line PQ represents the locus of the central zeros or turning points of the Morse wave functions, and it can be shown that on this locus the abscissa increases by x/a for each vibrational level, provided that $(vx)^2$ is small compared with vx. (x is generally a fraction of 0·01.) PQ is therefore nearly, but not quite, a straight line.

Now $U=Da^2\xi_0{}^2$, and ξ_1, $-\xi_2$ are the roots of $U=D(1-e^{-a\xi})^2$ and can be written $-a\xi=\ln[1\pm(U/D)^{1/2}]=\ln(1\pm a\xi_0)$, so that $\xi_1=-2{\cdot}303a^{-1}\log_{10}(1-a\xi_0)$, $\xi_2=2{\cdot}303a^{-1}\log_{10}(1+a\xi_0)$.

Write $\mathrm{CD}=z$. Then $\partial z/\partial v=x/a$; but $\partial U/\partial v\simeq\omega_e$ so that $\partial z/\partial U=x/a\omega_e$, and $z=0$ for $U=0$, thus $z=xU/a\omega_e=U/4Da=\frac{1}{4}a\xi_0{}^2$. Hence in Figure 1

$$\mathrm{DF}=-2{\cdot}303a^{-1}\log_{10}(1-a\xi_0)-\tfrac{1}{4}a\xi_0{}^2,$$

$$\mathrm{BD}=\ \ 2{\cdot}303a^{-1}\log_{10}(1+a\xi_0)+\tfrac{1}{4}a\xi_0{}^2.$$

The simple harmonic wave functions are tabulated already for $\frac{1}{4}$ integral values of ξ_0/d where $d^2 = \hbar/4\pi^2 c\mu\omega_e$. The plot of such a function is shown in Figure 2. In plotting the distorted function shown in Figure 3 the 'centre' D is placed at approximately the Morse 'centre' for the corresponding level, i.e. at $r = r_e + (v+1)x/a$. Now lay out the abscissae along the axis so that if, for instance, the point $\xi_0/d = 1{\cdot}5$ originally lay at a distance CE (Figure 1) from 0, it now lies

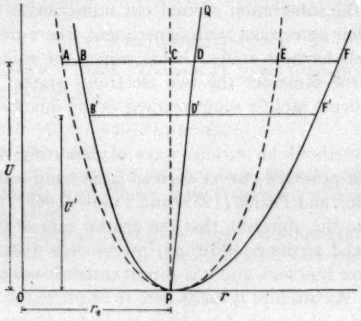

Figure 1.

Figure 2.

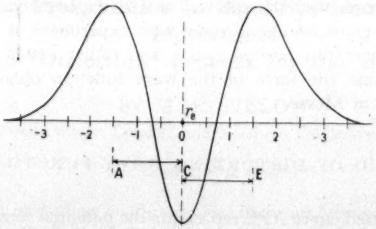

Figure 3.

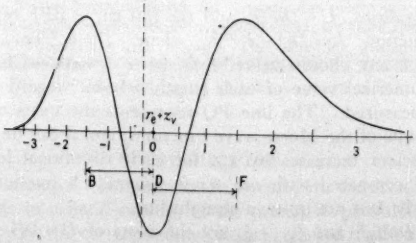

at DF, while $\xi_0/d = -1{\cdot}5$ lies at BD behind 0. On these abscissae plot the ordinates as for the simple harmonic wave function, and so obtain the distorted graph.

The previous distortion method consisted essentially in the use of CF, BC, where now DF, BD are used, and in practice these distances were read off from the graph of the potential curve instead of being calculated.)

Method B.

Another method of distortion tried, but not found very successful, is as follows: For each vibrational level, a value r_v can be obtained from the rotational constant B_v for that state, using the relation $B_v = \hbar/8\pi^2 c\mu r_v^2$. r_v might then be considered as a 'mean' internuclear distance for that level, and as the 'centre' for the wave function. A locus similar to PQ in Figure 1 was plotted using these values. The distortion was then carried out as described above, except that the distances were read off from a potential curve graph instead of being calculated. In the case tried, that of N_2^+, the slope of PQ was considerably greater when found in this way, and PQ roughly bisected such lines as BF. There is much doubt as to whether the function of the internuclear distance which is averaged by this means is the appropriate one for the purpose, and comparison of the results with experiment did not seem to justify investigating the method further.

§ 3. DIRECT COMPARISON OF WAVE FUNCTIONS

It was considered interesting to compare the actual form of the wave functions obtained from the Morse expression with those obtained by the present method of distortion (Method A). This has been done, using first a state in which the anharmonicity of the vibrations is large, and the approximations involved in the distortion method are therefore considerable. Dr. K. E. Shuler, of the Johns Hopkins University, kindly furnished the figures from which he had already plotted the Morse functions for the $v' = 0$, 1, 2 levels of the excited $^2\Sigma^+$ state for OH, and from these the Morse wave functions have been plotted, together with the distorted form. It can be seen that even here the agreement is close (Figure 4).

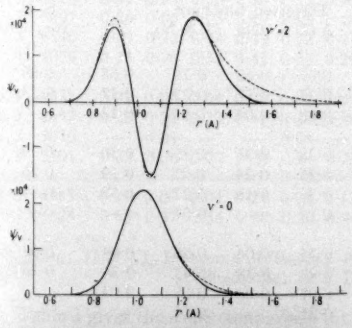

Figure 4. Wave functions for OH excited state :—Morse function; - - - 'distorted' function.

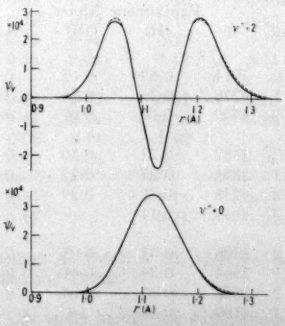

Figure 5. Wave functions for N_2^+ ground state :—Morse function; - - - 'distorted' function.

A more favourable state is the $^2\Sigma_g^+$ ground state of N_2^+. The Morse functions for $v'' = 0$, 1, 2 have been calculated, and plotted together with the distorted functions (Figure 5), and the diagrams show how very close is the agreement. Comparison has also been made in the same way for the excited state of N_2^+, and the agreement here is equally close*.

* From figures kindly supplied by Mr. D. R. Bates.

§4. COMPARISON OF RESULTS FOR TRANSITION PROBABILITIES OR INTENSITIES

In Table 1, a number of results for the first negative N_2^+ system are shown. The experimental values are estimates of transition probabilities made from intensity measurements due to Herzberg (1928), and these have already been compared by Bates (1949) with values calculated from Morse functions, and by Stephenson (1951) with those from simple harmonic functions. Calculations have now been made by the previous approximate method, and by both the modified methods of distortion described here. Since Bates' calculations were made, Herzberg (1950) has suggested amended vibrational constants for the excited state, and as the results are very sensitive to these constants the values for transition probabilities have been calculated from both sets, so that comparison can be made both with previous calculations and with experiment. All are expressed on such a scale that the sum of probabilities in one complete progression is as nearly as possible equal to 1.

In a recent paper Turner and Nicholls (1951) have calculated the same probabilities by a distortion method, and for completeness their results are included in the Table. They do not quote the values used for the molecular constants, neither do they make clear whether the method used is that of Gaydon and Pearse (1939) or that of Pillow (1949). These are not quite the same, and would probably give somewhat different results.

Table 1. First Negative N_2^+ Bands. Transition Probabilities

$B^2\Sigma_u^+$ (1) $\omega_e' = 2419{\cdot}84$, $x\omega_e' = 20{\cdot}95$, $r_e' = 1{\cdot}074$ A.
(2) $\omega_e' = 2419{\cdot}84$, $x\omega_e' = 23{\cdot}19$, $r_e' = 1{\cdot}075$ A.
$X^2\Sigma_g^+$ $\omega_e'' = 2207{\cdot}19$, $x\omega_e'' = 16{\cdot}14$, $r_e'' = 1{\cdot}114$ A.

		Experiment	Morse	Distorted functions					S. H.
v', v''	λ	(H)	(B)	A (1)	A (2)	Old	(T & N)	(B)	functions (S)
0, 0	3914	0·69	0·65	0·65	0·67	0·65	0·70	0·65	0·69
0, 1	4278	0·26	0·26	0·23	0·23	0·17	0·22	0·37	0·23
0, 2	4709	0·04	0·07	0·08	0·08	0·04	0·05	0·13	—
1, 0	3582	0·23	0·30	0·29	0·28	0·31	0·33	0·30	0·29
1, 1	3884	0·27	0·22	0·26	0·25	0·24	0·27	0·19	0·26
1, 2	4236	0·38	0·29	0·24	0·26	0·18	0·27	0·38	0·41
1, 3	4652	0·11	—	—	0·14	—	0·07	—	—
2, 0	3308	0·07	0·05	0·05	0·04	0·04	0·06	0·04	0·02
2, 1	3564	0·39	0·41	0·38	0·42	0·38	0·43	0·34	0·26
2, 2	3858	0·07	0·04	0·08	0·07	0·08	0·08	0·03	—
2, 3	4199	0·25	—	—	0·21	—	0·24	—	—
2, 4	4600	0·18	—	—	0·20	—	0·09	—	—
3, 0	3078	0·00	0·00	0·00	0·00	0·00	0·00	0·00	0·00
3, 1	3299	0·08	0·11	0·11	0·11	0·08	0·15	0·08	—
3, 2	3549	0·36	0·41	0·45	0·42	0·46	0·44	0·31	0·29
3, 3	3835	0·03	—	—	0·03	—	0·01	—	—
3, 4	4167	0·20	—	—	0·14	—	0·17	—	—
3, 5	4554	0·27	—	—	0·17	—	0·08	—	—

(H), Herzberg; (B), Bates; A, B, methods A, B; (S), Stephenson; (T & N), Turner and Nicholls.

Table 2 shows a similar comparison made for the C_2 Swan bands. The Morse function has not been applied to these bands, but two pairs of workers, McKellar and Buscombe (1948) and Patel and Tawde (1950) have made estimates of transition probabilities from simple harmonic wave functions. The experimental values quoted here were obtained by King (1948) and by Johnson and Tawde (1932) from their intensity measurements. In each case the temperature of the source was estimated by the workers concerned, and used in reducing the values to probabilities. Comparison should therefore be valid for ratios in one v'' progression, but there is room for a constant factor of error in passing from one progression to another.

Table 2. C_2 Swan Bands. Transition Probabilities

A $^3\Pi_g$ $\omega_e' = 1788{\cdot}22$, $x\omega_e' = 16{\cdot}44$, $r_0' = 1{\cdot}266$ A.
X $^3\Pi_u$ $\omega_e'' = 1641{\cdot}35$, $x\omega_e'' = 11{\cdot}67$, $r_e'' = 1{\cdot}312$ A.

v', v''	λ	Experimental values (K)		Experimental values (J & T)				Distorted functions A	Distorted functions Old	Simple harmonic functions (McK & B)	Simple harmonic functions (P & T)
0, 0	5165	0·67	0·54	0·49	0·61	0·53	0·67	0·77	0·83	0·72	0·73
0, 1	5635	0·16	0·23	0·27	0·22	0·28	0·29	0·20	0·15	0·25	0·24
0, 2	6191	0·03	0·23	0·24	0·17	0·19	0·04	0·05	0·02	0·04	0·03
1, 0	4737	0·24	0·22	0·27	0·20	0·17	0·40	0·23	0·38	0·23	0·23
1, 1	5129	0·35	0·29	0·20	0·24	0·24	0·22	0·38	0·40	0·31	0·34
1, 2	5585	0·36	0·23	0·25	0·19	0·25	0·26	0·28	0·21	0·37	0·36
1, 3	6122	0·08	0·26	0·29	0·37	0·33	0·11	0·11	0·04	0·09	0·07
2, 0	4382	0·03	0·02	0·01	0·03	0·02	0·02	0·02	0·07	0·02	0·04
2, 1	4715	0·35	0·33	0·36	0·30	0·15	0·45	0·38	0·55	0·30	0·30
2, 2	5097	0·26	0·06	0·05	0·07	0·09	0·06	0·18	0·23	0·10	0·12
2, 3	5540	0·33	0·32	0·24	0·19	0·22	0·27	0·25	0·24	0·39	0·39
2, 4	6059	0·13	0·26	0·33	0·42	0·53	0·20	0·18	0·08	0·14	0·13
3, 1	4371	0·07	0·04	0·04	0·08	0·02	0·09	0·08	0·17	0·11	0·10
3, 2	4697	0·48	0·32	0·33	0·41	0·18	0·50	0·44	0·56	0·28	0·28
3, 3	5070	—	0·01	—	—	0·04	—	0·08	0·11	0·02	—
3, 4	5501	0·53	0·26	0·27	0·24	0·24	0·24	0·22	0·20	0·36	0·36
4, 2	4365	0·17	0·09	0·04	0·23	0·02	0·13	0·13	—	0·15	0·15
4, 3	4684	0·63	0·37	0·36	0·50	0·20	0·44	0·46	—	0·24	0·24

(K), King; (J & T), Johnson and Tawde; A, method A; (McK & B), McKellar and Buscombe; (P & T), Patel and Tawde.

Table 3 gives the same comparison for the CN violet bands, the experimental values being due to Ornstein and Brinkman (1931) and to Tawde (1936). The calculations from simple harmonic wave functions were made by McKellar and Buscombe (1948) and by Patel and Tawde (1950).

Table 4 shows values for the α-system of BO. Elliott (1933) set out to compare the results of calculations from both Morse and simple harmonic functions with those of experiments made by himself on this system, which he chose because there is very little overlapping of bands. His experimental values for the intensities are the result of integrating over the whole of each band. For the results of his calculations he quotes intensities at infinite temperature instead

of transition probabilities, and since he has not estimated the temperature of his source the comparison with experiment can be made only within one v'' progression.

Table 3. CN Violet Bands. Transition Probabilities

$B^2\Sigma^+$ $\omega_e' = 2164{\cdot}15$ $x\omega_e' = 20{\cdot}25$, $r_e' = 1{\cdot}150$ A.
$X^2\Sigma^+$ $\omega_e'' = 2068{\cdot}7$ $x\omega_e'' = 13{\cdot}15$, $r_e'' = 1{\cdot}172$ A.

v', v''	λ	Experimental value (O & B)	Experimental value (T)	Distorted functions A	Distorted functions Old	S. H. functions (McK & B)
0, 0	3883	0·91	0·84	0·91	0·91	0·90
0, 1	4216	0·05	0·13	0·09	0·03	0·09
0, 2	4606	0·00	0·02	0·02	0·00	0·00
1, 0	3590	0·15	0·09	0·09	0·13	0·08
1, 1	3871	0·79	0·68	0·77	0·81	0·73
1, 2	4197	0·09	0·21	0·12	0·06	0·15
1, 3	4578	0·01	0·05	0·02	0·00	0·01
2, 1	3585	0·26	0·17	0·16	0·19	0·14
2, 2	3861	0·70	0·52	0·71	0·71	0·60
2, 3	4180	0·11	0·27	0·14	0·08	0·22
2, 4	4553	0·01	0·05	0·06	0·00	0·01
3, 2	3584	0·22	0·13	0·23	0·31	0·19
3, 3	3855	0·70	0·52	0·65	0·58	0·49
3, 4	4167	0·14	0·38	0·15	0·11	0·27
4, 3	3583	0·18	—	0·24	0·41	0·23
4, 5	4158	0·17	0·47	0·15	0·09	0·31
5, 6	4152	0·23	—	0·15	0·11	0·51

(O & B), Ornstein and Brinkman; (T), Tawde; A, Method A; (McK & B), McKellar and Buscombe.

Table 4. α-Bands of BO. Intensities

$A^2\Pi_{inv}$ $\omega_e' = 1259{\cdot}1$, $x\omega_e' = 10{\cdot}6$, $r_e' = 1{\cdot}348$ A.
$X^2\Sigma^+$ $\omega_e'' = 1885{\cdot}4$, $x\omega_e'' = 11{\cdot}71$, $r_e'' = 1{\cdot}199$ A.

v', v''	λ	Experiment (E)		Morse (E)	Distorted functions	S. H. functions (E)
0, 0	4248	40	46	30	21	40
0, 1	4613	96	102	88	69	75
0, 2	5040	84	94	75	81	80
0, 3	5548	64	80	55	66	61
0, 4	6160	34	41	Not calc.	31	37
1, 0	4036	88	92	73	85	110
1, 1	4363	100	100	100	100	100
1, 2	4744	49	49	39	37	42
2, 0	3847	—	158	82	158	152
2, 1	4143	45	85	41	73	36
2, 2	4485	0	0	7	0	0
2, 3	4883	26	56	17	31	12
2, 4	5351	32	81	Not calc.	24	13

(E), Elliott.

The scale here is so chosen that the intensity is 100 for the (1, 1) band. We should expect therefore that in the $v'=0$ progression the calculated values would be lower than the experimental, and that in the $v'=2$ progression they would be higher, and this is roughly true.

§ 5. CONCLUSION

The 'distortion' method of plotting wave functions requires the preliminary tabulation of the simple harmonic functions; this has already been done for levels up to $v=16$, and the values are applicable to any molecule. The calculation required to distort one wave function takes about the same time as that for the Morse function of zero quantum number; and when this has been done any other function in the range of levels covered by the table can be plotted in a few minutes, whereas each Morse function requires a separate evaluation, the complexity of the working increasing with v. The results here suggest that at least for fairly low values of v the additional labour is not justified. Any loss of accuracy involved in the numerical integration is probably within the limits of other errors in the method.

While the older method of distortion could cause large departures from normalization, the functions obtained by the new method are more nearly normalized, at least for low values of v.

So far, the modified method of distortion has been applied only to low vibrational levels, with the deliberate purpose of comparison with Morse and simple harmonic functions, and in each case a Morse potential form has been assumed. The method has still to be applied, with any necessary modifications, to higher levels, and to electronic states for which the dissociation energy is known to differ widely from the Morse value, $\omega_e^2/4x\omega_e$. This is being considered for some of the oxygen systems, which had previously been investigated by the earlier distortion process.

It must be noted that none of the methods discussed here takes any account of the interaction of rotational and vibrational energies. The method of estimating the intensity of a band experimentally is likely therefore to affect to some extent the agreement between theoretical and experimental results. The comparisons are strictly valid only if made between corresponding lines in the bands, or for the integrated intensities over whole bands, which is possible only where there is very little overlapping of bands. In addition, the effect of temperature must be accurately calculated before the comparison can be made. The experimental results collected here show that the values obtained by different workers can differ at least as widely from each other as from the calculated values.

ACKNOWLEDGMENTS

The author's thanks are due to Dr. R. W. B. Pearse for his suggestions and help, to Mr. D. R. Bates and Dr. K. E. Shuler for the use of their calculated values, and to Dr. G. Stephenson for discussion of his own methods and results before publication.

Note added in proof. This newer method is an improvement on older ones, particularly for low vibrational levels, but still has the defect of giving excessive values to the wave functions for large internuclear distances, thus making the functions far from orthonormal when moderately high vibrational levels are considered, and limiting the usefulness of the method.

A further modification, which gives promise of greatly improved results in these respects, at the cost of a slight addition to the calculation, is indicated shortly here, using the same notation as above. There the distortion is accomplished by substituting abscissae BD, DF for AC, CE, both taken at the same energy level U. But on the simple harmonic potential curve the vibrational levels correspond to $U=\omega_e(v+\frac{1}{2})$, while on the Morse curve, still used as the most useful approximation to the actual curve for the state, the corresponding level is $U'=\omega_e(v+\frac{1}{2})-x_e\omega_e(v+\frac{1}{2})^2$.

The distortion here suggested is the substitution of B′D′, D′F′ at the level U' for AC, CE at level U. A calculation similar to that used before then gives

$$\mathrm{B'D'}=\frac{2{\cdot}303}{a}\log\{1+a\xi_0(1-\tfrac{1}{4}a^2\xi_0^2)^{1/2}\}+\tfrac{1}{4}a\xi_0^2(1-\tfrac{1}{4}a^2\xi_0^2)/(1-\tfrac{1}{2}a^2\xi_0^2),$$

$$\mathrm{D'F'}=-\frac{2{\cdot}303}{a}\log\{1-a\xi_0(1-\tfrac{1}{4}a^2\xi_0^2)^{1/2}\}-\tfrac{1}{4}a\xi_0^2(1-\tfrac{1}{4}a^2\xi_0^2)/(1-\tfrac{1}{2}a^2\xi_0^2)$$

where $\xi_0=\mathrm{AC}=\mathrm{CE}$ as before. This rather more elaborate formula does not increase to any serious extent the work involved.

Results so far obtained indicate that the functions obtained in this way are more satisfactory than the other approximations so far tried.

REFERENCES

Bates, D. R., 1949, *Proc. Roy. Soc.* A, **196,** 217.

Elliott, A., 1933, *Proc. Phys. Soc.*, **45,** 627.

Gaydon, A. G., and Pearse, R. W. B., 1939, *Proc. Roy. Soc.* A, **173,** 37.

Herzberg, G., 1928, *Ann. Phys., Lpz.*, **86,** 191; 1950, *Molecular Spectra and Molecular Structure*, I, 2nd ed. (New York : Van Nostrand).

Hutchisson, E., 1930, *Phys. Rev.*, **36,** 410.

Johnson, R. C., and Tawde, N. R., 1932, *Proc. Roy. Soc.* A, **137,** 575.

King, R. B., 1948, *Astrophys. J.*, **108,** 429.

McKellar, A., and Buscombe, W., 1948, *Publ. Dom. Astrophys. Obs., Victoria*, B.C., **7,** No. 24.

Ornstein, L. S., and Brinkman, H., 1931, *Proc. K. Ned. Akad. Wet.*, **34,** 33.

Patel, J. M., and Tawde, N. R., 1950, *Astrophys. J.*, **112,** 210.

Pillow, M. E., 1949, *Proc. Phys. Soc.* A, **62,** 237; 1950, *Ibid.*, **63,** 940.

Stephenson, G., 1951, *Proc. Phys. Soc.* A, **64,** 209.

Tawde, N. R., 1936, *Proc. Indian Acad. Sci.* A, **3,** 140.

Turner, R. G., and Nicholls, R. W., 1951, *Phys. Rev.*, **82,** 290.

The Free Energy of the Double Layer of a Colloidal Particle

By S. LEVINE
Department of Mathematics, University of Manchester

MS. received 27th March 1951

ABSTRACT. Some theorems concerning the free energy of the electric double layer of a colloidal particle in a dilute sol are developed by making use of the Poisson–Boltzmann equation. It is shown that this free energy can be derived by employing the fictitious process of charging the excess ions in the double layer and that the surface density of ions may be an arbitrary function of the degree of charging. By integrating with respect to the charging parameter at constant surface density of ions we obtain an alternative form for the free energy which is expressed in terms of the electrostatic energy of the double layer and the excess osmotic pressure in the diffuse layer. The latter expression for the energy can also be derived by attributing to each volume element in the diffuse layer an energy term due to the thermal motion of the ions and an (electrostatic) field energy term.

§ 1. INTRODUCTION

In a series of previous papers (Levine 1946, 1948, 1950, 1951 a, b, hereafter to be referred to as I–V), the author derived a number of theorems relating to the free energy of the double layers of colloidal particles. We have found since that there exist other theorems of a similar nature, and it is the purpose of this paper to present these in a unified form. We shall consider the case of a single colloidal particle of general shape immersed in a very large (infinite) volume of electrolyte and make use of the Poisson–Boltzmann equation. The extension to more than one particle is fairly obvious. Also, we shall neglect the contribution to the free energy of our system from the Coulomb interaction of the ions in the interior of the dispersion medium (see V).

Three main results will be derived in this paper. The first, which is given by equation (12), is a generalization of a theorem obtained by Casimir (1948). Equation (12) states that the use of a Lippmann equation in deriving the free energy of the double layer is equivalent to imagining that all the ions in the colloidal system are subject to a charging process which is carried out in such a way that the density of surface ions varies quite arbitrarily with the degree of charging. The second result was first obtained by Verwey and Overbeek (1948, p. 78) in the particular case of two parallel plates. The electrical free energy of the double layer can be determined by charging under the condition that the density of surface ions remains fixed. It is possible to transform this expression into one which involves the electrostatic energy of the double layer and the integral of the (excess) osmotic pressure over the volume of the diffuse outer layer; this theorem is expressed by equation (14). The third result is an alternative derivation of the theorem just referred to, using an entirely different approach, which throws further light on the nature of the approximations introduced in the Poisson–Boltzmann equation. Associated with each volume element in the diffuse outer layer we have an osmotic term and an electrical term (namely the ordinary field energy in electrostatics); these are the last two terms

on the right of equation (26). A similar expression has been used by Debye (1927) in his theory of 'salting-in' effect, and also appears in the work of Frumkin (1943) (mentioned by Frenkel 1946), Derjaguin (1940) and Coolidge and Juda (1946).

The question arises as to the value of the various theorems put forward. As yet, we have not applied equation (12) to any practical problem, and it may be regarded as further evidence for the self-consistency of the general theory. However, the other two results are of immediate use. The equation (14) (or rather the equivalent first relation in (21)) has been applied in a forthcoming paper by Levine and Suddaby to determine the free energy of two parallel plates immersed in a 1–2 valency type of electrolyte. Also, work is now in progress on the numerical evaluation of the free energy of two spherical particles, and here again the right-hand side of (14) is found to be a suitable form for the energy. Finally, the expression (16) for the free energy differs from the other forms obtained, both in this paper and the earlier ones, in that it is equally applicable to either concentrated or dilute colloidal systems; at present it is being used by the author to study concentrated sols. The equivalence of the various charging processes proposed by Derjaguin (1940), Verwey and Overbeek (1948) and the author is based on the assumption that the volume of electrolyte is infinite, and a number of difficulties, which remain to be resolved, are apparently encountered when extending these processes to finite volumes.

Various authors have attempted to improve upon the Poisson–Boltzmann equation when applied to the electric double layer. Among the types of deviations there are: (i) fluctuation terms (Casimir 1944, Loeb 1951), (ii) effect of finite size of hydrated ions (Grimley and Mott 1947, Grimley 1950), (iii) dielectric saturation* (Grahame 1950), (iv) electrostrictive effects (Mueller 1935) and (v) image forces (Loeb 1951). These extensions are undoubtedly desirable but, in the opinion of the author, a satisfactory analysis of the corrections to the Poisson–Boltzmann equation entails the simultaneous treatment of all the above effects, particularly since they partially compensate one another. The Poisson–Boltzmann equation can be considered a useful first approximation and the basis from which a more exact equation can be developed. It is likely that considerably more experimentation would be required on the stability properties of colloidal systems, accompanied by a detailed application to special cases of the general theorems developed here and in the earlier papers, before we can establish the precise limitations of the Poisson–Boltzmann equation. This point of view receives support from the fact that at colloidal surfaces we may have such complications as the formation of the Stern layer of counter ions (Levine 1951 c) and the distribution of charge in the crystal lattice of the colloidal particle (Grimley and Mott 1947, Grimley 1950). Finally, it should be mentioned that equation (12) and the left-hand member of (14) may still be valid with the 'corrected' Poisson–Boltzmann equation, whereas this is not true of either the right-hand member of (14) or of the expression (26) for the free energy.

§ 2. FIRST FORM FOR ELECTRICAL FREE ENERGY

It is assumed that the surface charge on the colloidal particle arises from the adsorption of n ions of type 1, charge e_1, and that ν is the density of such ions at position $\mathbf{S}$ on the surface, which has an area S. The volume density of ions of species i ($i=1, \ldots, s$) in the interior of the solution is assumed constant

* More recently Booth (1951) and Conway *et al.* (1951).

(independent of n) and denoted by n_i^0. Then, according to the analysis in the earlier papers (see, in particular, III and IV), the part of the free energy of our system which depends on n is written as

$$U(n) = f_0(n) - n\Delta\chi_1(1) + F_e(n), \qquad \ldots\ldots(1)$$

$$F_e(n) = 2\int_0^1 \frac{1}{\lambda} E(\lambda, n)\, d\lambda = e_1 \int_0^n \bar{\psi}(1, n)\, dn, \qquad \ldots\ldots(2)$$

$$E(\lambda, n) = \tfrac{1}{2}\lambda e_1 n\bar{\psi}(\lambda, n) + \tfrac{1}{2}\int_V \psi\rho\, dv = \frac{D}{8\pi}\int_V |\operatorname{grad}\psi|^2\, dv, \qquad \ldots\ldots(3)$$

$$\bar{\psi}(\lambda, n) = \frac{1}{n}\int_S \psi\nu\, dS = \int_S \psi\nu_0(\mathbf{S})\, dS, \qquad \ldots\ldots(4)$$

where λ denotes the degree of charging, $f_0(n)$ is the free energy (depending on n) of our system in the completely discharged state $\lambda = 0$, $-\Delta\chi_1(1)$ is the change in the electrical self-energy of an ion of type 1 when it is transferred from the solution to the particle surface, $F_e(n)$ is the so-called electrical part of the free energy associated with the double layer and is defined by the first equation in (2), the quantity $E(\lambda, n)$ in the integrand being the average electrostatic energy of the double layer at degree λ. We imagine that the integration with respect to λ is carried out subject to the condition of a fixed distribution of surface ions. As in III and IV, we write this distribution as $\nu = \nu(\mathbf{S}) = n\nu_0(\mathbf{S})$, where $\nu_0(\mathbf{S})$ is subject to the normalization condition $\int_S \nu_0(\mathbf{S})dS = 1$, but is otherwise an arbitrary function of position $\mathbf{S}$. In the surface integral in (4) ψ is the potential at position $\mathbf{S}$ (and stage λ) on the particle surface. In the volume integrals in (3), ψ and ρ are the corresponding potential and charge density respectively at position $\mathbf{r}$ in the diffuse outer layer; these integrals are taken over the volume V of the outer layer, which can be assumed to extend to infinity, where the potential ψ vanishes. $\bar{\psi}(\lambda, n)$ is the average potential (at stage λ) over the surface, the weight function being $\nu_0(\mathbf{S})$. D is the dielectric constant of the dispersion medium.

At stage λ and position $\mathbf{r}$ the volume density of ions is given by the Boltzmann distribution law

$$n_i = n_i(\lambda, \mathbf{r}) = n_i^0 \exp(-\lambda e_i\psi/kT), \qquad \ldots\ldots(5)$$

where k is Boltzmann's constant and T the absolute temperature, and the Poisson–Boltzmann equation for the potential ψ is expressed as

$$\nabla^2\psi = -4\pi\rho/D = \lambda f(\lambda\psi), \qquad \ldots\ldots(6)$$

$$f(\lambda\psi) = -\frac{4\pi}{D}\sum_{i=1}^{s} n_i^0 e_i \exp(-\lambda e_i\psi/kT). \qquad \ldots\ldots(7)$$

Inside the particle the potential, which we denote by ψ^1, satisfies Laplace's equation since there is no charge. At the surface we have the boundary conditions

$$\psi = \psi^1,\ D\frac{\partial\psi}{\partial n_s} - D^1\frac{\partial\psi^1}{\partial n_s} = -4\pi\lambda e_1\nu, \qquad \ldots\ldots(8)$$

where n_s denotes the outward normal at the particle surface into the region of integration and D^1 is the dielectric constant of the colloidal particle. It should be observed that the second equation in (2), which was derived in III, is valid for an arbitrary function $f(\lambda\psi)$, provided that the latter vanishes at infinity, where ψ is zero; we note that $\sum_{i=1}^{s} n_i^0 e_i = 0$.

§3. GENERALIZATION OF CASIMIR EQUIVALENCE THEOREM

Instead of charging under the condition of fixed density of adsorbed ions, we shall imagine that this density varies quite arbitrarily with λ. For simplicity we first consider the case of uniform density of surface ions ($\nu_0(\mathbf{S})=1$) which would apply to a sphere, or to a section of a cylinder of infinite length or of an infinite plate. Then the function $n=n(\lambda)$ will represent the variation of the number of surface ions with the stage λ. Also $\psi(\lambda, n)$ will denote the (uniform) potential at the surface, a function of λ and n; this potential now replaces $\bar{\psi}(\lambda, n)$ in the equations of the preceding section.

We begin by equating the first expression in (3) for $E(\lambda, n)$ to an alternative formula which was obtained in III (equation (30)), namely,

$$E(\lambda, n)=\tfrac{1}{2}\lambda e_1 \int_0^n [\lambda\psi(\lambda, n)]_\lambda \, dn, \qquad \ldots\ldots(9)$$

where the subscript λ indicates partial differentiation, i.e. subject to fixed n. Since the relations (3) and (9) are identities in λ and n, we can choose $n=n(\lambda)$, which, therefore, becomes the upper limit of integration in (9). We readily derive now that

$$\frac{1}{\lambda}\int_V [\psi\rho]_{n=n(\lambda)}\, dv = -e_1 \int_0^{\psi[\lambda,\, n(\lambda)]} n(\lambda, \psi)\, d\psi + \lambda e_1 \int_0^{n(\lambda)} \psi_\lambda(\lambda, n)\, dn, \qquad \ldots\ldots(10)$$

where the function $n=n(\lambda, \psi)$ is the inverse to $\psi=\psi(\lambda, n)$. But

$$\int_0^{n(\lambda)} \psi_\lambda(\lambda, n)\, dn = -\frac{d}{d\lambda}\int_0^{\psi[\lambda,\, n(\lambda)]} n(\lambda, \psi)d\psi + n(\lambda)\psi'[\lambda, n(\lambda)], \qquad \ldots\ldots(11)$$

after integrating by parts; the prime denotes total differentiation with respect to λ. If we substitute (11) into the right-hand side of (10) and then integrate (10) with respect to λ, we obtain

$$\begin{aligned} -e_1 \int_0^{\psi[1,\, n(1)]} & n(1, \psi)d\psi + e_1 \lim_{\lambda\to 0} \lambda \int_0^{\psi[\lambda,\, n(\lambda)]} n(\lambda, \psi)d\psi \\ &= \int_0^1 \frac{d\lambda}{\lambda}\int_V [\psi\rho]_{n=n(\lambda)}\, dv - e_1 \int_0^1 \lambda n(\lambda)\psi'[\lambda, n(\lambda)]d\lambda. \qquad \ldots\ldots(12) \end{aligned}$$

The first term on the left of (12) can be obtained by integrating the well-known Lippmann equation from electrocapillarity theory. It occurs in the expression $U(n)$ for the free energy in the following way. The number of surface ions is not arbitrary but is determined by the condition of thermodynamic equilibrium, which is that $U(n)$ is a minimum, i.e. $U'(n)=0$. If $\bar{n}$ is the equilibrium value of n, we readily derive from (1) and (2)

$$U(\bar{n})=f_0(\bar{n})-\bar{n}f_0'(\bar{n})-\int_0^{\psi(1,\, \bar{n})} n(1, \psi)d\psi. \qquad \ldots\ldots(13)$$

If we identify $\bar{n}$ with $n(1)$ then the integral term on the right of (13) is given by (12). Now the resulting form for $U(n)$ can also be obtained from thermodynamic, statistical reasoning by imagining the charging process carried out along the path $n=n(\lambda)$, the end point being $\lambda=1$, $n(1)=\bar{n}$. In this thermodynamic proof, the details of which will not be given here, the potential of the mean force at an adsorbed ion is identified with the corresponding mean potential, and the same potential function is assumed for the different types of ions in the diffuse layer. In view of this alternative derivation of (12) it might appear that we have shown the Poisson–Boltzmann equation to be a good approximation yielding reliable estimates of the free energy of the double layer. It should be pointed out,

however, that (12), like the second relation in (2), is based on the use of (6) and is valid for any form of $f(\lambda\psi)$. The interesting feature is that as we choose different functions for $f(\lambda\psi)$, the two members of the equation (12) will have different values, but they will always be equal to one another. Thus the relation (12) is less specific than the Poisson–Boltzmann equation, and it seems that no conclusions concerning the reliability of the latter can be reached in this way.

If we can choose a path $n=n_0(\lambda)$ such that (i) the surface potential $\psi[\lambda, n(\lambda)]=\psi_0$, a constant independent of λ, and (ii) the second term on the left of (12) vanishes, then (12) reduces to the theorem of equivalence proved by Casimir (1948). These two conditions are satisfied in the case of an infinite plate-like particle or a cylindrical particle of infinite length, even though in the latter case $n_0(0)$ is infinite. However, for a spherical particle (and probably for any particle of finite extent) $n_0(0)$ is again infinite, and the second term on the left of (12) no longer vanishes (see III).

The result (12) can be generalized to apply to a particle of general shape, the surface of which is at a uniform potential, say $\psi_0(\lambda)$, which is an arbitrary function of λ. The analysis is quite similar to that given at the end of § 4 in III, where we considered a more particular case, namely $\psi_0(\lambda)=\psi_0$, a constant independent of λ. We first choose an arbitrary path of integration $n=n(\lambda)$. Then at each stage λ the surface ions are so distributed over the particle that the latter is at a uniform potential $\psi_0(\lambda)$, the value of which depends therefore on $n(\lambda)$. In this way we obtain (12), provided the function $\psi[\lambda, n(\lambda)]$ is replaced by $\psi_0(\lambda)$.

§ 4. SECOND FORM FOR ELECTRICAL FREE ENERGY

The following theorem will be proved: Let $\Delta p(\mathbf{r})$ denote the difference between the ideal osmotic pressure of the ions at position $\mathbf{r}$ in the diffuse layer and that in the interior of the solution; then the electrical free energy $F_e(n)$ can be expressed as

$$e_1\int_0^n \bar{\psi}(1,n)dn = -\int_V \Delta p(\mathbf{r})dv - E(1,n) + e_1 n\bar{\psi}(1,n). \quad \ldots\ldots(14)$$

Whereas the left-hand member is valid for arbitrary $f(\lambda\psi)$, the right-hand member is derived by using the Boltzmann form (7) for $f(\lambda\psi)$. If we substitute the first equation in (3) into (2), then we have two terms in the resulting expression for $F_e(n)$. The first term reads

$$e_1\int_0^1 d\lambda \int_S \psi\nu\, dS, \quad \ldots\ldots(15)$$

and the second term can be written as

$$\int_0^1 \frac{d\lambda}{\lambda}\int_V \psi\rho\, dv = -\frac{D}{4\pi}\int_0^1 d\lambda \int_V f(\lambda\psi)(\lambda\psi)_\lambda dv + \frac{D}{4\pi}\int_0^1 d\lambda \int_V \psi_\lambda \nabla^2\psi\, dv. \quad \ldots\ldots(16)$$

To obtain (16), we write $\psi=(\lambda\psi)_\lambda-\lambda\psi_\lambda$, where the subscript λ again denotes partial differentiation, and make use of the first equation in (6). It is understood that the integration in (15) and (16) is carried out subject to fixed surface distribution of ions, so that $\nu_\lambda=0$. On introducing the formula (7) for $f(\lambda\psi)$, interchanging the order of integration and making use of (5), the first term on the right of (16) reduces to

$$-kT\sum_{i=1}^{s}\int_V \{n_i(1,\mathbf{r})-n_i^0\}dv = -\int_V \Delta p(\mathbf{r})dv. \quad \ldots\ldots(17)$$

It is assumed here that $\lambda\psi \to 0$ as $\lambda \to 0$, which is true for a single particle immersed in an infinite volume of electrolyte. The second term in the right-hand member of (16) can be expressed as

$$\frac{D}{4\pi}\int_V \left\{[\psi\nabla^2\psi]_{\lambda=1} - \int_0^1 \psi\nabla^2\psi_\lambda d\lambda\right\} dv$$
$$= \frac{D}{8\pi}\int_V [\psi\nabla^2\psi]_{\lambda=1} dv + \frac{D}{8\pi}\int_0^1 d\lambda \int_S \left\{\psi\,\frac{\partial\psi_\lambda}{\partial n_s} - \psi_\lambda\,\frac{\partial\psi}{\partial n_s}\right\} dS. \quad \ldots\ldots(18)$$

The surface integral on the right is obtained by substituting Green's theorem, applied to the functions ψ and ψ_λ. We note here that when $\lambda = 0$, $\psi = 0$, or possibly $\psi =$ constant, throughout the dispersion medium, in which case $[\nabla^2\psi]_{\lambda=0} = 0$; the latter applies to an infinite plate. The second term on the right of (18) can be written as

$$\tfrac{1}{2}e_1 \int_0^1 d\lambda \int_S (\lambda\psi_\lambda - \psi)\nu\, dS, \quad \ldots\ldots(19)$$

substituting the boundary conditions (8). To derive (19) we also make use of the relation $\nu_\lambda = 0$ and of the result that the surface integral on the right of (18) vanishes when we replace the function ψ by ψ^{I}. The latter follows on transforming the surface integral by means of Green's theorem into a volume integral taken inside the particle itself and applying the conditions that both ψ^{I} and $\psi_\lambda{}^{\mathrm{I}}$ satisfy Laplace's equation. If we now add (15) and (19), we obtain

$$\tfrac{1}{2}e_1 \int_0^1 d\lambda \int_S (\lambda\psi)_\lambda \nu dS = \tfrac{1}{2}e_1 \int_S [\psi]_{\lambda=1}\nu\, dS = \tfrac{1}{2}e_1 n\bar{\psi}(1,n), \quad \ldots\ldots(20)$$

integrating by parts with respect to λ and putting $\nu_\lambda = 0$. The free energy $F_e(n)$ consists of three terms, namely, the quantities (17) and (20) and the volume integral on the right of (18). By making use of (3) it is readily verified that the sum of these three terms is identical with the right-hand member of (14). The formula (14) will be applied in later papers to determine the interaction of colloidal particles.

If the particle is metallic, the preceding analysis must be modified, but since the details are quite similar to those described in paper V, we shall omit them. Although ν_λ may no longer vanish, it can be verified that there are no additional terms in (19) and (20), since ψ is constant over the surface and $n = \int_S \nu\, dS$ is independent of λ. It follows that for a metallic particle the potential $\bar{\psi}(1,n)$ in (14) is replaced by $\psi(1,n)$.

Verwey and Overbeek (1948) considered the case of a dielectric particle for which the potential is uniform over the surface. Thus, if the particle is an ionic crystal and an adsorbed ion is identical with one of the lattice ions, then under thermodynamic equilibrium no (isothermal, reversible) work is required to transfer such an ion from one part of the surface to another. If we now assume that both the non-electrical (chemical) energy of adsorption and the electrical self-energy change are constant over the surface of the particle (which is of general shape), it follows that the particle surface is at uniform potential. (We identify the electrical potential of the mean force at an adsorbed ion with the corresponding mean potential and ignore possible surface imperfections.) In these circumstances the charging process which yields the second relation in (2) is carried out under the condition of fixed surface density of ions $\nu = n\nu_0(\mathbf{S}, n)$, where the function $\nu_0(\mathbf{S}, n)$ is so chosen that the potential is uniform over the surface at the final

stage. We note that because of the non-linearity of the Poisson–Boltzmann equation $\nu_0(\mathbf{S}, n)$ actually varies with n; in the case of very small n we may apply the linear Debye–Hückel equation and then $\nu_0(\mathbf{S}, n)$ no longer depends on n.

There are differences between a metallic particle and a dielectric particle at uniform surface potential in the normal equilibrium state $\lambda = 1$. First, in the former (metallic) case the potential is uniform over the surface at any intermediate stage during the charging (owing to the presence of free electrons), even though the distribution of adsorbed ions is fixed, whereas in the latter case this is not true. Secondly, for a metallic particle the second relation in (2) is valid when $\bar{\psi}(1, n)$ is replaced by the uniform potential $\psi(1, n)$, the relative distribution of adsorbed ions $\nu_0(\mathbf{S})$ being quite arbitrary. But again this property does not apply to a dielectric particle of general shape, since it becomes necessary to replace $\nu_0(\mathbf{S})$ by the definite distribution $\nu_0(\mathbf{S}, n)$ in (4), in order to achieve a uniform potential $\psi(1, n)$ at each value of n.

In the case of either a metallic particle or a dielectric particle of general shape under the conditions specified above, we may replace $\bar{\psi}(1, n)$ in (14) by $\psi(1, n)$, which we denote simply by ψ_0. On integrating by parts the left-hand side of (14) we now obtain

$$-e_1 \int_0^{\psi_0} n(1, \psi) d\psi = -\int_V \Delta p(\mathbf{r}) dv - E(1, n)$$

$$= \int_0^1 \frac{d\lambda}{\lambda} \int_V [\psi\rho]_{\psi_0} dv - e_1 \lim_{\lambda \to 0} \lambda \int_0^{\psi_0} n(\lambda, \psi) d\psi, \quad \ldots\ldots (21)$$

the second relation following from (12), where the subscript ψ_0 denotes that the integration is carried out subject to the condition that the surface potential is uniform and given by ψ_0, i.e. it is independent of state λ and position $\mathbf{S}$. For a metallic particle this condition is attained by suitable choice of the total number of ions as a function of λ and ψ_0. For a dielectric particle we would also need to specify the relative distribution of adsorbed ions as a function of λ and ψ_0.

The equation (37 *b*) of Verwey and Overbeek (1948, p. 80), which applies to the case of two parallel plates, is equivalent to the second equation in (21), and it is possible to derive the latter by generalizing the proof of these authors. The first term on the right of this second equation is first written in the form (16), and we again obtain the formulae (17) and (18). Making use of the condition $\psi_i = 0$ on the surface of the particle, we interchange the order of integration in the second term on the right of (18) and then integrate by parts. This second term thus simplifies to

$$\frac{D\psi_0}{8\pi} \int_S \left[\frac{\partial \psi}{\partial n_s}\right]_{\lambda=0}^{\lambda=1} dS = -\tfrac{1}{2} e_1 n \psi_0 + \tfrac{1}{2} e_1 \psi_0 \lim_{\lambda \to 0} \lambda n(\lambda, \psi_0). \quad \ldots\ldots (22)$$

The right-hand side follows on application of the boundary conditions (8), since $\psi^1 = \psi_0$, a constant. (In the case of a spherical particle the second term on the right of (22) does not vanish.) Now

$$\tfrac{1}{2}\psi_0 \lim_{\lambda \to 0} \lambda n(\lambda, \psi_0) = \lim_{\lambda \to 0} \int_0^{\psi_0} n(\lambda; \psi) d\psi, \quad \ldots\ldots (23)$$

which can be shown from the theory of electrostatics as follows. When $\lambda = 0$, but $q \neq 0$, where q is the charge on the particle, we simply have a charged conductor immersed in a dielectric and q is proportional to the surface potential, being

related by the coefficient of capacity. This coefficient is independent of the value of q, and hence (23) is valid. By substituting (22) for the second term on the right of (18) and making use of (23), we readily find that (16) becomes identical with the second relation in (21).

§ 5. TWO PARALLEL PLATES

The analysis which yields the expression on the right of (14) for $F_e(n)$ must be modified to apply to sections of two parallel plates of infinite area. We shall consider the double layer on the inner face only of such a section, which for simplicity has unit area, so that we write $n=\nu$ in the following analysis. The diffuse layer of this section extends from the plate face to the median plane; if R is the separation of the plates, the volume of the diffuse layer is $R/2$. If we charge at constant density ν of surface ions, then, as already explained in the earlier papers (see, in particular, II), the potential over the whole of the double layer tends to a common infinite value as $\lambda \to 0$, namely $\lambda\psi \to \lambda\psi(\lambda, \nu) = m$, say, a finite quantity different from zero. For finite plates (i.e. in a real sol) $m=0$ and the origin of a non-vanishing m is therefore the incorrect use of the model of *two infinite* plates to represent two finite plates in the vicinity of $\lambda=0$. As a consequence we have a spurious initial (or residual) electrical free energy in the completely discharged state, which can be expressed in one of two forms, namely,

$$-e_1 \int_0^{\nu} m \, d\nu = \tfrac{1}{2}kTR \sum_{i=1}^{s} n_i^0 \{\exp(-e_i m/kT) - 1\} + \tfrac{1}{4}mR \sum_{i=1}^{s} n_i^0 e_i \exp(-e_i m/kT) - \tfrac{1}{2}e_1 \nu m. \quad \ldots\ldots (24)$$

This can be shown in the following way. The formula (14) is always true for a particle of finite extent, provided that the Poisson–Boltzmann equation is used and the volume of electrolyte is infinite. We can also apply (14) to each of two identical finite parallel plates (with edges in line); the volume of electrolyte is divided into two by the median plane and the diffuse outer layer of each plate is assumed to extend over an (infinite) half-volume. Since no charging process is involved in the equation (14), the troublesome behaviour at $\lambda=0$, described above, does not arise when we imagine the area of the two plates to increase indefinitely. Consequently (14) remains valid for each of the two unit sections taken from the inner faces of the infinite plates and $\bar{\psi}(1, n)$ is now replaced by the uniform potential over each plate $\psi(1, \nu)$. But we can apply the first formula in (2) for $F_e(n) = F_e(\nu)$ to unit (inner) area of each infinite plate and by suitable transformations obtain two equivalent forms for $F_e(\nu)$. The first form, which was derived in III, is the sum of the left-hand members of (14) and (24), since $\bar{\psi}(1, n) = \psi(1, \nu)$; the second form is obtained by adding the right-hand sides of (14) and (24). The validity of the equation (24) follows immediately. It remains to indicate the derivation of the three terms on the right of (24). The first term must be added to (17) and accounts for a difference in the densities of ions between the plates and in the bulk of the electrolyte at $\lambda=0$. The second term would occur in the right-hand member of (18) and is due to a non-vanishing value for $\psi\nabla^2\psi = \lambda\psi f(\lambda\psi)$ at $\lambda=0$. Finally, the last term in (24) would appear on the extreme right of (20).

The validity of (24) can be verified in another way. In an earlier paper (Levine and Suddaby 1951) a series expansion for the potential in the double layer which applies to the case of a binary symmetrical electrolyte ($n_1^0 = n_2^0$,

$e_1 = -e_2$) and moderate potentials has been obtained by solving the Poisson–Boltzmann equation. Making use of this expansion, we find that

$$m = m_0 - \frac{1}{6}\left(\frac{e_1}{kT}\right)^2 m_0^3 + \frac{3}{40}\left(\frac{e_1}{kT}\right)^4 m_0^5 - \ldots, \qquad \ldots\ldots(25)$$

where $m_0 = \nu kT/Re_1 n_1^0$. The approximation $m = m_0$ is obtained if we replace the Poisson–Boltzmann equation by the linear Debye–Hückel equation. If we substitute (25) into (24) and then expand each side of (24) in powers of ν^2, we obtain identical coefficients of the first three powers of ν^2.

§ 6. ALTERNATIVE DERIVATION OF SECOND FORM FOR FREE ENERGY

The free energy of our system, consisting of one particle immersed in a very large volume of electrolyte, is assumed to have the form

$$F(n) = \sum_{i=1}^{s} N_i\xi_i - n\xi_1 + f_s(n) + \sum_{i=1}^{s} N_i\chi_i(1) - n\Delta\chi_1(1) + kT\int_V \left(\sum_{i=1}^{s} n_i \ln n_i\right) dv + E(1, n). \qquad \ldots\ldots(26)$$

In this section all quantities refer to the actual physical state $\lambda = 1$. The quantities $\xi_i (i = 1, \ldots, s)$ are functions of volume (or pressure) and temperature only and represent the part of the chemical potential of the ions due to the short-range van der Waals interaction with the surrounding solvent molecules.*

$f_s(n)$ is the non-electrical part of the free energy associated with the surface phase of n adsorbed ions of type 1. $\chi_i(1)$ is the electrical self-energy of an i ion in the dispersion medium. The last two terms on the right of (26) can be interpreted as follows. Consider an element of volume dv in the dispersion medium, containing $n_i\,dv$ ions of type i ($i = 1, \ldots, s$). The free energy attributed to these ions includes an osmotic term $kTn_i \ln n_i\,dv$ and an electrostatic term $n_i e_i\psi\,dv$ which arises from the Coulomb interaction of the ions. Thus in the chemical potential expression of an i ion in the volume element dv we have the contribution $e_i\psi + kT \ln n_i$ which has the same value throughout the whole of the dispersion medium. If we compare the element dv with another dv_0, the density of i ions and potential in the latter being n_i^0 and $\psi = 0$ respectively, then the condition of equal chemical potentials obviously yields the Boltzmann distribution law (5). We now integrate over the dispersion medium and halve the resulting electrostatic contribution since we have been counting the Coulomb interaction energy of each ion pair twice by this method. The corresponding electrostatic contribution (again halved) from the surface ions is finally added. If we use the second form in (3) for $E(1, n)$ then alternatively we can assign the usual form for the field energy to each volume element dv.

If we substitute (5) for n_i (after putting $\lambda = 1$), we derive that the 'osmotic term' on the right of (26) becomes

$$kT\sum_{i=1}^{s}\int_V n_i(\ln n_i^0 - e_i\psi/kT)\,dv = kT\left\{\sum_{i=1}^{s} N_i \ln n_i^0 - n \ln n_1^0\right\} - \int_V \psi\rho\,dv, \quad \ldots(27)$$

since $\rho = \sum_{i=1}^{s} n_i e_i$. Applying the Boltzmann distribution law, we have

$$n_i^0 V\left[1 + \frac{1}{V}\int_V \{\exp(-e_i\psi/kT) - 1\}dv\right] = \begin{cases} N_1 - n, & i = 1, \\ N_i, & i = 2, \ldots, s, \end{cases}$$

* Instead of $n_i \ln n_i$, one should write $n_i(\ln n_i - 1)$, but the additional term is absorbed into ξ_i.

and thus, if the volume V is large, a very good approximation is

$$\ln n_i^0 + \frac{1}{V}\int_V \{\exp(-e_i\psi/kT)-1\}dv = \begin{cases} \ln\{(N_1-n)/V\}, & i=1, \\ \ln(N_i/V), & i=2,\ldots,s. \end{cases} \quad \ldots\ldots(28)$$

On substituting this approximate form for $\ln n_i^0$ into (27) and making use of (3), we find that (26) can be expressed in the form

$$F(n) = F_0(n) + \sum_{i=1}^{s} N_i\chi_i(1) - n\Delta\chi_1(1) + F_e(n), \quad \ldots\ldots(29)$$

very nearly, where $F_e(n)$ is given by the right-hand side of (14) and

$$F_0(n) = \sum_{i=1}^{s} N_i\{\xi_i + kT\ln(N_i/V)\} + f_0(n), \quad \ldots\ldots(30)$$

where

$$f_0(n) = f_s(n) - n\xi_1 - nkT\{1+\ln(N_1/V)\}. \quad \ldots\ldots(31)$$

The quantity $F_0(n)$ is the free energy of our system in the completely discharged state. To derive the expression (31) for $f_0(n)$ we have expanded $F_0(n)$ in powers of n/N_1 and neglected terms of order $(n/N_1)^2$.

The physical significance of the preceding method of evaluating the free energy can be described as follows. We imagine that the ions are all discharged and that those in the dispersion medium are uniformly distributed. Then these *discharged* ions are redistributed so as to be in their final average positions, corresponding to the fully charged state. The second last term on the right of (26) (the osmotic term) represents the work done against thermal motion in this redistribution. The last term in (26) (the electrostatic term) is the work done in charging all the ions against the potential ψ, assuming the ions are fixed in their average final positions. This method of charging is not an isothermal, reversible, process, and the approximation introduced thereby is implied in the Poisson–Boltzmann equation itself.

REFERENCES

Booth, F., 1951, *J. Chem. Phys.*, **19**, 391.

Casimir, H. G. B., 1944, *Tweede symposium over sterke electrolyten en over de electrische dubbellaag*, Utrecht, ed. Ned. Chem. Ver., 6; 1948, *see* Verwey E. J. W., and Overbeek, J. Th. G., 1948, p. 63.

Conway, B. E., Bockris, J. O'M., and Ammar, I. A., 1951, *Trans. Faraday Soc.*, **47**, 756.

Coolidge, A. S., and Juda, W., 1946, *J. Amer. Chem. Soc.*, **68**, 608.

Debye, P., 1927, *Z. Phys. Chem.*, **130**, 56.

Derjaguin, B., 1940, *Trans. Faraday Soc.*, **36**, 203.

Frenkel, J., 1946, *Kinetic Theory of Liquids* (Oxford : University Press), p. 362.

Frumkin, H., 1943, *Acta Physicochimica, U.S.S.R.*, **18**, 473.

Grahame, D. C., 1950, *J. Chem. Physics*, **18**, 903.

Grimley, T. B., 1950, *Proc. Roy. Soc.* A, **201**, 40.

Grimley, T. B., and Mott, N. F., 1947, *Discussions of the Faraday Society*, **1**, 3.

Levine, S., 1946, *Trans. Faraday Soc.*, **42B**, 102; 1948, *Ibid.*, **44**, 833; 1950, *Phil. Mag.*, **41**, 53; 1951 a, *Proc. Camb. Phil. Soc.*, **47**, 217; 1951 b, *Ibid.*, **47**, 230; 1951 c, *J. Colloid Science*, **6**, 1.

Levine, S., and Suddaby, A., 1951, *Proc. Phys. Soc.* A, **64**, 287.

Loeb, A. W., 1951, *J. Colloid Science*, **6**, 75.

Mueller, H., 1935, *J. Phys. Chem.*, **39**, 743.

Verwey, E. J. W., and Overbeek, J. Th. G., 1948, *Theory of the Stability of Lyophobic Colloids* (Amsterdam : Elsevier).

The Conversion and Auger Electrons of Radium D

By D. K. Butt and W. D. Brodie
Department of Natural Philosophy, University of Edinburgh

Communicated by N. Feather; MS. received 18th April 1951

ABSTRACT. The conversion and Auger electrons of Radium D have been studied in a lens β-ray spectrometer with a post-focusing electron accelerator. The number of conversion electrons due to the 46·7 kev. γ-ray is found to be $59{\cdot}2 \pm 5$ per hundred disintegrations but reasons are given which suggest that this value be regarded as a lower limit. The Auger electrons have been compared with those resulting from the ThB–ThC transition.

§1. Introduction

Because of the softness of the Ra D radiations doubt remains regarding its mode of disintegration. For many years attempts have been made to detect the primary β-radiation, but the problem is a difficult one since the end point is believed to be in the 15 kev. region. The expansion chamber results of Richardson and Leigh-Smith (1937) are the most reliable to date, and these workers estimate that 60% of the β-rays have energies less than 4 kev. It has been suggested that the spectrum is complex, there being a second component with an end point of some 60 kev. (Kinsey 1948, Cranberg 1950), but this has not been observed.

The presence of a 46·7 kev. γ-ray has long been known both in emission and through the natural photoelectrons from the L, M and N shells of the residual atom. The unconverted γ-radiation is known, with fair certainty, to have an intensity of $3{\cdot}5 \pm 0{\cdot}4\%$ (Bramson 1930, Gray 1932, Von Droste 1933, Stahel 1935), but the values given by various workers for the intensity of the internal conversion lines range from 15% to 80% (Kikuchi 1927, Stahel 1931, Lee and Libby 1939, Ouang, Surugue and Tsien 1943).

Besides the 46·7 kev. γ-ray, other weaker γ-rays have been discovered more recently (see Feather 1949) and, in all, seven γ-rays are assumed to be known. Their energies and intensities are listed in Table 1. Internal conversion electrons of one of these γ-rays have been reported by Cranberg (1950).

Table 1. The γ-Rays of Ra D

Quantum energy (kev.)	46·7	42·6	$37 \pm 0{\cdot}5$	$31{\cdot}3 \pm 0{\cdot}8$	$23{\cdot}2 \pm 0{\cdot}6$	$16{\cdot}1 \pm 0{\cdot}4$	$7{\cdot}3 \pm 0{\cdot}7$
Emission intensity (%)	3·5	$0{\cdot}2 \pm 0{\cdot}1$	$0{\cdot}2 \pm 0{\cdot}1$	$0{\cdot}4 \pm 0{\cdot}2$	~1	~0	~10

The present investigation of the electron and β-ray spectrum of Ra D was made with a β-ray lens spectrometer which incorporates a post-focusing electron accelerator, enabling electron spectra to be studied conveniently down to energies as low as 4 kev. A thin-windowed Geiger–Müller counter is used as detector. Details of the spectrometer have already been published (Butt 1949, 1950).

§2. SOURCE PREPARATION

Ra D was extracted from a supply of old glass radon needles. The needles were boiled in chromic acid, rinsed in distilled water and finely crushed under about 10 ml. of concentrated HNO_3. This solution was boiled and centrifuged, and the concentrated HNO_3 containing the Ra D was decanted. The solution was then evaporated to dryness and taken up again with about 2 ml. of 0·1N HNO_3. The Ra D was collected on a platinum foil 0·3 cm^2 in area by an electrolysis in which the platinum foil was positive with respect to the platinum crucible containing the solution. A current of 10^{-4} amp. was passed for 10 hours. By this means only Ra D was collected on the anode, since it alone of the elements present forms a complex negative ion. In particular this method of collection has the advantage of rejecting any traces of mercury that might have been included in the radon tubes. The Ra D was finally transferred to a piece of gold leaf 0·22 mg/cm^2 in thickness and 0·6 cm. in diameter, backed, for extra strength, by a collodion film of weight negligible compared with that of the gold. This transfer was accomplished electrolytically. The platinum was mounted horizontally and a drop of 0·1N HNO_3 spread over its upper surface. The gold leaf was then lowered until contact with the HNO_3 was made. A current of 10^{-4} amp. was passed for one hour through the cell so formed, the gold leaf being the anode. From this, after washing with distilled water, the surplus liquid was removed with the corner of a piece of filter paper. The source so formed was a disc of about 4·5 mm. diameter and was a practically invisible deposit on the gold leaf. The strength of the source was approximately 10 μc.

§3. THE INTERNAL CONVERSION ELECTRONS OF THE 46·7 kev. TRANSITION

Figures 1 and 2 show the spectrum obtained after equilibriun between the Ra D and Ra E had been established. With maximum current in the spectrometer coil it was impossible to focus electrons with momenta greater than 2,500 gauss cm. so the upper part of the Ra E spectrum was taken from the results of Neary (1940). This part is drawn with a dotted line in Figure 2.

The two most prominent lines, *e* and *f* ($H\rho = 600$ and 720 gauss cm. respectively) are formed by internal conversion electrons due to the 46·7 kev. transition. Line *e* corresponds to conversion in the L_I, L_{II} and L_{III} shells of the Ra E product nucleus and line *f* to conversion in the M and N shells. Of necessity the resolution was too low for the lines due to the individual shells to be resolved.

Since, for all practical purposes, the only mode of disintegration of Ra E is to the ground state of Ra F by β-emission, a comparison of the areas of lines *e* and *f* with the area of the Ra E β-spectrum gives the fraction of the decays involving excited atomic levels of the Ra E atom due to the internal conversion of the 46·7 kev. γ-ray. Before this comparison can be made, however, it is necessary to estimate the effect on the spectrum of back-scattering from the source support. This work falls into two parts.

(i) *Correction of the Ra E β-spectrum.* When compared with that of Neary our Ra E spectrum shows deviations due to back-scattering at energies below 180 kev. ($H\rho = 1{,}550$ gauss cm.). Accordingly the Ra E spectrum was corrected below 180 kev. using Neary's results, and the area under the corrected curve was taken to represent the intensity of the β-rays of Ra E.

(ii) *Corrections to be applied to the area of the conversion lines e and f.* The intensity due to Ra E in the region of the conversion lines was found by examining in the spectrometer the β-radiation from a source of pure Ra E deposited electrolytically on a gold foil similar to that used for the Ra D. The source was prepared by the method of Broda and Feather (1947). Fitting of the resulting curve to the previous one gave the line marked 'Ra E' in Figure 1. This line was used

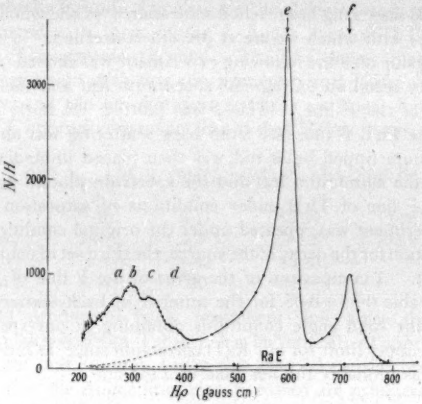

Figure 1.

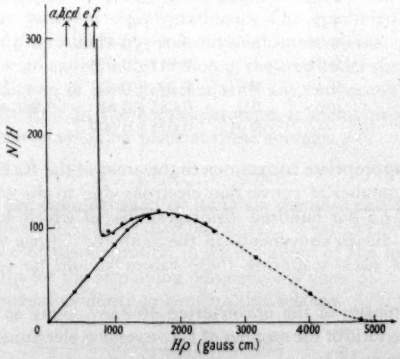

Figure 2.

as a base line when the intensity of the conversion electrons was being considered. To correct the area of the conversion lines for back-scattering use was made of the formula given by Hamilton and Gross (1950). These authors state that the back-scattering ratio (the number of scattered electrons per primary) reaches an asymptotic value called the back-scattering constant S for a thickness t_0 of scattering material at an energy V_e given by $V_e = 800[(Z^2/A)t_0]^{1/2}$, where V_e is in kev., Z and A are the atomic number and mass number of the scatterer and

t_0 its thickness in gm/cm². The value of S has little energy dependence. Applying this equation to the source support used in the present investigation we obtain $V_c = 67$ kev. This value appears to be a reasonable one for saturation back-scattering since our Ra E spectrum begins to depart from that of Neary at about 180 kev. It is nevertheless possible that the source backing was actually thinner than 0·22 mg/cm² owing to the solution of some of the gold in the 0·1N HNO_3 during the electrolysis of the Ra D. However this may be, we assume that back-scattering has reached saturation over the whole range of energy (45 kev. and less) with which we are at present concerned.

To find the value of S the following experiment was carried out. Thorium B was deposited by recoil on 0·2 mg/cm² aluminium leaf and the spectrum in the neighbourhood of the F line (148 kev.) was plotted. A fairly reliable estimate of the area of the Th B F line free from back-scattering was obtained from this curve. A platinum tipped brass rod was then placed immediately behind and in contact with the aluminium leaf and the spectrum plotted again. This gave the area of the F line of Th B under conditions of saturation back-scattering. Finally, the experiment was repeated under the original conditions to make sure that, after correction for the decay of the source, the third set of counts corresponded with the first set. A comparison of the areas of the F line of Th B in the two cases gave the value $0{\cdot}55 \pm 0{\cdot}05$ for the number of back-scattered electrons per primary under the solid angle conditions obtaining in our spectrometer. We regard this as an upper limit for our Ra D correction since, as indicated above, the source mount was probably thinner than 0·22 mg/cm².

Table 2. The Relative Intensities of the Conversion Lines of the 46·7 kev. γ-Ray

	Ellis	Curtis	Cranberg	Butt and Brodie
L_I	1·0	1·0	1·0	
L_{II}	0·04	0·06	$0{\cdot}09 \pm 0{\cdot}015$	1·0
L_{III}	0·01	—	$0{\cdot}019 \pm 0{\cdot}004$	
M	0·4	0·5	$0{\cdot}29 \pm 0{\cdot}02$	
N	0·2	0·2	$0{\cdot}085 \pm 0{\cdot}01$	$0{\cdot}266 \pm 0{\cdot}03$
O	—	0·01	$0{\cdot}021 \pm 0{\cdot}007$	

Applying the appropriate corrections to the areas of the Ra E spectrum and of lines *e* and *f*, the number of conversion electrons due to the 46·7 kev. γ-ray was calculated as $59{\cdot}2 \pm 5$ per hundred disintegrations, of which $46{\cdot}7 \pm 4$ (i.e. 79%) were found to be due to conversions in the L shells. Since we have probably over-corrected for back scattering these values should be regarded as lower limits.

Taking the intensity of the unconverted 46·7 kev. γ-ray as 3·5 per hundred disintegrations, the ratio of the number of L-conversion electrons to the number of unconverted γ-rays is 13·5.

An indirect method of finding the number of conversion electrons depends upon the determination of (i) the number of L x-rays produced as a result of internal conversion in the L shells, (ii) the fluorescence yield of the L shells and (iii) the fraction of the internal conversion electrons which originate from the L shells. Stahel's (1935) result for (i) is 25·1 per hundred disintegrations, and Kinsey (1948) has obtained 0·47 for the fluorescence yield. These figures, with the present result of 79% for (iii) give 67·5 conversion electrons per hundred disintegrations. This method eliminates the fitting of our incomplete Ra E

spectrum to Neary's, but ignores any ionization of the L shells which may be produced by conversion of the recently discovered low energy γ-rays.

Since there is still some uncertainty regarding the relative intensities of the conversion lines, Table 2 has been compiled giving the results up to date.

§4. THE VERY LOW ENERGY REGION OF THE SPECTRUM

Lines *b*, *c* and *d* of Figure 1 are L-Auger lines associated with the ionization of the L shells of the Ra E product nucleus by the various γ-rays present. Their energies are compared with those of the L-Auger lines of Th C, an isotope of Ra E, in Table 3. The agreement is good. The Th C Auger lines were obtained in a previous investigation with this spectrometer (Butt 1950). Line *a* has an energy of 6·85 kev. and can be identified either as an Auger line, as shown in Table 3, or as the L internal conversion line of the 23·2 kev. γ-ray. This internal

Table 3. The L-Auger Lines of Th C and Ra E

		a	*b*	*c*		*d*
Th C	kev.	7·10	8·11	10·39	12·26	12·62
	$H\rho$ (gauss cm.)	284·2	303·5	343·5	373·0	378·5
Ra E	kev.	(6·85)	7·93	10·20		12·70
	$H\rho$ (gauss cm.)	(279)	300	340		379

conversion should produce a fairly prominent line, since the unconverted 23·2 kev. radiation, as seen from Table 1, has an intensity of approximately 1%; we therefore suggest that line *a* is due to this internal conversion.

If we assume that the Auger lines just discussed are produced by ionization of the L shells as represented by line *e* only, then, using Kinsey's value of 0·47 for the fluorescence yield the Auger lines should have a combined intensity of $0{\cdot}53 \times 46{\cdot}7 = 25$ per hundred disintegrations. The combined intensity of all four lines *a*, *b*, *c* and *d* is roughly 24 per hundred disintegrations. This agreement is accidental because an appreciable fraction of the area under these lines may well be due to the β-radiation of Ra D together with any conversion electrons of the 23·2 kev. γ-ray. In view of these considerations it seems probable that some source self-absorption was taking place at these energies.

§5. CONCLUSIONS

It is clear that the disintegration of Ra D via the 46·7 kev. transition can, at most, account for about 70% of the disintegrations. Feather (1949) has suggested an alternative mode of disintegration involving some of the low energy γ-rays which might account for the remaining percentage (Figure 3). So far, however, there is no experimental evidence to confirm this scheme.

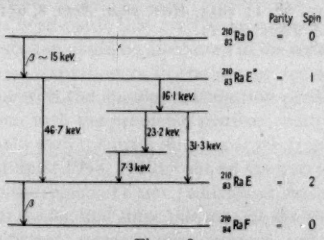

Figure 3.

As regards spin and parity relations, since the even–even nuclei Ra D and Ra F have zero spin and even parity and since the Ra E β-spectrum is almost certainly second forbidden (Feather and Richardson 1948) we conclude that the ground state of the Ra E nucleus has spin 2 and even parity (this assumes the Gamow–Teller selection rules). Again, assuming the end point of the Ra D β-spectrum is about 15 kev. the transition is an allowed one (Feather and Richardson 1948), and the Ra E* nucleus has spin 1 and even parity. From this we conclude that the 46·7 kev. radiation carries away one unit of angular momentum, and that, since there is no parity change, magnetic dipole radiation will probably be of comparable importance with electric quadrupole. The high value of 13·5 for the L internal conversion coefficient points to the presence of a large amount of magnetic dipole radiation.

As has been indicated, we have obtained no convincing evidence regarding the Ra D continuous spectrum. Its end point could easily be masked by the presence of the intense Auger lines and its expected rapid rise partially annulled by self-absorption in the source. Efforts to obtain a cleaner source by activation with radon gas have so far failed.

It will have been noted that no internal conversion line of any of the five recently reported γ-rays has been detected, with the possible exception of the 6·8 kev. line. This can be explained on the grounds of the weakness of the radiations and the fact that the resolving power of the instrument was too low.

ACKNOWLEDGMENT

The authors' thanks are due to Professor N. Feather for his continued support throughout the work.

REFERENCES

Bramson, S., 1930, *Z. Phys.*, **66**, 721.
Broda, E., and Feather, N., 1947, *Proc. Roy. Soc.* A, **190**, 20.
Butt, D. K., 1949, *Proc. Phys. Soc.* B, **62**, 551; 1950, *Ibid.*, **63**, 986.
Cranberg, G., 1950, *Phys. Rev.*, **77**, 155.
Feather, N., 1949, *Nucleonics*, July, 22.
Feather, N., and Richardson, H. O. W., 1948, *Proc. Phys. Soc.*, **61**, 452.
Gray, J., 1932, *Nature, Lond.*, **130**, 738.
Hamilton, D. R., and Gross, L., 1950, *Rev. Sci. Instrum.*, **21**, 912.
Kikuchi, S., 1927, *Jap. J. Phys.*, **4**, 143.
Kinsey, B., 1948, *Canad. J. Res.*, **26**, 421.
Lee, D. D., and Libby, W. F., 1939, *Phys. Rev.*, **55**, 252.
Neary, G. J., 1940, *Proc. Roy. Soc.* A, **175**, 71.
Ouang, T. T., Surugue, J., and Tsien, S. T., 1943, *C. R. Acad. Sci., Paris*, **217**, 535.
Richardson, H. O. W., and Leigh-Smith, A., 1937, *Proc. Roy. Soc.* A, **160**, 454.
Stahel, E., 1931, *Z. Phys.*, **68**, 1; 1935, *Helv. phys. Acta*, **8**, 651.
Von Droste, G., 1933, *Z. Phys.*, **34**, 17.

The Angular Distribution of Neutrons from the (d, n) Reaction in Light Elements

By J. HUGHES
Department of Physics, University of Liverpool

Communicated by H. W. B. Skinner; MS. received 2nd April 1951

ABSTRACT. A proton recoil chamber with a thick polythene layer was used to determine the angular distribtuion of the neutrons from thick targets of various light elements bombarded with 8 MeV. deuterons. In all cases a pronounced forward maximum in intensity was found, the half width of the distribution decreasing with increasing atomic number. The absolute intensity of neutrons in the forward direction decreases as the atomic number increases but the dependence on atomic number is not a smooth function. Most elements show the presence of multiple forward peaks. In a few elements the effect of reducing the incident deuteron energy was investigated.

§ 1. INTRODUCTION

For low bombarding energies the (d, n) reaction has usually been considered to proceed in two successive steps, in accord with the compound nucleus theory of nuclear reactions (Bohr 1936). Measurements made on the angular distribution of the neutrons emitted from light elements bombarded with deuterons of energy approximately 6 MeV. are in agreement with predictions from this theory (Pool 1938).

At higher energies however, because of the low binding energy of the deuteron and its consequent extended structure, other types of interaction have been predicted (Oppenheimer 1935, Dancoff 1947 a). In one possible interaction the deuteron grazing the edge of the nucleus, or coming within the range of the specifically nuclear forces, may cause the proton to be 'stripped off' and captured, while the neutron continues in approximately the same direction as the incident deuteron with approximately the same velocity. Calculations have shown that at 200 MeV. this stripping process is the most important reaction (Serber 1947, Dancoff 1947 b). Experiments with incident deuterons of energy 200 MeV. (Helmholz, McMillan and Sewell 1947) and of 15 MeV. (Roberts and Abelson 1947) showed the existence of this stripping process, characterized by the pronounced forward maximum in intensity of the neutrons.

The suggestion has been made that even at relatively low energies the major part of the (d, n) cross section could be attributed to the stripping process (Peaslee 1948, Butler 1950 a, b). Experiments in the energy region 15–20 MeV. showed approximate agreement with the angular distribution predicted by the stripping theory, but disagreement with the predicted neutron energy distribution and the variation of neutron yield with the mass number of the target element (Ammiraju 1949, Falk, Creutz and Seitz 1948, 1949). As no measurements have been made on the (d, n) reaction in the region of 8 MeV., which is above the potential barrier for most light and medium nuclei, and since this may be the transition region for the onset of stripping, the present series of measurements was made.

§ 2. APPARATUS

Deuterons were accelerated by the 37-inch cyclotron in this laboratory, and had an initial energy of approximately 8 MeV. The deuteron beam entered a subsidiary target chamber through a 5-foot extension tube connected to the main target chamber. Adjustable slits in this extension tube served to limit the angular spread of the beam, and achieved some small measure of energy resolution in the cyclotron stray field. The main features of this subsidiary target chamber were an insulated target box of thin brass, in which the various targets were mounted, and an insulated flap of lead which could be rotated through a vacuum-tight joint, so that it either intercepted the beam before it struck the target or lay completely out of the path of the beam. Since both the target box and the lead flap were insulated from earth, it was possible by connecting them to a beam-integrating circuit to measure the total charge which either had received during a particular experiment. All parts of the target chamber which could be bombarded by stray beams were covered with thick lead foil, to reduce the neutron background.

Most of the experiments cited above were performed with radioactive threshold detectors to measure the neutron angular distribution. The present measurements were made using a proton recoil chamber, with a thick polythene layer. Although the energy resolution of the thick layer proton recoil chamber is very poor, it has been shown that the efficiency is high, and increases approximately linearly with incident neutron energy (Allen and Wilkinson 1948). This form of neutron detector will therefore give more weight to the higher energy neutron groups. By varying the bias on the recording instrument it is possible to use the chamber as a threshold detector with variable threshold (Barschall and Bethe 1947). The proton recoils were detected in a parallel plate ionization chamber with a grid (Bunemann, Cranshaw and Harvey 1949). Argon at a pressure of 10 atmospheres was used as the chamber filling.

At this pressure the dimensions of the chamber were such that a proton with energy greater than 8 MeV. passed through the grid. A higher pressure would have been desirable to contain all the recoils within the region between the polythene layer and the grid, but the intense γ-ray background from the cyclotron tank caused too much piling up of pulses. Although it was not possible to run the chamber with voltage saturation of the pulses, the change in pulse amplitude for any reasonable voltage variation of the regulated high voltage supply, due to mains variation, was negligible. An amplifier with a rise time of $\frac{1}{2}$ μsec. was used, as the chamber operated under electron collection conditions. The differentiating time constant was made approximately 10 μsec., in order to minimize the piling up effect of γ-ray and neutron recoils formed in the high-pressure argon. The pre-amplifier was mounted directly on the recoil chamber, and the pulses fed back through a cable to the main amplifier and recording gear, located remotely. The pulses were recorded by a 20-channel pulse analyser. The use of a pulse analyser enabled the data obtained to be treated so that the effect of varying the threshold energy could be investigated. The recoil chamber was mounted on a light framework, which moved around the target on an arc of a circle of one metre radius, in such a way that the centre of the chamber was at the same level as the beam. The experimental arrangement was such that the neutrons could be detected at angles up to 75° with respect to the cyclotron beam. The monitoring beam integrator and the analyser recording counters could be simultaneously switched on. To keep

down the background of stray neutrons from the cyclotron tank itself, a thick wall of paraffin was used. All the targets were 'thick', i.e. thicker than the deuteron range in the target material.

§ 3. PROCEDURE

The current to the target was approximately 0·1 μa. throughout the experiments, and at each angle the neutron counts were recorded for two runs each of 33 μ-coulombs. Since, as was to be expected theoretically and was actually found in preliminary experiments, the neutron angular distribution was symmetrical about the direction of the incident deuteron beam, measurements were made on one side of this direction only. Despite the paraffin shielding there was still a considerable background of stray neutrons from the cyclotron tank, and so the following procedure was adopted to enable corrections to be made for this effect. Measurements had shown that the neutron yield from lead at 8 MeV. is very small, probably the major contribution being due to light element impurities, and an oxygen surface film. At each angle therefore the neutron yield was measured both from the target and from the lead flap, with equal irradiations. The whole of the neutron yield when the lead flap was being irradiated was taken to be a measure of the background effect, and was subtracted from the yield obtained when the target proper was irradiated. This background correction varied from approximately 2½% of the yield in the forward direction in the best cases (Li, Be, B) to approximately 15% in the worst case (O_2). Of this correction only about 30% was attributable directly to the yield from the lead flap. The energy of the deuteron beam was varied by putting lead foils of known thickness in front of the lead flap, so that the beam energy was lowered both when measuring the yield from the target, and while measuring the background effect.

§ 4. RESULTS

The measurements of the angular distribution are presented graphically in Figures 1 to 12. The relative intensities of recoil protons, and consequently of the emitted neutrons, are plotted as a function of the angle of emission of the neutrons with respect to the incident deuteron beam direction, the laboratory coordinate system. All of the distribution curves are characterized by the narrow forward peak of intensity, similar to that found in the measurements at higher energies. Since the amplitudes of the recoils were recorded on a 20-channel pulse it was possible to count all proton recoils with energies greater than a certain 'bias energy', obtainable from a calibration of the detecting equipment with α-particles of known energy.

All the measurements, except those of Figures 8 and 10, were taken with a bias corresponding to 1·5 MeV., this being the lowest bias which could be used without γ-ray pile-up making a significant contribution to the counting rate. The measurements of Figures 8 and 10 were recorded at a bias energy of 2 MeV. Figures 1, 2, 8 and 10 show the presence of subsidiary maxima, such as have been previously reported (Allen, Nechaj, Sun and Jennings 1949). From Figures 7, 8, 9 and 10 it is seen that in magnesium and aluminium the subsidiary maxima appear only at the higher bias. Almost all these elements which do not show subsidiary maxima at the lowest bias show the feature at high bias values. In certain elements (Figures 2, 8 and 10) the effect of lowering the beam energy by about 1 MeV. is

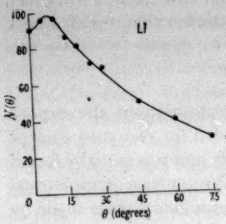

Figure 1.

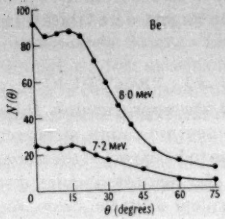

Figure 2.

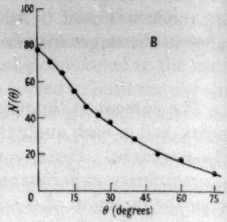

Figure 3.

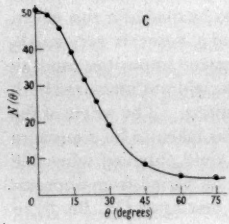

Figure 4.

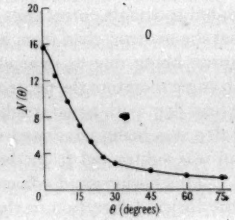

Figure 5.

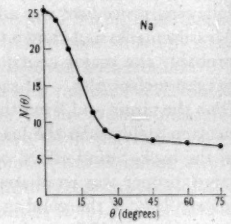

Figure 6.

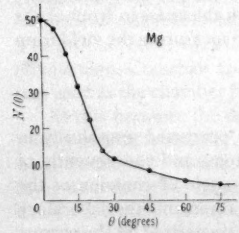

Figure 7.

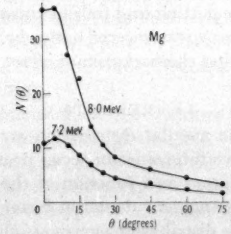

Figure 8.

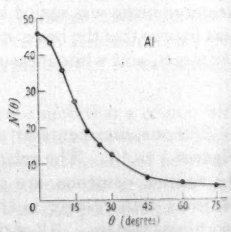

Figure 9.

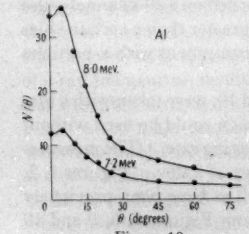

Figure 10.

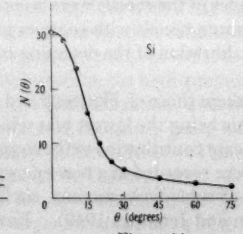

Figure 11.

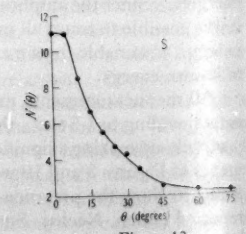

Figure 12.

In Figures 1 to 12 $N(\theta)$ is the relative number of neutrons emitted into a fixed solid angle making an angle θ with the incident deuteron beam, in the laboratory coordinate system.

shown. It can be seen that, although the yield is considerably reduced by this decrease in incident deuteron energy, the general form of the angular distribution function is unchanged. Interpretation of the results in any detail is difficult compared with recent (d, p) experiments (Holt and Young 1950, Rotblat 1950, Burrows, Gibson and Rotblat 1950), since neutron groups arising from different states are not resolved, and so the angular distribution measured is the cumulative effect of the distributions from many states. The presence of the forward peak however tends to add weight to the suggestions that even at low energies the major part of the (d, n) cross section can be attributed to a stripping process.

ACKNOWLEDGMENT

The author wishes to thank the Department of Scientific and Industrial Research for a Senior Research Award.

REFERENCES

ALLEN, A. J., NECHAJ, F. J., SUN, K. H., and JENNINGS, B., 1949, *Phys. Rev.*, **77**, 752.
ALLEN, K. W., and WILKINSON, D. H., 1948, *Proc. Camb. Phil. Soc.*, **44**, 581.
AMMIRAJU, P., 1949, *Phys. Rev.*, **76**, 1421.
BARSCHALL, H. H., and BETHE, H. A., 1947, *Rev. Sci. Instrum.*, **18**, 147.
BOHR, N., 1936, *Nature, Lond.*, **137**, 344.
BUNEMANN, O., CRANSHAW, T. E., and HARVEY, J. A., 1949, *Canad. J. Res.* A, **27**, 191-206.
BURROWS, H. B., GIBSON, W. M., and ROTBLAT, J., 1950, *Phys. Rev.*, **80**, 1095.
BUTLER, S. T., 1950 a, *Proceedings of Harwell Nuclear Physics Conference*, p. 54; 1950 b, *Phys. Rev.*, **80**, 1095.
DANCOFF, S. M., 1947 a, *Phys. Rev.*, **72**, 163; 1947 b, *Ibid.*, **72**, 1017.
FALK, C. E., CREUTZ, E., and SEITZ, F., 1948, *Phys. Rev.*, **74**, 1226; 1949, *Ibid.*, **76**, 322.
HELMHOLZ, A. C., MCMILLAN, E. M., and SEWELL, D. C., 1947, *Phys. Rev.*, **72**, 1003.
HOLT, J. R., and YOUNG, C. T., 1950, *Proc. Phys. Soc.* A, **63**, 833.
OPPENHEIMER, J. R., 1935, *Phys. Rev* , **47**, 845.
PEASLEE, D. C., 1948, *Phys. Rev.*, **74**, 1001, 1223.
POOL, M. L., 1938, *Phys. Rev.*, **53**, 707.
ROBERTS, R. B., and ABELSON, P. H., 1947, *Phys. Rev.*, **72**, 76.
ROTBLAT, J., 1950, *Proceedings of Harwell Nuclear Physics Conference*, p. 33.
SERBER, R., 1947, *Phys. Rev.*, **72**, 1008.

Deuteron Bombardment of Neon

BY R. MIDDLETON AND C. T. TAI
The Physical Laboratories, University of Liverpool

Communicated by H. W. B. Skinner; *MS. received 22nd March* 1951

ABSTRACT. Neon gas of normal isotopic constitution was bombarded by 7·8 MEV. deuterons from the Liverpool University cyclotron. Photographic plates were used as detectors, enabling the protons from the reactions ^{20}Ne(d, p) and ^{22}Ne(d, p) and alpha-particles from ^{20}Ne(d, α) and ^{22}Ne(d, α) to be studied, as well as a group of inelastically scattered deuterons.

§ 1. INTRODUCTION

THE reactions ^{20}Ne(d, p) and ^{22}Ne(d, p) have recently been studied by several authors (Elder, Motz and Davison 1947, Zucker and Watson 1950) but all in cases low bombarding energies have been used, and few proton groups have been observed. The reactions ^{20}Ne(d, α) and ^{22}Ne(d, α) have not

been previously investigated and are capable of giving information about the low-lying states of ^{18}F. By using the gas scattering technique of Chadwick, May, Pickavance and Powell (1944) it is possible to study the spectra and angular distributions of the charged particles emitted by ^{20}Ne and ^{22}Ne under deuteron bombardment. This paper describes measurements of the energy of the particles emitted by ^{20}Ne and ^{22}Ne when bombarded with 8 Mev. deuterons. The recent theory of Butler (1950) for stripping reactions makes the angular distributions for (d, p) reactions of use in determining the spins and parities of the states involved which will be discussed in a later paper.

§ 2. EXPERIMENTAL TECHNIQUE

The experimental method used has recently been described by Rotblat *et al.* (to be published) who give details of the scattering geometry. Spectroscopically pure neon of normal isotopic constitution was used at pressures between 10 and 20 cm. of mercury. Ilford C2 and E1 emulsions 100 μ thick were used as detectors, the plates being so located as to enable measurements to be made on the scattered particles over an angular range of 15° to 165° with respect to the deuteron beam, and at distances of 5 to 20 cm. from the scattering volume. Exposures of about 1 micro-coulomb of deuterons were found to give a suitable track density.

Observations of proton and alpha-particle tracks were made at various angles, using standard microscope technique. At each angle the horizontal projections of all the tracks were measured within an area of about 10 mm^2 containing some 3,000 tracks. A collective correction to determine the true range was applied to the track lengths at each angle, corresponding to the angle of incidence of the particles in the emulsion. The particles were identified by general appearances (e.g. grain density and end-scattering) and by comparison of the measurements with the calculated Q-values corresponding to the different angles.

§ 3. RESULTS

(i) *Proton Groups*

Range measurements have been made for ten angles, in the region from 30° to 150°. Figure 1 shows a typical histogram for the angle 110°. The mean ranges of particle groups and their half widths were deduced from the histogram by fitting gaussian curves to the individual groups. In the case of a weak group the results of several different angles were superposed to obtain the Q-value corresponding to that group. By comparing two such superposed histograms at fairly widely separated angles it was possible in most cases to detect an incorrect assignment of the neon isotope responsible for the group of particles.

The energies of the groups were obtained by using the range–energy relationship of Rotblat (to be published). A correction was applied to the range of a group according to the distance travelled by the particles through neon gas. For this purpose we assumed the value of the atomic stopping power of neon to be 1·250 for protons and deuterons, and 1·235 for alpha-particles (Livingston and Bethe 1937). Since the correction for most of the proton and deuteron groups is less than 0·1 Mev., any uncertainty in the value of the atomic stopping power has a negligible effect on the calculated Q-values.

The energy of the incident deuteron beam at the centre of the scattering volume was determined by measurement of the mean range of the elastically scattered

deuterons at various angles. The contribution to the elastically scattered peaks due to the presence of 10% of ^{22}Ne was subtracted on the assumption that the isotopes have equal differential scattering cross sections. At certain angles, see Figure 1, there is a proton group merged in the deuteron peak which was either subtracted or, if sufficiently small compared with the elastic peak, neglected. Since the position of the centre of the scattering volume changes slightly with the angle, there is also a corresponding change in the incident deuteron energy due to a slightly different path length through the neon gas. In Table 1 are listed the measured values of the incident deuteron energy as a function of angle, and also the values corrected to the 90° position. From the average of the latter values were deduced the deuteron energies at various angles which were later used for the calculation of Q-values.

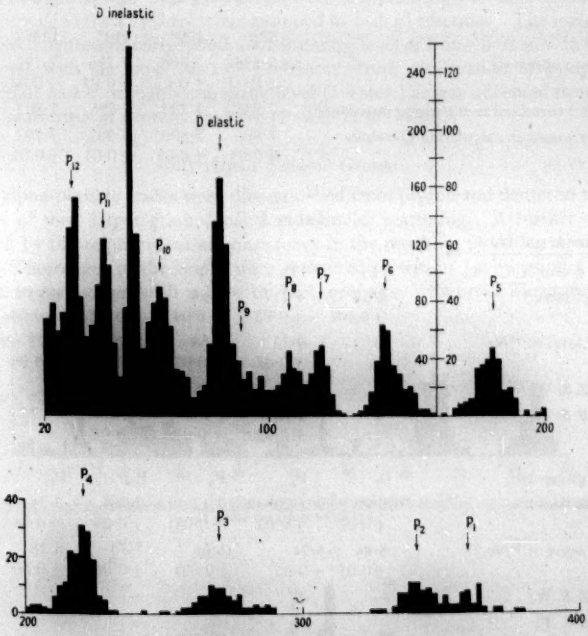

Figure 1. Histogram of proton and deuteron groups at 110°. (1 scale division = 1·7 μ)

With statistically well-established groups, it is possible to assign a particular proton group to ^{20}Ne or ^{22}Ne by comparing the Q-values calculated from the range at various angles. If the reaction has been assigned to the incorrect isotope a systematic deviation occurs in the Q-values of more than 0·1 to 0·15 MeV. in the complete angle range. In the case of such groups, this deviation is quite apparent, and immediate differentiation can be made between the isotopes possibly responsible for the reaction. The reaction responsible for groups statistically not well

established, having a probable error of the order of ±0·07 MeV., was determined by a method of superposition of histograms. This method of superposition has yielded fairly definite assignment of most groups, only one or two remaining uncertain.

Table 1. Incident Deuteron Energy as deduced from the Range of the elastically scattered Deuterons

Angle	30°	37½°	45°	52½°	60°
E_D (MeV.) observed	7·815 ±0·03	7·773 ±0·03	7·830 ±0·03	7·815 ±0·03	7·791 ±0·03
E_D (MeV.) corrected to scattering position 90°	7·800	7·785	7·823	7·809	7·786
E_D (MeV.) used in calculating Q-values	7·815 ±0·01	7·810 ±0·01	7·808 ±0·01	7·807 ±0·01	7·805 ±0·01

Angle	82½°	100°	110°	135°	150°
E_D (MeV.) observed	7·834 ±0·03	7·800 ±0·03	7·796 ±0·03	7·795 ±0·03	7·795 ±0·03
E_D (MeV.) corrected to scattering position 90°	7·835	7·799	7·798	7·802	7·809
E_D (MeV.) used in calculating Q-values	7·800 ±0·01	7·800 ±0·01	7·797 ±0·01	7·793 ±0·01	7·785 ±0·01

Table 2

(*a*) ^{20}Ne (d, p) ^{21}Ne

Proton group No.	P_1	P_2	P_3	P_4	P_5	P_6
Q-values (MeV.)	4·54 ±0·04	4·21 ±0·03	2·86 ±0·04	1·75 ±0·02	0·81 ±0·04	−0·17 ±0·02
Energy level of ^{21}Ne	0	0·33 ±0·05	1·68 ±0·07	2·79 ±0·05	3·73 ±0·06	4·71 ±0·05
Level (Z & W)	0	0·34	1·78	2·84	3·6	—
Level (F & T)	0	0·38 ±0·02	1·75 ±0·04	2·76 ±0·05	—	—

Proton group No.	P_7	P_8	P_9	P_{10}	P_{11}	P_{12}
Q-values (MeV.)	−0·90 ±0·02	−1·20 ±0·02	(−2·12 ±0·08)	−2·76 ±0·04	−3·74 ±0·04	−4·37 ±0·04
Energy level of ^{21}Ne	5·44 ±0·05	5·74 ±0·05	(6·66 ±0·09)	7·30 ±0·06	8·28 ±0·06	8·91 ±0·06
Level (Z & W)	—	—	—	—	—	—
Level (F & T)	—	—	—	—	—	—

(*b*) ^{22}Ne (d, p) ^{23}Ne

Proton group No.	1	2
Q-value (MeV.)	1·17 ±0·05	(−0·04 ±0·08)
Q-value (Z & W)	1·13	—

The values in parentheses are uncertain as to the responsible isotope. They are listed with the more likely isotope.

(Z & W) Zucker and Watson 1950; (F & T) French and Thomson 1951.

In Table 2 are listed the results obtained for the various proton groups with their probable errors, together with the recent results of other workers. Errors, other than statistical errors, may be attributed to: (i) an uncertainty in the incident deuteron energy of $\pm 0{\cdot}01$ Mev., (ii) an error in the range–energy relation of $\pm 0{\cdot}02$ Mev. (since our Q-values are averaged over different angles, different portions of the range energy relation are used, thus minimizing the error), (iii) an uncertainty in the position of the photographic plates, which will affect the Q-values by about $\pm 0{\cdot}002$ Mev. In the most unfavourable case, the sum of these errors would introduce an error of $\pm 0{\cdot}025$ Mev. in the Q-values of Table 2.

(ii) *Inelastically Scattered Deuterons*

In addition to the observed proton groups an inelastic deuteron group due to ^{20}Ne has been observed. The deuterons were identified by the large systematic error occurring in the Q-values when assigned to a (d, p) reaction. The inelastically scattered deuterons correspond with an energy level of $1{\cdot}66 \pm 0{\cdot}02$ Mev. in ^{20}Ne. This agrees with the level of $1{\cdot}64 \pm 0{\cdot}05$ Mev. from observation of γ-rays by Jelley (1950) and is probably the same level (1·4 Mev.) as was observed from the inelastic scattering of protons by ^{20}Ne (Powell *et al.* 1940).

(iii) *Alpha-Particle Groups*

The alpha-particle tracks were distinguished from proton and deuteron tracks by virtue of their larger grain density and smaller scattering. A further check was given by the requirement of consistency in the resulting Q-values at various angles. The ranges of the tracks were measured to within $\frac{1}{4}\mu$ by using a 96× objective in conjuction with a 10× or 15× eyepiece. Figure 2 illustrates two

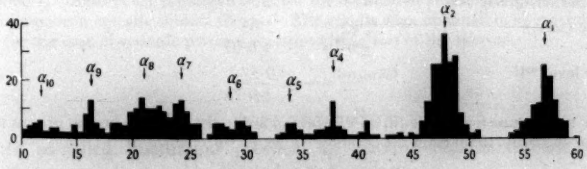

Figure 2 (*a*). Histogram of alpha-particles at 35°.
(1 scale division = 0·83 μ)

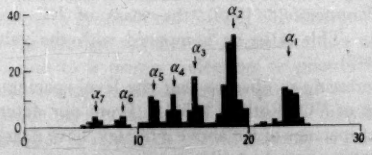

Figure 2 (*b*). Histogram of alpha-particles at 132½°.
(1 scale division = 1 μ)

typical histograms (35° and 132½°). The alpha-particle tracks were measured for ten angles and a similar analysis applied to the histograms as for the case of the protons. In the case of the alpha-particles the assignment of the responsible neon

isotope is easier, since the corresponding difference in the Q-values for different angles is larger. The contribution of ^{22}Ne was found to be very weak, and at many angles unobservable, as was also the case with the protons.

The correction due to the stopping power of neon is larger than that for protons and deuterons. An intrinsic check on the adopted value of the atomic stopping power of neon, namely 1·235, was obtained by comparing the calculated energies for alpha-particles belonging to the same group, but having traversed different path lengths in the neon. The Q-values obtained are listed in Table 3. None of the groups listed from the ^{20}Ne(d, α) reactions has previously been observed.

Table 3

(*a*) ^{20}Ne (d, α) ^{18}F

Alpha-particle group No.	α_1	α_2	α_3	α_4	α_5
Q-value (MeV.)	2·78 ± 0·02	1·73 ± 0·02	0·95 ± 0·02	0·58 ± 0·05	0·17 ± 0·04
Energy level ^{18}F	Ground	1·05 ± 0·03	1·83 ± 0·05	2·20 ± 0·05	2·61 ± 0·05

Alpha-particle group No.	α_6*	α_7	α_8	α_9	α_{10}
Q-value (MeV.)	−0·45 ± 0·07	−1·14 ± 0·03	−1·64 ± 0·10	−2·23 ± 0·08	−2·83 ± 0·10
Energy level ^{18}F	3·23 ± 0·07	3·92 ± 0·04	4·42 ± 0·10	5·01 ± 0·08	5·61 ± 0·10

* Group may be a doublet.

(*b*) ^{22}Ne (d, α) ^{20}F

Alpha-particle group No.	1	2
Q-value (MeV.)	2·62 ± 0·10	2·05 ± 0·07
Energy level ^{20}F	Ground	0·57 ± 0·13

The two groups from ^{22}Ne (d, α) ^{20}F correspond to the first two proton groups observed by Allen and Rall (1950) from the reaction ^{19}F (d, p) ^{20}F.

By assuming that the observed alpha-particles of longest range correspond to the transition to the ground state of ^{18}F, and utilizing the known masses of ^{20}Ne (Mattauch and Flammersfeld 1949), the mass of ^{18}F was calculated to be 18·00672 ± 0·00006. This is to be compared with the value 18·0065 ± 0·0006 given by Bethe (1947).

Finally it is interesting to observe that the level spacing of ^{18}F bears a close resemblance to that of ^{17}O (Rotblat 1950). From our determinations it would appear that the level spacings of ^{18}F above 2·60 MeV. have nearly the same value, as for ^{17}O above 3·88 MeV., namely 0·60 MeV.

ACKNOWLEDGMENTS

The authors wish to express their thanks to Dr. J. R. Holt for helpful discussion. They also thank the University of Liverpool for the award of Fellowships which enabled this work to be carried out.

REFERENCES

ALLEN, R. C., and RALL, W., 1950, *Phys. Rev.*, **78**, 337.
BETHE, H. A., 1947, *Elementary Nuclear Theory* (New York : Wiley and Sons).
BUTLER, S. T., 1950, *Report on Harwell Conference, Sept.* 1950, p. 54, also *Phys. Rev.*, **80**, 1095.
CHADWICK, J., MAY, A. N., PICKAVANCE, T. G., and POWELL, C. F., 1944, *Proc. Roy. Soc.* A, **183**, 1.
ELDER, F. K., Jr., MOTZ, H. T., and DAVISON, P. W., 1947, *Phys. Rev.*, **71**, 917.
FRENCH, A. P., and THOMSON, D. M., 1951, *Proc. Phys. Soc.* A, **64**, 203.
JELLEY, J. V., 1950, *Proc. Phys. Soc.* A, **64**, 538.
LIVINGSTON, S. M., and BETHE, H. A., 1937, *Rev. Mod. Phys.*, **9**, 272.
MATTAUCH, J., and FLAMMERSFELD, A., 1949, *Z. Naturforsch.* (Special Issue).
POWELL, C. F., MAY, A. N., CHADWICK, J., and PICKAVANCE, T. G., 1940, *Nature, Lond.*, **145**, 893.
ROTBLAT, J., 1950, *Report on Harwell Conference, Sept.* 1950, p. 33.
ZUCKER, A., and WATSON, W. W., 1950, *Phys. Rev.*, **78**, 14.

Further Results on the Fluctuation Problem in Electron–Photon Cascade Shower Theory and the Probability Distribution Function

BY H. MESSEL

School of Theoretical Physics, Dublin Institute for Advanced Studies

Communicated by W. Heitler; *MS. received* 1*st May* 1951

ABSTRACT. Results are presented both for the fluctuation and distribution of electrons in electron–photon cascade shower theory. The results were obtained in approximation A and are for the case of a single primary electron giving rise to the shower.

§ 1. INTRODUCTION

THE so-called fluctuation problem in electron–photon cascade shower theory may be roughly divided into two parts:

(*a*) If we consider an electron (or photon) of energy E_0 impinging on a layer of material of thickness t, what is the probability that exactly N electrons (or photons) with energies greater than $E=\epsilon E_0$ will emerge?

(*b*) If we know the *average* number of particles above an energy $E=\epsilon E_0$ at any given depth t, due to a primary electron or photon of energy E_0, what fluctuations from this average number may we expect?

In order to answer (*a*) knowledge of the actual distribution function for electron–photon cascades is required. Until recently it was also believed that (*b*) could not be answered without solving (*a*) first (Arley 1949). This, however, has not proved to be the case.

Jánossy (1950) has shown that a cascade could be represented by the following set of equations, when ionization loss by electrons is neglected.

$$\frac{\partial G^{(i)}(\epsilon,t)}{\partial t}=\int_0^1\{G^{(i)}(\epsilon/(1-\epsilon_1),t)G^{(3-i)}(\epsilon/\epsilon_1,t)-G^{(i)}(\epsilon,t)\}w^{(i)}(\epsilon_1)\,d\epsilon_1 \quad i=1,2 \qquad \ldots\ldots(1)$$

where the index i refers to the nature of the primary: $i=1$, electron primary, $i=2$, photon primary, and $G^{(i)}$ is the generating function

$$G^{(i)}(\epsilon, U_1, U_2, t) = \sum_{n_1, n_2=0}^{\infty} \Phi^{(i)}(\epsilon, n_1, n_2, t) U_1^{n_1} U_2^{n_2} \qquad \ldots\ldots(2)$$

with $\Phi^{(i)}(\epsilon, n_1, n_2, t)$ the probability that at a depth t a primary of energy E_0 has given rise to n_1 electrons and n_2 photons with energies greater than $E=\epsilon E_0$ and an arbitrary number of electrons and photons with energies less than E. Note that in equation (1) we have omitted the variables U_1 and U_2 for convenience only.

In principle equation (1) should be capable of being evaluated by numerical methods, since the initial conditions are known, and thus, the answer to (*a*) obtained. However, this has proved to be a very difficult task and to date no satisfactory solution has been obtained.

Bhabha (1950), Bhabha and Ramakrishnan (1950) and Scott (private communication*) have also given the solution of the fluctuation problem a good deal of attention. They set up the fundamental equations for the distribution function in a manner different from that of Jánossy, but made no essential progress in their solution.

Recently Jánossy and Messel (1950, hereafter referred to as I) took a step forward. They gave analytical solutions and fairly extensive numerical results for the fluctuations in number about the average. The correlation between electrons and photons in a shower has also been worked out, and numerical results have been given. That work has confirmed quantitatively what had long been suspected, viz. that on either side of the cascade maximum the fluctuations deviate wildly from those which would be expected if the distribution in number were Poissonian. It should be pointed out that the solutions obtained in I were in approximation A, i.e. when ionization loss by electrons was neglected. The computations even in this approximation were extremely heavy and one wonders what hope there is of obtaining numerical results when ionization loss is included (approximation B). In fact the obtaining of an analytical solution in approximation B for the second moments of the distribution is most forbidding—especially when one considers that we have not as yet obtained a completely satisfactory method for obtaining values for the average numbers in approximation B!

The results as presented in I were of value for interpreting the physical behaviour of the fluctuations, but of little direct use to the experimentalist. We shall present in a Table below, numerical values of the relative fluctuation, which may be utilized more directly.

In view of the fact that there is little hope of immediately obtaining a solution for the electron–photon distribution function, we have decided to make use of an assumption first introduced by Arley (1949). He assumed that the distribution function could be well approximated by the Polya distribution (discussed below), which contains, essentially, two parameters, the first and second moments. Since we now have the values of the second moments it is directly possible, using the above assumption, to evaluate the distribution function. This is done below. (Note that Arley found values for the distribution function also; however, in his case he did not have the values of the second moments and had to approximate them.) We shall only present results for the case of a single primary electron producing electrons, since this is the case for which the second moments have been evaluated.

* The author is indebted to Dr. W. T. Scott for communicating his results prior to publication.

§2. THE POLYA DISTRIBUTION

The Polya distribution function expressing the probability of finding exactly N particles with energies greater than ϵE_0 at a depth t is given by

$$P(\epsilon, N, t) = \frac{1.(1+b)\ldots\{1+(N-1)b\}}{N!}\left(\frac{\overline{N}}{1+b\overline{N}}\right)^N P(\epsilon, 0, t)$$

$$(b \geqslant 0,\ \overline{N} \geqslant 0 \text{ and } N = 1, 2, \ldots.) \qquad \ldots\ldots(3)$$

with

$$P(\epsilon, 0, t) = (1+b\overline{N})^{-1/b}. \qquad \ldots\ldots(3\,a)$$

In our case $\overline{N}$ expresses the average number of electrons with energies greater than ϵE_0 at a depth t cascade units due to a single incident primary electron of energy E_0. The parameter b is expressed by

$$b = (\overline{N^2} - \overline{N}^2 - \overline{N})/\overline{N}^2. \qquad \ldots\ldots(3\,b)$$

One obtains the Poisson distribution function by simply allowing the parameter b to approach zero, thus

$$P(\epsilon, 0, t) \underset{b\to 0}{\to} \exp(-\overline{N}), \qquad P(\epsilon, N, t) \underset{b\to 0}{\to} \frac{\overline{N}^N \exp(-\overline{N})}{N!}. \qquad \ldots\ldots(4)$$

Note that for a Poisson distribution the relative fluctuation, defined as $\delta = (\overline{N^2} - \overline{N}^2)^{1/2}/\overline{N}$ is simply equal to $\overline{N}^{-1/2}$. The significance of the parameter b appearing in the Polya distribution is now obvious. It expresses the difference between the square of the relative fluctuation for the actual distribution and that for a Poissonian one.

If one knows both $\overline{N}$ and b then the distribution function $P(\epsilon, \overline{N}, t)$, given by (3), may be immediately evaluated. The value of $\overline{N}$ may be obtained from the extensive tables given by Jánossy and Messel (1951) and the value of b found using the results given in I.

§3. RESULTS

In Table 1 we have tabulated $\overline{N}, b, -1/b, 1+b\overline{N}$ and the relative fluctuation $\delta = (\overline{N^2} - \overline{N}^2)^{1/2}/\overline{N}$ as functions of the depth t measured in cascade units and the energy ratio expressed by $-\log\epsilon$. At a cascade maximum and its neighbourhood the value of the parameter b takes on negative values. In these cases we have omitted to give the value of b. It may be pointed out here that the fact that b takes on negative values proves by itself that the true distribution function is not exactly a Polya distribution, for if it were, then in all cases b would necessarily be greater than or equal to zero.

In Table 2 we have evaluated the Polya distribution function using Table 1 for the case $-\log\epsilon = 2{\cdot}0$. The values for a Poisson distribution are also given for comparison. For the cases in which $b<0$ we could use only the Poisson distribution function. This, however, should not bring in serious errors for, as shown in I, the fluctuations at the cascade maximum where $b<0$ are nearly Poissonian.

The value of $P(\epsilon, N, t)$ for $-\log\epsilon = 3{\cdot}0$, $4{\cdot}0$ and $6{\cdot}0$ and any N and t may also easily be obtained by using Table 1 and formula (3).

Figure 1 gives a plot of the relative fluctuation δ against the depth t for $-\log\epsilon = 2{\cdot}0$, $3{\cdot}0$, $4{\cdot}0$ and $6{\cdot}0$. We have also plotted the relative fluctuation assuming the distribution to be Poissonian, for comparison. Figure 2 gives the probability distribution curve for both a Polya and a Poisson distribution, for

Table 1. Showers initiated by a Single Electron of Energy E_0

The average number $\overline{N}$ of electrons with energies greater than ϵE_0, the relative fluctuation $\delta=(\overline{N^2}-\overline{N}^2)^{1/2}/\overline{N}$, the Polya parameter $b=(\overline{N^2}-\overline{N}^2-\overline{N})/\overline{N}^2$, and combinations of the above quantities useful in computing Table 2 are given as functions of the depth t measured in cascade units and $-\log\epsilon$.

t	$-\log\epsilon$	2·0	3·0	4·0	6·0
	$\overline{N}$	5·861	17·140	38·994	139·00
	b	—	0·072	0·128	0·189
2	$-1/b$	—	−13·908	−7·813	−5·291
	$1+b\overline{N}$	—	2·234	5·999	27·320
	δ	0·383	0·370	0·392	0·444
	$\overline{N}$	7·482	32·961	103·04	590·20
	b	—	0·040	0·089	0·151
3	$-1/b$	—	−24·876	−11·249	−6·623
	$1+b\overline{N}$	—	2·324	10·156	90·271
	δ	0·277	0·265	0·314	0·391
	$\overline{N}$	7·430	47·643	198·15	1762
	b	—	0·008	0·055	0·122
4	$-1/b$	—	−122·40	−18·083	−8·197
	$1+b\overline{N}$	—	1·389	11·953	216·09
	δ	0·264	0·171	0·245	0·351
	$\overline{N}$	6·295	56·624	306·90	4102
	b	—	—	0·033	0·096
5	$-1/b$	—	—	−30·211	−10·417
	$1+b\overline{N}$	—	—	11·161	394·89
	δ	0·318	0·074	0·191	0·310
	$\overline{N}$	4·797	58·210	403·65	7925
	b	—	—	0·013	0·070
6	$-1/b$	—	—	−76·336	−14·286
	$1+b\overline{N}$	—	—	6·260	555·82
	δ	0·429	0	0·124	0·265
	$\overline{N}$	3·404	53·827	468·81	13183
	b	0·026	—	—	0·050
7	$-1/b$	−41·300	—	—	−20·000
	$1+b\overline{N}$	1·088	—	—	660·20
	δ	0·566	0·086	0·046	0·244
	$\overline{N}$	2·291	45·814	490·91	19454
	b	0·101	0·008	—	0·032
8	$-1/b$	−9·901	−122·25	—	−31·250
	$1+b\overline{N}$	1·230	1·375	—	623·56
	δ	0·732	0·173	0	0·179

t	$-\log\epsilon$	2·0	3·0	4·0	6·0
	$\overline{N}$	1·483	36·644	474·24	25942
	b	0·186	0·039	—	0·020
9	$-1/b$	−5·376	−25·641	—	−50·000
	$1+b\overline{N}$	1·276	2·430	—	519·86
	δ	0·927	0·257	0	0·141
	$\overline{N}$	0·933	27·733	428·55	31·696
	b	0·390	0·088	0·014	0·010
10	$-1/b$	−2·564	−11·351	−71·429	−100·000
	$1+b\overline{N}$	1·363	3·442	7·014	317·97
	δ	1·208	0·352	0·128	0·100
	$\overline{N}$	0·344	14·158	298·54	38·548
	b	1·145	0·203	0·068	—
12	$-1/b$	−0·873	−4·926	−14·663	—
	$1+b\overline{N}$	1·394	3·880	21·369	—
	δ	2·012	0·523	0·268	0·005
	$\overline{N}$	0·119	6·412	177·01	37·411
	b	3·554	0·347	0·161	0·005
14	$-1/b$	−0·282	−2·882	−6·211	−200·000
	$1+b\overline{N}$	1·423	3·224	29·482	188·06
	δ	3·464	0·709	0·409	0·071
	$\overline{N}$	0·039	2·673	93·111	30·550
	δ	11·985	0·557	0·286	0·040
16	$-1/b$	−0·083	−1·795	−3·497	−25·000
	$1+b\overline{N}$	1·469	2·488	29·633	1223
	δ	6·140	0·965	0·564	0·200
	$\overline{N}$	0·012	1·042	44·566	21·777
	b	41·639	1·000	0·409	0·103
18	$-1/b$	−0·024	−1·000	−2·445	−9·709
	$1+b\overline{N}$	1·516	2·041	19·226	2244
	δ	11·045	1·400	0·657	0·321
	$\overline{N}$	0·004	0·385	19·861	13·932
	b	155·850	2·212	0·551	0·190
20	$-1/b$	−0·006	−0·452	−1·815	−5·263
	$1+b\overline{N}$	1·592	1·852	11·952	2648
	δ	20·469	2·193	0·776	0·436

Table 2. The Probability Distribution Function $-\log P(\epsilon, N, t)$

giving the negative logarithm of the probability of a shower containing exactly N electrons with energies greater than 1/100 of the primary energy, at a depth t cascade units. The shower was initiated by a single primary electron. We have also given the results for a Poisson distribution, for comparison. (The top line of each group is the Polya and the lower line the Poisson distribution.)

N \ t	2	3	4	5	6	7	8	9	10	12	14	16	18	20
0	2·545	3·249	3·227	2·734	2·083	1·513	0·890	0·569	0·345	0·126	0·0432	0·0139	0·0043	0·0012
						1·478	0·995	0·644	0·405	0·149	0·0517	0·0169	0·0052	0·0017
1	1·777	2·375	2·356	1·935	1·402	1·017	0·620	0·504	0·509	0·734	1·121	1·590	2·106	2·601
						0·946	0·635	0·473	0·435	0·613	0·976	1·426	1·926	2·400
2	1·310	1·802	1·786	1·437	1·022	0·812	0·609	0·665	0·832	1·311	1·841	2·353	2·879	3·307
						0·715	0·576	0·603	0·766	1·377	2·202	3·136	4·148	5·099
3	1·020	1·405	1·392	1·115	0·819	0·772	0·736	0·940	1·223	1·879	2·487	3·009	3·532	3·888
						0·661	0·693	0·909	1·274	2·318	3·603	5·022	6·546	7·974
4	0·854	1·134	1·123	0·918	0·740	0·846	0·953	1·284	1·654	2·441	3·100	3·619	4·135	4·420
						0·731	0·935	1·340	1·906	3·383	5·130	7·033	9·069	10·974
5	0·785	0·958	0·951	0·818	0·758	1·006	1·235	1·676	2·109	3·001	3·694	4·204	4·711	4·923
						0·898	1·274	1·868	2·635	4·546	6·753	9·141	11·688	14·071
6	0·795	0·863	0·858	0·797	0·855	1·236	1·565	2·103	2·582	3·560	4·277	4·774	5·270	5·409
						1·144	1·692	2·475	3·443	5·787	8·456	11·328	14·387	17·247
7	0·872	0·834	0·832	0·843	1·019	1·523	1·934	2·558	3·068	4·116	4·851	5·338	5·818	5·882
						1·451	2·177	3·149	4·318	7·096	10·225	13·582	17·153	20·490
8	1·007	0·863	0·864	0·947	1·241	1·858	2·335	3·034	3·564	4·672	5·418	5·888		
						1·828	2·720	3·880	5·252	8·462	12·053	15·894		
9	1·193	0·943	0·948	1·103	1·514	2·235	2·762	3·526	4·068	5·227	5·982			
						2·250	3·315	4·664	6·236	9·880	13·932			
10	1·425	1·069	1·077	1·304	1·833	2·648	3·211	4·034	4·578	5·781				
						2·718	3·954	5·492	7·266	11·344				
11	1·699	1·236	1·247	1·546	2·194	3·094	3·679	4·554	5·094					
						3·228	4·636	6·363	8·338					
12	2·010	1·442	1·455	1·826	2·592	3·568	4·164	5·084	5·614					
						3·775	5·355	7·271	9·447					
13	2·356	1·681	1·698	2·141	3·025	4·069	4·663	5·623						
						4·357	6·109	8·214						
14	2·734	1·954	1·973	2·488	3·490	4·593	5·175							
						4·971	6·895							
15	3·142	2·256	2·278	2·865	3·985	5·139	5·698							
						5·615	7·711							
16	3·578	2·586	2·612	3·271	4·508	5·705								
						6·287								
17	4·041	2·942	2·971	3·702	5·058									
18	4·528	3·323	3·355	4·158	5·632									
19	5·039	3·728	3·763	4·638	6·230									
20	5·572	4·155	4·193	5·140	6·850									

the case of $-\log\epsilon=2{\cdot}0$ and $t=8$ cascade lengths. Finally in Figure 3 we have plotted the logarithm of the ratio of the probability of finding N particles with energies greater than ϵE_0 at a depth t for a Polya and a Poisson distribution. Curves are given for $t=7$, 8, 10 and 14 cascade lengths.

§4. DISCUSSION OF RESULTS

The outstanding feature of the curves in Figure 1 is the extreme rapidity with which the relative fluctuation δ increases once the cascade maximum has been passed. We note in comparison the rather slow increase (as $\overline{N}^{-1/2}$) of δ for

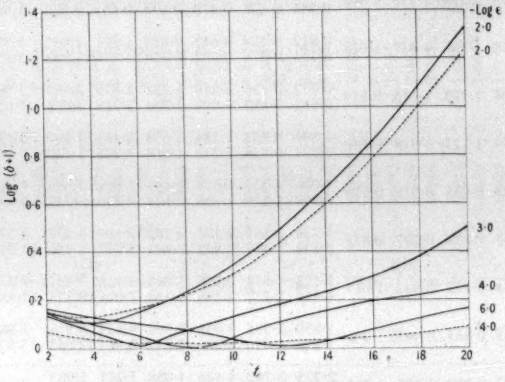

Figure 1. A plot of the relative fluctuation $\delta=(\overline{N^2}-\overline{N}^2)^{1/2}/\overline{N}$ for the case of a single primary electron of energy E_0 producing electrons at a depth t cascade units with energies greater than $E=\epsilon E_0$. (Log $(\delta+1)$ is plotted for convenience.) The full curves refer to the true relative fluctuation, the dotted curves to the relative fluctuations if the distribution were Poissonian. The minimum of each curve corresponds to the cascade maximum.

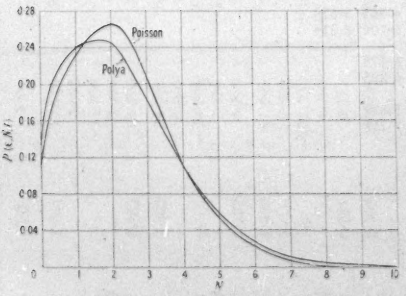

Figure 2. The probability distribution function $P(\epsilon, N, t)$ for the case of $-\log\epsilon=2{\cdot}0$ and $t=8$ cascade units. For comparison the curve for the corresponding Poisson distribution is also given.

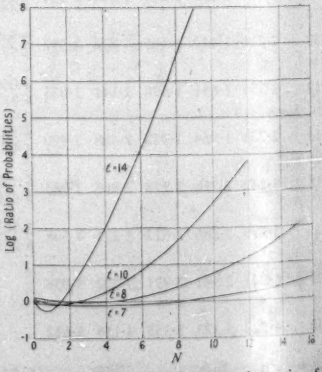

Figure 3. The logarithm of the ratio of finding N particles with energies greater than $E=\epsilon E_0$ at a depth t cascade units, for our distribution function (Polya) and a Poisson distribution. In all cases $-\log\epsilon=2{\cdot}0$.

a Poisson distribution. The above behaviour brings out forcibly the fact that the probability of finding two particles at a great depth is of the same order of magnitude as the probability of finding one particle. This behaviour had already been pointed out by Jánossy and Messel.

Both Figures 2 and 3 and Table 2 bring out the above feature more directly: that is, the probability distribution function for electron–photon cascades beyond the cascade maximum is heavily skewed in comparison with the Poisson distribution. For example, the probability of finding two electrons with energies greater than one hundredth of the primary electron energy at a depth of 18 cascade units is approximately 1·3 in 1,000 whereas for a Poisson distribution the probability is of the order of 7 in 100,000. The average number of electrons expected under these conditions is only 0·012. For larger values of N and greater t the difference is further accentuated.

The amount of confidence one can have, from a quantitative point of view, in our results depends solely on how well the Polya distribution function approximates to the true electron–photon distribution function. We recall the well-known theorem in statistics that in principle, if all the moments of the distribution are known, then the distribution function itself is fixed. Note that the Poisson distribution utilizes the first moments only. The Polya distribution contains both the first and second moments. From a qualitative standpoint our results do throw a good deal of light on the behaviour of electron showers and should be of value for the interpretation of these showers, observed in cloud chambers and photographic plate work.

The values of the relative fluctuation δ may be treated with confidence in approximation A.

ACKNOWLEDGMENTS

My thanks are due to Professor E. Schrödinger for continued encouragement to carry out the above work and to the Dublin Institute for Advanced Studies for provision of a Research Scholarship.

REFERENCES

Arley, N., 1949, *On the Theory of Stochastic Processes* (New York : Wiley and Sons).
Bhabha, H. J., 1950, *Proc. Roy. Soc.* A, **202,** 301.
Bhabha, H. J., and Ramakrishnan, A., 1950, *Proc. Indian Acad. Sci.*, **32,** 141.
Jánossy, L., 1950, *Proc. Phys. Soc.* A, **63,** 241.
Jánossy, L., and Messel, H., 1950, *Proc. Phys. Soc.* A, **63,** 1101; 1951, *Proc. Roy. Irish Acad.* A, **54,** 217.

On the Theory of Free Electron Ferromagnetism

By A. B. LIDIARD

Department of Theoretical Physics, King's College, London

Communicated by C. A. Coulson; MS. received 19th March 1951

ABSTRACT. A calculation has been made of the ferromagnetic properties of a system of electrons using plane wave functions and Bloch exchange integrals. Our results show that below a critical temperature T_c the spontaneous magnetization decreases slowly with increasing temperature. At T_c the magnetization drops suddenly to zero as if a change of phase were taking place and there is therefore a latent heat of demagnetization at this temperature. Above T_c the model is paramagnetic. The reasons for the differences between the results and those obtained by experiment and on Stoner's theory of collective electron ferromagnetism are discussed, and the possibility that they may be due to the neglect of positional correlations among the electrons is considered.

§1. INTRODUCTION

Before Stoner (1938, 1939a) introduced his theory of collective electron ferromagnetism there was no general scheme sufficiently flexible to account for the behaviour of the ferromagnetic metals and their alloys in any but qualitative terms. For example, the Heisenberg (1928) theory, although it explained the existence of ferromagnetism and the existence of the Curie point, could not (without *ad hoc* assumptions) be made to account for the non-integral numbers of spins per atom which the observed values of saturation moment at absolute zero required. Nor could it explain the departures of the susceptibility above the Curie point from the Curie–Weiss law. Stoner, using Fermi–Dirac statistics, calculated the properties of an assembly of electrons in a parabolic band when their exchange interactions could be represented by a term of the form $-N\boldsymbol{k}\theta'\zeta^2/2$ in the total free energy; ζ is the relative magnetization of the electron assembly, $(0 \leqslant \zeta \leqslant 1)$, N the total number of electrons, $\boldsymbol{k}$ is Boltzmann's constant and θ' is a constant which is supposed to be independent of temperature. With the further assumption that the holes at the top of a nearly filled band were magnetically and thermally equivalent to electrons in a parabolic band, this theory was able to explain the above facts which found no explanation on the Heisenberg theory. The scheme has recently been successfully developed by Wohlfarth (1949a, b) in a study of alloys of the ferromagnetic metals. But although successful in its application the basis of the theory is not above discussion (Van Vleck 1945). In particular, there is at the moment no rigorous theoretical foundation for the representation of the total exchange energy by an expression of the form used by Stoner; this can only be regarded as justified pragmatically by the success of the theory.

In the present paper we shall adopt a different approach; we shall calculate the ferromagnetic properties of an assembly of free electrons systematically using the exchange energies given by the quantum mechanics of this system. Our results show that below a critical temperature T_c the magnetization ζ decreases slowly from unity with increasing temperature. At T_c, ζ drops suddenly to zero as if a change of phase were taking place; there is therefore a latent heat of

demagnetization at $T = T_c$. Real ferromagnetics do not behave in this way, the magnetization falling steadily to zero at the Curie temperature. (This is not true for some alloys of manganese with the Group V elements phosphorus, arsenic and bismuth, which do behave in the same way as our hypothetical model; it is likely, however, that in this case the behaviour is due to other effects.) Our results are thus very different from those of Stoner's theory. However, using the same model as we have done, Wohlfarth (1949 c) has attempted to justify Stoner's assumption that the total exchange energy is $-N\boldsymbol{k}\theta'\zeta^2/2$ but his considerations were confined to the behaviour at absolute zero and thus failed to disclose a strong temperature dependence of the exchange energy.

Now this free electron model is relevant to a discussion of the ferromagnetism in iron, cobalt and nickel because of the equivalence to it of the holes in the nearly filled 3d bands of these metals. It is not directly applicable in the way it would be if the magnetically effective electrons were those in the almost empty 4s bands. However, the model is only ferromagnetic under certain conditions (discussed in § 3) and when these are not satisfied we should expect to be able to apply it to the nearly free valence electrons in, say, sodium. (Calculations by Von der Lage and Bethe (1947) have shown how closely the wave functions and kinetic energies of the 3s electrons in sodium approximate to those for perfectly free electrons.) This has been done by Wohlfarth (1950) who has shown that the free electron model only gives a specific heat of the same order as the observed electronic specific heat provided we make a correction to the exchange energy for the correlation effect: otherwise it is very much less than is observed. It is possible in our case also that inclusion on the correlation correction would give better agreement with experiment and, in particular, make the change from the ferromagnetic to the paramagnetic state less abrupt. Unfortunately it is extremely difficult to estimate the changes which the inclusion of a correction for electron correlation will bring about. Further consideration is being given to this problem.

§ 2. THE ONE-ELECTRON APPROXIMATION AND CALCULATION OF THE FREE ENERGY

It is well known (Seitz 1940) that on the basis of the *one-electron approximation* in the theory of metals, the energy of an assembly of electrons is

$$U = \frac{-h^2}{8\pi^2 m}\sum_n \int \psi_n^*(\mathbf{r})\nabla^2\psi_n(\mathbf{r})\,d\mathbf{r} + \sum_n \int \psi_n^*(\mathbf{r})V(\mathbf{r})\psi_n(\mathbf{r})\,d\mathbf{r}$$
$$+ \sum_{m\neq n}\iint \frac{e^2}{r_{12}}|\psi_n(\mathbf{r}_1)|^2\,|\psi_m(\mathbf{r}_2)|^2\,d\mathbf{r}_1\,d\mathbf{r}_2$$
$$- \sum_{m\neq n}{}'\iint \frac{e^2}{r_{12}}\psi_n^*(\mathbf{r}_1)\psi_m^*(\mathbf{r}_2)\psi_n(\mathbf{r}_2)\psi_m(\mathbf{r}_1)\,d\mathbf{r}_1\,d\mathbf{r}_2. \quad \ldots\ldots(2.1)$$

Here $\psi_n(\mathbf{r})$ is the space dependent part of the wave function for state n of an electron, and $V(\mathbf{r})$ is the potential energy of an electron at $\mathbf{r}$ due to the ion cores of the lattice. The summations in the first two terms are over all occupied electron states n, and in the third term over all pairs of occupied states. These three terms are respectively the kinetic energy of the electrons and the Coulomb energy of the electrons with the lattice and among themselves. In the fourth

term, which is the exchange energy, the summation is over all pairs of states occupied by electrons with mutually parallel spins.

Now for perfectly free electrons the wave functions ψ are of the form $\psi = V^{-1/2}\exp(i\mathbf{k}.\mathbf{r})$, where V is the volume of the metal and $\mathbf{k}$ is the momentum vector. The integral in the first term in equation (2.1) is then just k^2. The integrals in the second and third terms are independent of the states for which they are taken and thus these two terms in U are independent of any change in the occupation of states. That is, we can ignore the Coulomb energy in considering changes in magnetization or changes brought about by temperature. The exchange integral between an electron in state $\mathbf{k}$ and another (with parallel spin in state $\mathbf{k}'$ was first evaluated by Bloch (1928) who obtained

$$J_{\mathbf{k},\mathbf{k}'} = \frac{4\pi e^2}{V}\frac{1}{|\mathbf{k}-\mathbf{k}'|^2}. \qquad \ldots\ldots(2.2)$$

The absence of an exchange integral between two states of opposite spin allows us to consider our assembly of N electrons as two independent sub-assemblies, one of n_1 parallel spins, the other of n_2 anti-parallel spins. The relative magnetization ζ is defined by

$$\zeta = (n_1 - n_2)/N. \qquad \ldots\ldots(2.3)$$

Hence, if we can find the free energy of the parallel spins F_1 say, and thus also of the anti-parallel spins F_2, the free energy of the whole assembly is $F(\zeta) = F_1 + F_2$. The equilibrium magnetization is that for which $F(\zeta)$ has its least value. The problem, then, is the calculation of the free energy for an assembly of electrons with individual kinetic energies $h^2\mathbf{k}^2/8\pi^2 m$ and exchange energies given by (2.2), where only one electron can be assigned to each allowed value of $\mathbf{k}$. These allowed values are determined by the Born cyclic condition, which requires all components of $\mathbf{k}$ to be integral multiples of $2\pi/V^{1/3}$. If we assign to each state $\mathbf{k}$ a distribution number $\phi(\mathbf{k})$ which can be zero or unity only, then the energy of any particular configuration is

$$U = \sum_{\mathbf{k}} \frac{h^2}{8\pi^2 m} k^2 \phi(\mathbf{k}) - \frac{1}{2}\sum_{\mathbf{k}}\sum_{\mathbf{k}'\neq\mathbf{k}} \frac{4\pi e^2}{V}\frac{\phi(\mathbf{k})\phi(\mathbf{k}')}{|\mathbf{k}-\mathbf{k}'|^2}, \qquad \ldots\ldots(2.4)$$

with

$$\Sigma_{\mathbf{k}}\phi(\mathbf{k}) = n_1. \qquad \ldots\ldots(2.5)$$

The summations are over all allowed $\mathbf{k}$ vectors; for a cubical volume V these form a simple cubic lattice of points in $\mathbf{k}$-space. In principle we can now obtain the free energy F from the partition function Z calculated from (2.4) and the equation

$$Z = e^{-F/kT} = \sum_{(\varphi(\mathbf{k}))} e^{-U/kT}, \qquad \ldots\ldots(2.6)$$

where the summation is over all sets of $\phi(\mathbf{k})$ consistent with $\phi(\mathbf{k}) = 0, 1$ and the equation (2.5). However, it appears that the present resources of statistical mechanics are not adequate for evaluating a partition function of this type which is equivalent to solving the general order–disorder problem where each atom interacts with every other one. We therefore look for an approximate method. The average distribution $\bar{\phi}(\mathbf{k})$ will be a function of the temperature and of the magnitude of $\mathbf{k}$ only: we write it as $f(k)$. If the exchange energy in (2.4) were

absent $f(k)$ would be just the Fermi–Dirac function. We take as the internal energy $E=\overline{U}$

$$E=\sum_{\mathbf{k}}\frac{h^2}{8\pi^2 m}k^2 f(k)-\frac{1}{2}\sum_{\mathbf{k}}\sum_{\mathbf{k}'}\frac{4\pi e^2}{V}\frac{f(k)f(k')}{|\mathbf{k}-\mathbf{k}'|^2}.$$

This is not quite accurate since the average of $\phi(k)\phi(k')$ is not just the product of the averages of $\phi(k)$ and $\phi(k')$. To get the free energy we need now an expression for the entropy. As the main approximation we assume that the entropy S is the same function of f as it is for the Fermi–Dirac assembly where no exchange interactions are present. This is not to assume that the entropy is unaltered because f will be a different function of k when we include the exchange interactions $S=-\boldsymbol{k}\Sigma_{\mathbf{k}}[f\ln f+(1-f)\ln(1-f)]$. This assumption is due to Koppe (1947). Hence for the free energy we have

$$F=E-TS=\sum_{\mathbf{k}}\frac{h^2}{8\pi^2 m}k^2 f(k)-\frac{1}{2}\sum_{\mathbf{k}}\sum_{\mathbf{k}'\neq\mathbf{k}}\frac{4\pi e^2}{V}\frac{f(k)f(k')}{|\mathbf{k}-\mathbf{k}'|^2}$$
$$+\boldsymbol{k}T\sum_{\mathbf{k}}[f\ln f+(1-f)\ln(1-f)].$$

Let us in the usual way replace these sums by integrals in $\mathbf{k}$-space introducing the density of states factor $k^2V/2\pi^2$ (one electron to each state $\mathbf{k}$), then

$$F=\frac{h^2V}{16\pi^4 m}\int_0^\infty f(k)k^4\,dk-\frac{e^2V}{4\pi^3}\int_0^\infty\int_0^\infty f(k_1)f(k_2)k_1k_2\ln\left|\frac{k_1+k_2}{k_1-k_2}\right|dk_1\,dk_2$$
$$+\boldsymbol{k}T\frac{V}{2\pi^2}\int_0^\infty[f\ln f+(1-f)\ln(1-f)]k^2\,dk, \qquad \ldots\ldots(2.7)$$

with
$$n_1=\frac{V}{2\pi^2}\int_0^\infty f(k)k^2\,dk. \qquad \ldots\ldots(2.8)$$

The form of $f(k)$ is found by putting the variation $\delta F=0$. In this way we get the equation

$$\frac{h^2}{8\pi^2 m}k^2-\frac{e^2}{\pi k}\int_0^\infty k'f(k')\ln\left|\frac{k+k'}{k-k'}\right|dk'-\eta=\boldsymbol{k}T\ln\left(\frac{1-f(k)}{f(k)}\right).$$

The parameter η, which is equal to the chemical potential, is determined by (2.8). This is the equation Bardeen (1936) assumed for the distribution function, since the second term on the left-hand side is just the exchange energy of an electron in state $\mathbf{k}$ with all the others in the assembly. However we have little hope of solving this equation for $f(k)$ or of evaluating the integrals in (2.7): we therefore apply the approximate method used by Koppe (1947). This consists in assuming a form for $f(k)$ containing two parameters: one of these is eliminated through the condition that the total number of electrons is constant (2.8), the other by making F a minimum, a condition necessary for thermodynamic consistency.

We shall use two forms for $f(k)$, one for 'low' temperatures when the electron gas is degenerate, the other for 'high' temperatures.

(i) *Low Temperatures.*

$$f=1,\ 0\leqslant k\leqslant\frac{\alpha-1}{\beta},\quad f=\alpha-\beta k,\ \frac{\alpha-1}{\beta}\leqslant k\leqslant\frac{\alpha}{\beta},\quad f=0,\ k\geqslant\frac{\alpha}{\beta} \qquad \ldots\ldots(2.9)$$

Very low temperatures correspond to $\alpha\gg 1$.

(ii) *High Temperatures.*

$$f=\alpha-\beta k, \quad 0\leqslant k\leqslant \alpha/\beta. \qquad f=0, \quad k\geqslant \alpha/\beta. \qquad \ldots\ldots(2.10)$$

It might be thought that (2.9), and (2.10) would give a very crude approximation indeed. But it appears that the free energy F is rather insensitive to the form used for f. A calculation, in the same manner as below, was made for the electron gas without exchange interactions and the results compared with the accurate functions tabulated by Stoner (1939 b). The differences were no more than a few per cent, whilst the internal energy at high temperatures was given accurately as $3n_1\boldsymbol{k}T/2$. Curves of the free energy, internal energy and entropy are given in Figure 2, and details of the calculation are given in Appendix A.

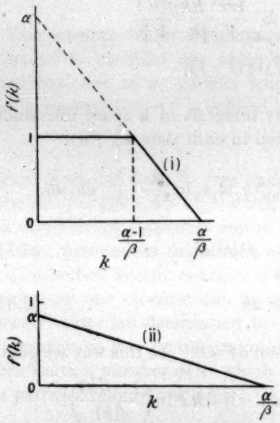

Figure 1. Approximate forms for the function $f(k)$: (i) $a\geqslant 1$; (ii) $a\leqslant 1$.

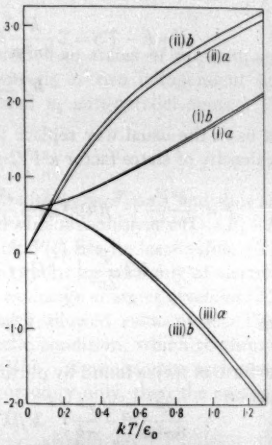

Figure 2. Thermodynamic functions for a perfect Fermi–Dirac gas. Curves marked a are obtained using the approximate forms for $f(k)$ and those marked b from the accurate values obtained by Stoner: (i) internal energy; (ii) entropy; (iii) free energy.

The form of the integrals in (2.7) is such that it is more convenient to work with the parameters α/β and $1/\alpha=x$ than with α and β themselves. Thus (2.9) gives $f(k)$ for $x\leqslant 1$ and (2.10) applies to $x\geqslant 1$. By (2.8) we get as the equations for eliminating α/β

$$n_1=\frac{V}{6\pi^2}\left(\frac{\alpha}{\beta}\right)^3\left(1-\frac{3x}{2}+x^2-\frac{x^3}{4}\right), \qquad x\leqslant 1.$$

$$=\frac{V}{24\pi^2}\left(\frac{\alpha}{\beta}\right)^3\frac{1}{x}, \qquad x\geqslant 1.$$

Using equations (2.9) and (2.10) to evaluate the integrals in (2.7), we find that F_1 has the form

$$F_1=\frac{3}{5}n_1{}^1\epsilon_0 A(x)-\frac{3}{4}n_1{}^1\epsilon_j B(x)-n_1\frac{3\boldsymbol{k}T}{2}C(x), \qquad \ldots\ldots(2.11)$$

where ${}^1\epsilon_0 = \frac{h^2}{8m}\left(\frac{6n_1}{\pi V}\right)^{2/3}$ and ${}^1\epsilon_j = e^2\left(\frac{6n_1}{\pi V}\right)^{1/3}$; $A(x)$, $B(x)$, and $C(x)$ are the following functions of x, in which $P(x) = (1-3x/2+x^2-x^3/4)^{-1}$.

$$\left.\begin{aligned} A(x) &= P^{5/3}[1-(1-x)^6]/6x, && x \leqslant 1, \\ &= 2.4^{2/3}x^{2/3}/3, && x \geqslant 1. \end{aligned}\right\} \qquad \ldots\ldots(2.12)$$

$$\begin{aligned} B(x) = {} & \frac{4P^{4/3}}{45x^2}\{[1+(1-x)^6]\ln(1-\tfrac{1}{2}x)-(1-x)^6\ln(1-x)\} \\ & + \frac{7P^{4/3}}{45}(8-16x+14x^2-6x^3+x^4) \\ & + P^{4/3}\left(\frac{x^2}{6}-\frac{x^3}{6}+\frac{2x^4}{45}\right)\ln\left(\frac{x}{2-x}\right), \qquad x \leqslant 1, \\ = {} & \frac{4^{1/3}}{45}(28-16\ln 2)x^{-2/3}, \qquad x \geqslant 1. \end{aligned}$$

$$\left.\begin{aligned} C(x) &= P(x-x^2+\tfrac{11}{36}x^3), && x \leqslant 1, \\ &= \frac{2}{3}\ln x - \frac{2}{3}(x-1)^4\ln\left(\frac{x}{x-1}\right)+\frac{26x}{9}-\frac{7x^2}{3}+\frac{2x^3}{3}, && x \geqslant 1. \end{aligned}\right\} \qquad (2.13)$$

The parameter x is determined by putting $\partial F/\partial x = 0$, which gives

$$\tfrac{3}{5}\,{}^1\epsilon_0 A'(x) - \tfrac{3}{4}\,{}^1\epsilon_j B'(x) - \tfrac{3}{2}\boldsymbol{k}TC'(x) = 0, \qquad \ldots\ldots(2.14)$$

where the primes indicate differentiation with respect to x. At least in principle we have thus solved the main problem, which was the calculation of the free energy of either of the sub-assemblies of electrons. As we have already remarked, we may consider them separately because the exchange energy is zero between two electrons of opposite spin. There are n_1 electrons in the sub-assembly of parallel spins and n_2 in the sub-assembly of anti-parallel spins. Then by the definition (2.3) of ζ we have $n_1 = \frac{1}{2}N(1+\zeta)$ and $n_2 = \frac{1}{2}N(1-\zeta)$. Thus it follows from equation (2.11) that the free energy of the whole assembly of electrons, which is simply the sum of the free energies of the two sub-assemblies, is given by

$$\begin{aligned} \frac{F(\zeta)}{N\epsilon_0} = {} & \frac{3}{10}\{(1+\zeta)^{5/3}A(x_1)+(1-\zeta)^{5/3}A(x_2)\} \\ & - \frac{3}{8}\frac{\epsilon_j}{\epsilon_0}\{(1+\zeta)^{4/3}B(x_1)+(1-\zeta)^{4/3}B(x_2)\} \\ & - \frac{3}{4}\frac{\boldsymbol{k}T}{\epsilon_0}\{(1+\zeta)C(x_1)+(1-\zeta)C(x_2)\}, \qquad \ldots\ldots(2.15) \end{aligned}$$

where

$$\epsilon_0 = \frac{h^2}{8m}\left(\frac{3N}{\pi V}\right)^{2/3} \quad \text{and} \quad \epsilon_j = e^2\left(\frac{3N}{\pi V}\right)^{1/3}. \qquad \ldots\ldots(2.16)$$

ϵ_0 is just the Fermi energy, whilst ϵ_j measures the strength of the exchange interactions. The parameters x_1 and x_2 are given as functions of ζ and $\boldsymbol{k}T/\epsilon_0$ by the equations

$$\left.\begin{aligned} \frac{3}{5}(1+\zeta)^{2/3}A'(x_1) - \frac{3}{4}\frac{\epsilon_j}{\epsilon_0}(1+\zeta)^{1/3}B'(x_1) - \frac{3}{2}\frac{\boldsymbol{k}T}{\epsilon_0}C'(x_1) = 0, \\ \frac{3}{5}(1-\zeta)^{2/3}A'(x_2) - \frac{3}{4}\frac{\epsilon_j}{\epsilon_0}(1-\zeta)^{1/3}B'(x_2) - \frac{3}{2}\frac{\boldsymbol{k}T}{\epsilon_0}C'(x_2) = 0. \end{aligned}\right\} \qquad \ldots\ldots(2.17)$$

Just as kT/ϵ_0 gives a convenient measure of temperature for the assembly, so ϵ_j/ϵ_0 gives the strength of the exchange interaction. We shall work entirely in terms of these reduced quantities ζ, kT/ϵ_0 and ϵ_j/ϵ_0. However, before considering the numerical analysis of these equations, let us examine the conditions under which the model is ferromagnetic.

§ 3. THE EXISTENCE OF FERROMAGNETISM

If we reduce the temperature T to zero, then equations (2.17) give for all ζ, $x_1=x_2=0$; $A(0)$ and $B(0)$ are both unity, so that

$$\frac{F(\zeta)}{N\epsilon_0}=\frac{E(\zeta)}{N\epsilon_0}=\frac{3}{10}[(1+\zeta)^{5/3}+(1-\zeta)^{5/3}]-\frac{3}{8}\frac{\epsilon_j}{\epsilon_0}[(1+\zeta)^{4/3}+(1-\zeta)^{4/3}]$$

where $E(\zeta)$ is simply the internal energy. The equilibrium value of ζ is clearly that which gives $E(\zeta)$ its least value. The curves of $[E(\zeta)-E(0)]/N\epsilon_0$ against ζ for particular values of ϵ_j/ϵ_0 (Figure 3) show that equilibrium is given by

$$\left.\begin{aligned}\zeta=1 \quad &\text{for} \quad \epsilon_j/\epsilon_0>4(2^{1/3}+1)/5,\\ \zeta=0 \quad &\text{for} \quad \epsilon_j/\epsilon_0<4(2^{1/3}+1)/5.\end{aligned}\right\} \qquad \ldots\ldots(3.1)$$

The model is thus only ferromagnetic if $\epsilon_j/\epsilon_0>1{\cdot}81$. No intermediate values of ζ are possible as they are in Stoner's theory. This sudden change in ζ as

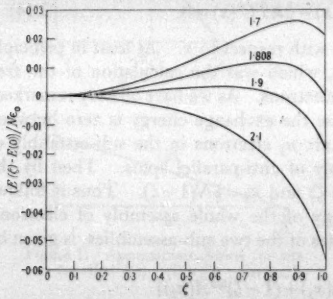

Figure 3. The internal energy as a function of ζ at $T=0$. Numbers on the curves are the values of ϵ_j/ϵ_0.

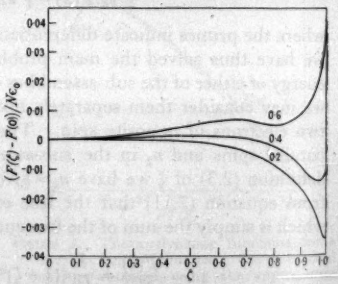

Figure 4. Curves of free energy against relative magnetization for $\epsilon_j/\epsilon_0=2{\cdot}0$. The numbers on the curves are the values of kT/ϵ_0.

kT/ϵ_0 is increased, was noticed by Wohlfarth (1949 c). Equation (3.1) corrects an error he made in locating the transition point. The lowest value of ϵ_j/ϵ_0 for which $E(\zeta)<E(0)$ for all ζ is $\epsilon_j/\epsilon_0=2$: in fact $d^2E/d\zeta^2$ at $\zeta=0$ is less than, equal to, or greater than zero according as ϵ_j/ϵ_0 is greater than, equal to, or less than two.

§ 4. MAGNETIZATION–TEMPERATURE CURVES

Temperature effects are in principle deducible from the equations (2.15) and (2.17), which by elimination of x_1 and x_2, give F as a function of ζ and T. However, owing to the very complicated nature of the functions A, B and C and their derivatives, this elimination can only be done numerically. This we have done for $\epsilon_j/\epsilon_0=2$ and for $kT/\epsilon_0=0{\cdot}2$, $0{\cdot}4$ and $0{\cdot}6$. These three curves are sufficient to demonstrate the magnetic behaviour of the model. The method was to

tabulate the functions A, B and C and their derivatives, and then, using equations (2.17) to prepare tables of $(1 \pm \zeta)^{-1/3}$ as a function of x for the three chosen temperatures. Inverse interpolation in the tables of $(1 \pm \zeta)^{-1/3}$ against x then gave x_1 and x_2 corresponding to any particular ζ. These could then be substituted in (2.15) to give $F(\zeta)/N\epsilon_0$ for this value of ζ.

The results of the calculation are shown as curves of $[F(\zeta) - F(0)]/N\epsilon_0$ against ζ in Figure 4. In general, we see that $dF(\zeta)/d\zeta = 0$ has three roots (one of which is always $\zeta = 0$), so that in considering the variation of equilibrium magnetization with temperature, it would not be sufficient merely to use this equation: that is why we have obtained complete curves of the free energy. It is also to be seen from Figure 4 that the equilibrium value of ζ decreases slowly from unity (at $T = 0$) with increasing $\boldsymbol{k}T/\epsilon_0$ until a Curie temperature T_c is reached at which $F(\zeta) = F(0)$: for $\epsilon_j/\epsilon_0 = 2$ we find $\boldsymbol{k}T_c/\epsilon_0 = 0{\cdot}52$. Above this temperature the equilibrium value of ζ is zero, and so at $T = T_c$ there is a latent heat of demagnetization equal to $E(0) - E(\zeta)$: for $\epsilon_j/\epsilon_0 = 2$ this is about $0{\cdot}05\, N\epsilon_0$. Rough values of the equilibrium magnetization against $\boldsymbol{k}T/\epsilon_0$ have been obtained by eliminating x_1 and x_2 from (2.17) and the equation $dF(\zeta)/d\zeta = 0$: these are shown in Figure 5.

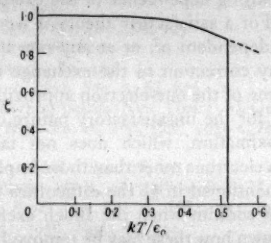

Figure 5. Curve of equilibrium magnetization ζ against temperature for $\epsilon_j/\epsilon_0 = 2{\cdot}0$.

With these results for the special case $\epsilon_j/\epsilon_0 = 2$, and Figure 3, we can see qualitatively how the magnetization will vary with temperature for other values of this parameter. Firstly, as ϵ_j/ϵ_0 and the corresponding Curie temperature decrease, the (approximately) rectangular area enclosed by the (ζ, T) curve, will become thinner, the value of ζ for $T = 0$ being always unity. This will continue until $\epsilon_j/\epsilon_0 = 4(2^{1/3} + 1)/5$ when the rectangle is vanishingly thin: we have already seen that below this value the model is not ferromagnetic. Clearly if we now increase ϵ_j/ϵ_0 above 2, this effect will be reversed, and the area enclosed by the magnetization curve will become broader. We should also expect the value of ζ at $T = T_c$ to decrease, and it is possible that, by increasing the exchange interaction sufficiently, we might get a completely second order transition to the paramagnetic state, without the abrupt change in magnetization found here. However, we cannot be certain of this without repeating the calculations for other values of ϵ_j/ϵ_0, and in view of the general divergence of our results from experiment, it was felt that the labour would not be justified. Thus, even if we suppose that for a sufficiently high value of ϵ_j/ϵ_0 the model would reproduce the behaviour of, say, nickel, dilution of nickel with copper must bring the value down into the region we have examined, whereas none of the ferromagnetic nickel–copper alloys show any behaviour such as we have found.

§5. DISCUSSION

The general conclusion to be drawn from our calculations is, therefore, that although the model reproduces several of the characteristic features of ferromagnetism, it cannot be used to provide an exact detailed description. This arises because it predicts a sudden drop in magnetization at the Curie point instead of the steady fall to zero found experimentally. Also the specific heat curve of, say, iron (see Awbery and Griffiths 1940) has a fairly broad (finite) peak at the Curie point whereas our model yields a latent heat, which would be observed as an extremely narrow tall peak. We can conveniently discuss why the model fails to predict the correct behaviour by comparing it with Stoner's theory which agrees well with experiment. The basic assumption of Stoner's theory is that the total exchange energy is a certain function of the magnetization, but not explicitly a function of the temperature. Clearly a sufficient condition for this result to be true is that the exchange interaction between two electrons, one in state $\mathbf{k}$, the other in state $\mathbf{k}'$, is independent of $\mathbf{k}$ and $\mathbf{k}'$. It is interesting to notice, however, that the condition is also *necessary*; this result is demonstrated in Appendix B. This suggests that the difference between our results and those of Stoner is due to the strong dependence of the exchange integral on $\mathbf{k}$ and $\mathbf{k}'$, namely as $|\mathbf{k}-\mathbf{k}'|^{-2}$. For a satisfactory theory it would be necessary to derive an exchange integral independent of, or at any rate much less dependent on $\mathbf{k}$ and $\mathbf{k}'$ than (2.2). Any correction to the exchange integral must however be sought outside the scheme of the one-electron approximation.

A very likely reason for the unsatisfactory nature of our model is the use of the one-electron approximation, which does not take account of positional correlations between the electrons other than those implied by the Pauli principle. Now we have already mentioned in §1 the difficulties which arise in connection with the specific heat of sodium when the Bloch exchange terms are included. Wohlfarth (1950) has shown how these may be removed by replacing the Coulomb potential integral by a screened potential

$$V(r_{12}) = e^2 r_{12}^{-1} \exp(-\lambda r_{12}), \qquad \ldots\ldots(5.1)$$

while the one-electron character of the wave function is retained. (This suggestion was first made by Landsberg (1949) to explain the width of the tail of the soft x-ray emission curve for sodium.) Modification of the Coulomb potential in this way is regarded as an empirical way of taking into account the positional correlations of the electrons. We may therefore enquire whether a similar modification of the potential would not remove the difference between our results and experiment. The potential (5.1) gives as the modified exchange integral

$$J_{\mathbf{k},\mathbf{k}'} = \frac{4\pi e^2}{V} \frac{1}{|\mathbf{k}-\mathbf{k}'|^2+\lambda^2}, \qquad \ldots\ldots(5.2)$$

which has a weaker dependence on $\mathbf{k}$ and $\mathbf{k}'$ than the Bloch integral (obtained by putting $\lambda=0$). It is clear then that by choosing suitable values of λ, the dependence of (5.2) on $\mathbf{k}$ and $\mathbf{k}'$ could be made sufficiently weak to give a second order transition from ferromagnetism to paramagnetism in the way predicted by Stoner's theory. It does not seem likely, however, that calculations with (5.2) would be of much significance since (5.1) is merely an empirical expression without a theoretical basis. In addition the formula is open to criticism on

qualitative grounds. The correlations we are considering are of short range and arise from the terms in the total Hamiltonian representing electron repulsions. The 'correlations' taken into account by the screened potential (5.1) would seem to represent long-range effects, since the term $\exp(-\lambda r_{12})$ effectively reduces the product of wave functions in the exchange integral only at large separations r_{12}. It is difficult to see how these long-range effects are to be interpreted (see, however, a note by Bohm and Pines (1950)). In view of this, further consideration is being given to the problem of positional correlations.

ACKNOWLEDGMENTS

The author wishes to thank Mr. F. Booth for his kind encouragement and interest in this problem and for checking the calculation of the functions $A(x)$, $B(x)$ and $C(x)$; he also wishes to acknowledge a grant from the Department of Scientific and Industrial Research.

REFERENCES

Awbery, J. H., and Griffiths, E., 1940, *Proc. Roy. Soc.* A, **174,** 1.
Bardeen, J., 1936, *Phys. Rev.*, **50,** 1098.
Bloch, F., 1928, *Z. Phys.*, **57,** 545.
Bohm, D., and Pines, D., 1950, *Phys. Rev.*, **80,** 903.
Heisenberg, W., 1928, *Z. Phys.*, **49,** 619.
Koppe, H., 1947, *Z. Naturforsch.*, **2a,** 429.
Landsberg, P. T., 1949, *Proc. Phys. Soc.* A, **62,** 806.
Seitz, F., 1940, *Modern Theory of Solids* (New York : McGraw-Hill).
Stoner, E. C., 1938, *Proc. Roy. Soc.* A, **165,** 372; 1939 a, *Ibid.*, **169,** 339; 1939 b, *Phil. Mag.*, **28,** 257.
Van Vleck, J. H., 1945, *Rev. Mod. Phys.*, **17,** 27.
Von der Lage, F. C., and Bethe, H. A., 1947, *Phys. Rev.*, **71,** 612.
Wohlfarth, E. P., 1949 a, *Proc. Roy. Soc.* A, **195,** 434; 1949 b, *Phil. Mag.*, **40,** 1095; 1949 c, *Ibid.*, **40,** 703; 1950, *Ibid.*, **41,** 534.

APPENDIX A

We give here the details of the calculation of the thermodynamic functions for a perfect Fermi–Dirac gas using the approximate forms (2.9) and (2.10) for the distribution function. When there are no exchange interactions there can be no ferromagnetism: we therefore obtain an approximate expression for the free energy of the perfect Fermi–Dirac gas by putting $x_1=x_2$, $\zeta=0$ and $\epsilon_f=0$ in equation (2.15). This yields

$$\frac{F}{N\epsilon_0}=\frac{3}{5}A(x)-\frac{3}{2}\frac{kT}{\epsilon_0}C(x). \qquad \ldots\ldots(A1)$$

In this equation $3A(x)/5$ is the reduced internal energy $E(x)/N\epsilon_0$, and $3C(x)/2$ is the reduced entropy $S(x)/Nk$. The equilibrium value of x is that for which $F(x)$ is a minimum; this gives the equation

$$kT/\epsilon_0=2A'(x)/5C'(x). \qquad \ldots\ldots(A2)$$

From the tabulated values of $A(x)$, $C(x)$ and their derivatives it was therefore simple to obtain $F/N\epsilon_0$ and kT/ϵ_0 as functions of x. Figure 2 was then constructed from these results. We give below the forms taken by the functions at very high and very low temperatures.

(*a*) *Very low temperatures.* From equations (2.12) and (2.13) we find, for $x \ll 1$, $A(x) = 1 + 5x^2/12$ and $C(x) = x$. Therefore, by (A 2), $x = 3\boldsymbol{k}T/\epsilon_0$ so that the internal energy E is given by

$$\frac{E}{N\epsilon_0} = \frac{3}{5}\left[1 + \frac{5}{12}\left(\frac{3\boldsymbol{k}T}{\epsilon_0}\right)^2\right],$$

whereas the accurate expression is

$$\frac{E}{N\epsilon_0} = \frac{3}{5}\left[1 + \frac{5}{12}\left(\frac{\pi\boldsymbol{k}T}{\epsilon_0}\right)^2\right].$$

(*b*) *Very high temperatures.* The limiting forms of $A(x)$ and $C(x)$ for large values of x are $A(x) = 2 \cdot 4^{2/3}x^{2/3}/3$ and $C(x) = 25/18 + (2/3)\ln x$. Therefore $x^{2/3} = 15\boldsymbol{k}T \cdot 4^{-2/3}/4\epsilon_0$ which gives for the internal energy and entropy respectively $E = 3N\boldsymbol{k}T/2$ and

$$\frac{S}{Nk} = \ln\left\{\frac{(2\pi m\boldsymbol{k}T)^{3/2}}{N}\frac{2V}{h^3}\right\} + \frac{25}{12} + \ln\left[\frac{5}{8}\left(\frac{15}{\pi}\right)^{1/2}\right]$$

$$= \ln\left\{\frac{(2\pi m\boldsymbol{k}T)^{3/2}}{N}\frac{2V}{h^3}\right\} + 2{\cdot}396.$$

In this equation we have substituted for ϵ_0 from equation (2.16). We note that whereas the expression for the internal energy is accurate, the entropy is in error by a constant amount, the accurate expression being

$$\frac{S}{Nk} = \ln\left\{\frac{(2\pi m\boldsymbol{k}T)^{3/2}}{N}\frac{2V}{h^3}\right\} + \frac{5}{2}.$$

the difference in the constant terms is, however, only 0·104.

APPENDIX B

We shall find below the conditions under which the sum of the exchange and Coulomb energies for the whole assembly of electrons depends only on the magnetization and not on the temperature. The individual Coulomb and exchange integrals which appear in equation (2.1), we denote by $C_{\mathbf{k}\mathbf{k}'}$ and $J_{\mathbf{k}\mathbf{k}'}$ respectively. Let the distribution function for the sub-assembly of parallel spins be $f_1(k)$ and let it be $f_2(k)$ for the anti-parallel spins. The total exchange and Coulomb energy is then

$$G = \tfrac{1}{2}\sum_{\mathbf{k}}\sum_{\mathbf{k}'} f_1(k)f_1(k')J_{\mathbf{k}\mathbf{k}'} + \tfrac{1}{2}\sum_{\mathbf{k}}\sum_{\mathbf{k}'} f_2(k)f_2(k')J_{\mathbf{k}\mathbf{k}'}$$
$$+ \tfrac{1}{2}\sum_{\mathbf{k}}\sum_{\mathbf{k}'} f_1(k)f_1(k')C_{\mathbf{k}\mathbf{k}'} + \tfrac{1}{2}\sum_{\mathbf{k}}\sum_{\mathbf{k}'} f_2(k)f_2(k')C_{\mathbf{k}\mathbf{k}'}$$
$$+ \sum_{\mathbf{k}}\sum_{\mathbf{k}'} f_1(k)f_2(k')C_{\mathbf{k}\mathbf{k}'}. \qquad \ldots\ldots(\mathrm{B}1)$$

In this equation we have introduced implicitly a self-exchange integral, so that the inner summations in the first four terms may be over all allowed $\mathbf{k}'$ vectors, not only over all $\mathbf{k}' \neq \mathbf{k}$. Clearly, if we make $J_{\mathbf{k}\mathbf{k}} = -C_{\mathbf{k}\mathbf{k}}$ the self-exchange terms in the first and second summations will cancel the self Coulomb terms in the third and fourth. The last summation in (B1) represents the Coulomb energy of the parallel spins with the anti-parallel spins; terms in $C_{\mathbf{k}\mathbf{k}}$ will therefore occur here in any case.

Now if there are n_1 parallel spins and n_2 anti-parallel spins, $f_1(k)$ and $f_2(k)$ must satisfy the conditions $\Sigma_k f_1(k) = n_1$ and $\Sigma_k f_2(k) = n_2$. It is given that G is independent of temperature, and therefore the variation δG is zero, for all variations in f_1 and f_2

$$\begin{aligned}\delta G = 0 = &\sum_k \delta f_1(k) \sum_{k'} f_1(k') J_{kk'} + \sum_k \delta f_2(k) \sum_{k'} f_2(k') J_{kk'} \\ &+ \sum_k \delta f_1(k) \sum_{k'} f_1(k') C_{kk'} + \sum_k \delta f_2(k) \sum_{k'} f_2(k') C_{kk'} \\ &+ \sum_k \delta f_1(k) \sum_{k'} f_2(k') C_{kk'} + \sum_k \delta f_2(k) \sum_{k'} f_1(k') C_{kk'},\end{aligned}$$

subject to the conditions

$$\sum_k \delta f_1(k) = 0 \quad \ldots\ldots (B\,2), \qquad \sum_k \delta f_2(k) = 0. \quad \ldots\ldots (B\,3)$$

Introducing the undetermined Lagrange multipliers λ_1 and λ_2, we have therefore

$$\begin{aligned}\sum_k \delta f_1(k) \{\lambda_1 + \sum_{k'} [f_1(k') J_{kk'} + f_1(k') C_{kk'} + f_2(k') C_{kk'}]\} \\ + \sum_k \delta f_2(k) \{\lambda_2 + \sum_{k'} [f_2(k') J_{kk'} + f_2(k') C_{kk'} + f_1(k') C_{kk'}]\} = 0.\end{aligned}$$

As this must be true for all arbitrary variations δf_1 and δf_2 we must have

$$\sum_{k'} f_1(k')(J_{kk'} + C_{kk'}) + \sum_{k'} f_2(k') C_{kk'} = -\lambda_1, \quad \ldots\ldots (B\,4)$$

$$\sum_{k'} f_2(k')(J_{kk'} + C_{kk'}) + \sum_{k'} f_1(k') C_{kk'} = -\lambda_2. \quad \ldots\ldots (B\,5)$$

These two equations show that if the energy G is not an explicit function of temperature, then the total Coulomb and exchange energy of a *single* electron with the remaining electrons of the assembly is likewise independent of temperature. Equation (B 4) expresses this for an electron with parallel spin (in the f_1 distribution) and (B 5) for an electron with anti-parallel spin. Now take (B 4) and consider further variations δf_1 and δf_2, obtaining

$$\sum_{k'} \delta f_1(k')(J_{kk'} + C_{kk'}) + \sum_{k'} \delta f_2(k') C_{kk'} = 0.$$

Combining this with the conditions (B 2) and (B 3) by the aid of further undetermined Lagrange multipliers j_1 and j_2, we have

$$\sum_{k'} \delta f_1(k')(J_{kk'} + C_{kk'} + j_1) + \sum_{k'} \delta f_2(k')(C_{kk'} + j_2) = 0.$$

As this also must be true for all arbitrary variations δf_1 and δf_2 we must have $C_{kk'} = -j_2$ and $J_{kk'} + C_{kk'} = -j_1$ which can be put in the form $C_{kk'} = C$ and $J_{kk'} = J$. If we now substitute these results into equation (B 1), we find that the total Coulomb energy is simply $N^2C/2$ (where $N = n_1 + n_2$) and is therefore independent of magnetization. Likewise the total exchange energy is $\frac{1}{4}N^2J + \frac{1}{4}N^2J\zeta^2$ where, as before, ζ is the reduced magnetization. We have thus shown that if the sum of the exchange and Coulomb energies is to be a function only of the magnetization, then, within the scheme of the one-electron approximation the total Coulomb energy is a constant, whilst the total exchange energy can only have the form assumed by Stoner. As a corollary it follows that if the exchange energy is assumed to be some other function of ζ, it must contain parameters which depend on the temperature.

The Velocity of First Sound in Liquid Helium

By K. R. Atkins and C. E. Chase
Royal Society Mond Laboratory, Cambridge

Communicated by D. Shoenberg; *MS. received* 21*st May* 1951

ABSTRACT. The velocity u_1 of ordinary sound in liquid helium has been measured in the temperature range from 1·2° K. to 4·2° K. Its value extrapolated to 0° K. is compared with the velocity u_2 of second sound at 0·1° K. and a slight departure from the Landau relation $u_2=u_1/\sqrt{3}$ is indicated. The behaviour of u_1 in the neighbourhood of the λ-point has been studied in detail.

§1. Introduction

A study of ordinary sound in liquid helium is of interest for several reasons. First, a determination of the velocity at low temperatures would make it possible to test more critically the relation $u_2=u_1/\sqrt{3}$ between the velocities of first and second sound at absolute zero predicted by Landau (1941). Measurements of second sound velocity at temperatures down to 0·1°K. have recently been completed (Atkins and Osborne 1950), and it was desired to extend the existing first sound measurements to lower temperatures in order to make possible a more accurate extrapolation to absolute zero. Second, the behaviour of the velocity in the immediate vicinity of the λ-point is of interest. The Ehrenfest relations for a phase transition of the second order predict a discontinuity of 2½% at the λ-point, using accepted values of the thermodynamic parameters involved. Previous investigators have found no evidence for such a discontinuity under the saturated vapour pressure (Findlay, Pitt, Grayson Smith and Wilhelm 1938), although it has been observed at higher pressures (Findlay *et al.* 1939). A knowledge of the exact shape of the curve in this region might lead to a better understanding of the mechanism of the λ-transition. Third, the question of dispersion has never been adequately investigated. It is probable that there is no large dispersion in the region between 1 and 15 Mc/s. (Pellam and Squire 1947), but a small effect of a few per cent is not excluded in this range and nothing is known about the behaviour at other frequencies. Finally, the attenuation is of interest, particularly near the λ-point and in the low-temperature region, as it may provide information about the internal structure of the liquid.

Measurements of velocity were made by Findlay *et al.* (1938), using a continuous-wave resonance method at a frequency of 1·338 Mc/s., and of both velocity and attenuation by Pellam and Squire (1947), using a pulse technique at 15 Mc/s. The present work is in agreement with these previous results in the temperature range which they covered (from the normal boiling point down to 1·6° K.). In addition velocity and attenuation measurements have been extended to 1·2° K., and a much more detailed investigation of the behaviour in the neighbourhood of the λ-point has been made.

§2. DESCRIPTION OF APPARATUS

A pulsed ultrasonic method similar to that employed by Pellam and Squire was used. Pulses of approximately ten microseconds duration from a 14 Mc/s. oscillator were fed into a quartz crystal immersed in the liquid helium. The resulting ultrasonic pulses were reflected from a polished brass reflector, and the echoes received by the same crystal. After amplification and demodulation the echoes were displayed on a Cossor Model 1035 double-beam oscilloscope, together with timing pips provided by a standard radar unit (a 'Gee' unit).

Figure 1 shows the etalon with which the measurements were made. An X-cut quartz crystal G, 1·9 cm. in diameter, was mounted in a specially designed

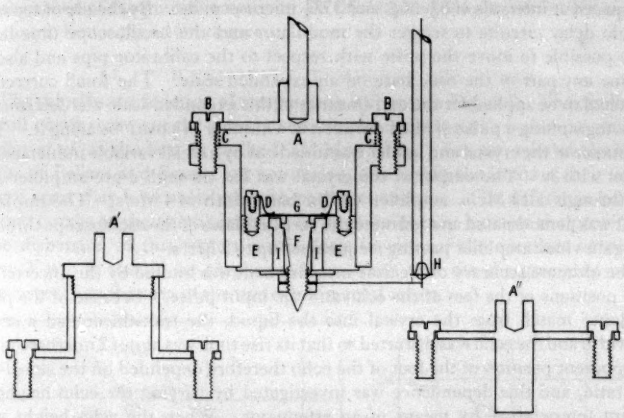

Figure 1.

Etalon. A : Polished reflector. F : Brass electrode.
B : Aligning screws. G : Quartz crystal.
C : Beryllium–copper spiral springs. H : Coaxial cable.
D : Beryllium–copper springs. I : Dystrene insulator.
E : Brass case.

holder. The top surfaces of the electrode F and brass case E were machined accurately plane, and the crystal was held against these surfaces by means of three beryllium copper springs D. The top face of the crystal was silvered, and contact with this face was made through these springs. The assembly was so designed that thermal contraction would not alter the alignment of the surfaces against which the crystal was pressed, thus making certain that the central electrode would remain in contact with the crystal face and that no stresses would act upon the quartz when the apparatus was cooled. The electrode was made in the shape of a cone to eliminate spurious echoes caused by the sound travelling back from the crystal. Such echoes would have to undergo many reflections before ever reaching the crystal again, and would be highly attenuated. The electrode was connected to the oscillator by a coaxial cable H extending to the cryostat head. The crystal holder assembly was attached to the reflector A by three aligning screws B, and was held in position by the beryllium copper springs C. By immersing the

apparatus in water and adjusting these screws to maximize the echoes, it was possible accurately to align the reflector and transducer, and it was then found that no appreciable misalignment occurred when the apparatus was cooled to liquid helium temperatures. The reflector was of brass, and was machined to be as plane and smooth as possible. Two alternative reflectors (A′ and A″) were provided in order to obtain longer or shorter path lengths. By interchanging them with A and varying the position of the aligning screws, it was possible to obtain a number of different path lengths.

All the electronic equipment was synchronized by means of the ' Gee ' unit, which provided trigger pulses at a repetition rate of 500 per second and calibrator pips spaced at intervals of $6\frac{2}{3}$, $66\frac{2}{3}$, and $333\frac{1}{3}$ microseconds. By the use of separate variable delay circuits to trigger the modulator and the oscilloscope time base, it was possible to move the pulse with respect to the calibrator pips and also to examine any part of the time base on an expanded scale. The small correction which had to be applied for the non-linearity of this expanded scale was determined by photographing a pulse of fixed duration at a number of positions along it. The capacitance of the crystal and holder was tuned out by a small variable inductance in parallel with it. The output of the crystal was fed through a pre-amplifier and then through a 14 Mc/s. amplifier with a bandwidth of 4 Mc/s. The amplifier output was demodulated and fed on to the vertical plates of the oscilloscope through a low-gain video amplifier passing frequencies up to 2 Mc/s.

The ultimate accuracy of the time measurement was limited by the uncertainty in the positions of the feet of the echo and the input pulse. Because of the poor impedance match from the crystal into the liquid, the transducer had a small bandwidth and the echo was distorted so that its rise time was about 2 microseconds. The apparent position of the foot of the echo therefore depended on the signal-to-noise ratio, and this dependence was investigated by varying the echo height at constant temperature by means of an attenuator. When the echo height was approximately equal to the noise level this pulse amplitude correction amounted to 0·7 microsecond, but after it had been applied the position of the echo could be estimated to within 0·5 microsecond visually and 0·1 microsecond from enlarged photographs. The uncertainty in the position of the foot of the input pulse arose because this pulse was many orders of magnitude larger than the echo, so that any small build-up region at its foot could have been unduly emphasized and could conceivably have introduced an error as large as 0·5 microsecond. The length of the etalon could not be measured to better than 0·05 mm., or $\frac{1}{4}\%$. A correction of $\frac{1}{2}\%$ was applied for contraction of this length upon cooling, but this was only an approximate estimate. As a consequence of all these sources of error it is believed that relative values of the velocities are accurate to within $\frac{1}{3}\%$, but that the absolute values may be in error by as much as 1%.

Temperature measurements were made with a mercury manometer at pressures above 4 cm. Hg, and with a butyl phthalate manometer at lower pressures (the accuracy being of the order of $\frac{1}{10}$ mm. in both cases). A differential butyl phthalate manometer was also provided to register small changes of pressure, and proved to be of particular value near the λ-point. By comparing the oil and mercury manometers at one or two temperatures the conversion factor relating the density of oil to the density of mercury was obtained. Above the λ-point a correction was applied to allow for the temperature gradient in the helium bath due to the hydrostatic pressure head. This will be discussed in more detail in § 5. The

λ-point, as determined by the sudden cessation of boiling, occurred at a pressure of 3·77 cm. Hg, which corresponds to a temperature of 2·179° K. on the 1949 scale (van Dijk and Shoenberg 1949). Since the accepted value (2·186° K.) of the λ-transition temperature is probably not very accurate, the observed deviation from it is not very significant. In any case, although this deviation may possibly be accounted for by errors in manometry which have been overlooked, temperature differences measured from the λ-point are certainly correct to within 0·001° K. In order to obtain very accurate temperature control near the λ-point, a constantan heater was wound round the etalon, and the power fed into it varied in such a way that a balance was maintained between the amount of liquid helium evaporating and the speed of the pumping system. In this way the temperature could be kept constant to better than 10^{-4} degree.

§ 3. THE VELOCITY–TEMPERATURE CURVE

The velocity as a function of temperature is shown in Figure 2. The circles and the full curve represent the present results; the broken curve is the one given by Findlay *et al.* as the best fit to the 1·338 Mc/s. data. For the sake of clarity the results of Pellam and Squire are not shown, but within the limits of their experimental error they are consistent with both sets of data. The difference between the two curves in the neighbourhood of the λ-point may indicate the presence of some dispersion in this region, particularly in view of the excellent agreement above 3° K. It should be emphasized, however, that the disagreement is very little larger than the sum of the two experimental errors.

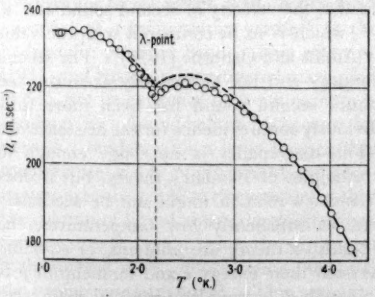

Figure 2.

Velocity of sound in liquid helium.
– – – Findlay, Pitt, Grayson Smith and Wilhelm.
–o–o– Present results. Path length = 4·310 cm.

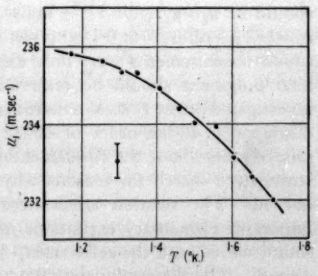

Figure 3.

Velocity of sound in liquid helium (low temperature range).
The vertical line indicates the size of the random error.

In Figure 2 there is a faint suggestion of a maximum near 1·3° K.; however it was believed that the apparent dip at the lowest temperatures was due to the small size of the echo there and the resulting difficulty in estimating the position of its foot.* Measurements were therefore made with a shorter etalon of length 4 mm., in order to have larger echoes. Figure 3 shows the results of these measurements, which were made photographically on the second echo, giving an effective path length of 1·6 cm., and a relative accuracy of within ± 0·2%. Since the error in

* The attenuation rises very rapidly below 1·4° K. This will be discussed in greater detail in a later paper.

measuring the length of the etalon was more important in this case, the absolute value has been adjusted to agree with the more precise absolute determinations made with the longer etalon. From this curve it may be seen that there is no evidence for a maximum in the velocity at low temperatures. The value extrapolated to absolute zero is 237 ± 2 m. sec^{-1}.

Figure 4 shows the adiabatic compressibility β_{ad} calculated from the usual formula $\beta_{ad} = 1/\rho u_1^2$, where ρ is the density and u_1 the velocity of sound. This calculation is based on the assumption that there is no dispersion between zero frequency and 14 Mc/s. Values above 2·5° K. have been given by Findlay *et al.*

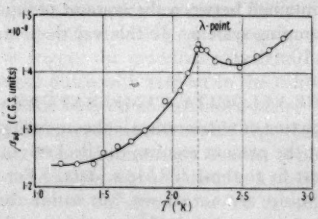

Figure 4.

Adiabatic compressibility of liquid helium at 14 Mc/s.

§ 4. VELOCITIES OF FIRST AND SECOND SOUND NEAR 0° K.

If the above extrapolation of the velocity of first sound u_1 from 1·2° K. to 0° K. is justifiable, then Landau's prediction is that the velocity of second sound at 0° K. should be $u_2 = u_1/\sqrt{3} = 137 \pm 1$ m.sec^{-1}, which is to be compared with the value $u_2 = 152 \pm 5$ m. sec^{-1} at 0·1° K. given by Atkins and Osborne (1950). The second sound measurements were only exploratory and not particularly accurate, and final judgment should be reserved until second sound has been more fully investigated below 1° K., but there is obviously some evidence for the existence of a discrepancy of the order of 10%. This discrepancy is not large enough to raise doubts about the fundamental principles of Landau's theory, but it does stimulate a search for reasons why Landau's relation might not be accurately obeyed. The relation arises because, at sufficiently low temperatures, the important elementary excitations in Landau's theory are phonons, or standing sound waves, and the relationship between their energy ϵ and momentum p is $\epsilon = u_1 p$. The thermodynamic functions such as entropy and internal energy can be derived from a knowledge of the elementary excitations, as in the Debye theory of the specific heats of solids, and the velocity of second sound can then be expressed in terms of the thermodynamic functions, giving the Landau relation $u_2 = u_1/\sqrt{3}$. It is important to notice, however, that at a temperature T the average frequency of the phonons is of the order of $\boldsymbol{k}T/\boldsymbol{h}$, which is still as high as 2×10^9 c/s. at 0·1° K. The discrepancy therefore suggests that the velocity of the phonons (i.e. the velocity of first sound) at a frequency of 2×10^9 c/s. is greater than the velocity measured at $1{\cdot}4 \times 10^7$ c/s. Dispersion always occurs when the absorption is so large that the wave is appreciably attenuated in a distance comparable with the wavelength, and present knowledge of the attenuation indicates that this may well be the case at a frequency of 2×10^9 c/s. and a temperature of 0·1° K. This will be discussed in greater detail in a later paper describing some results on the attenuation of first sound.

§ 5. BEHAVIOUR AT THE λ-POINT

The question of the behaviour of the velocity of sound near the λ-point is an interesting one. If the transition is assumed to be second order and the best possible values of the various quantities are taken to be those given by Keesom (1942), the Ehrenfest relations predict a discontinuity of approximately $2\frac{1}{2}\%$ in the velocity of sound. The experimental evidence on the magnitudes of the discontinuities in specific heat and thermal expansion is so inadequate, however, that this prediction is very approximate, and it is possible that a discontinuity much larger than this or even zero might still be consistent with the Ehrenfest relations.

The measurement of velocity near the λ-point is made difficult by the extremely high attenuation in this region (Pellam and Squire 1947). It is therefore necessary to extrapolate the curve over an interval of a few thousandths of a degree, and since the velocity depends strongly on the temperature in the vicinity of the λ-point, considerable uncertainty is introduced in this way. The use of a shorter etalon reduces the attenuation and makes it possible to approach closer to the λ-point, but the shorter time delays involved make the measurements less accurate. It is therefore necessary to compromise between these two sources of error. The procedure adopted was to approach as closely as possible using a long etalon for maximum accuracy, and then to make supplementary measurements with a much shorter etalon. The points obtained with the shorter etalon were then adjusted in absolute value to lie evenly about the more accurate curve in the region of overlap, and were sufficiently accurate to determine the shape of the curve very near the λ-point.

Another factor which made it difficult to come very near the λ-point was the existence of a temperature gradient in the liquid above the λ-point due to the hydrostatic pressure head. This effect is mentioned by Schmidt and Keesom (1937) and has been investigated more recently by Lock, Pippard and Shoenberg (1951), but its existence does not seem to be generally recognized. The thermal conductivity in liquid helium I is so poor that whenever there is a heat flow upwards there is a tendency for a large temperature gradient to be set up; however, the temperature at any point cannot rise above the temperature corresponding to a vapour pressure equal to the pressure at the surface plus the hydrostatic pressure of the column of liquid above the point, otherwise the liquid would vaporize. The temperature at a point below the surface is therefore greater than the temperature at the surface by an amount determined by the hydrostatic pressure and the slope of the vapour pressure curve. This amounts to somewhat over 0·001 deg/cm. near the λ-point. When, however, the surface of the liquid reaches the λ-point, it is no longer possible for this temperature gradient to be maintained because of the high thermal conductivity, and the entire volume becomes superfluid at once. This leads to a sudden jump in temperature, which may be as great as one or two hundredths of a degree near the bottom of the flask. The exact mechanism by which the transition takes place is obscure, and needs further study. The present work afforded an opportunity to demonstrate the existence of this hydrostatic effect in a very convincing fashion. Measurements of velocity were made both above and below the λ-point, first with a pressure head of about 20 cm. and then with a much lower pressure head of approximately 4 cm. The data from this experiment are shown in Figure 5, where velocity is plotted against surface temperature determined manometrically. The agreement of the two sets of points below the λ-point indicates that the etalon temperature was then the same as the surface temperature,

and hence no hydrostatic temperature gradient was present. Above the λ-point, however, the two curves are clearly separated, the upper curve corresponding to the higher pressure head. If this curve is shifted to the right by 0·019° K., the temperature difference resulting from a pressure head of 16 cm., it agrees well with the lower one. Because of the existence of this effect, measurements above the λ-point were made with the liquid level only a few millimetres above the reflector, and the theoretical correction was then applied, measuring the pressure head from the middle of the etalon path. In this way it was possible to approach within 0·002° K. of the λ-point from above.

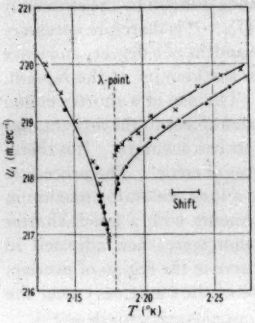

Figure 5.

Effect of hydrostatic pressure head.
× Pressure head = 20 cm.
● Pressure head = 4 cm.
Shift = Expected shift due to the change in hydrostatic pressure head.

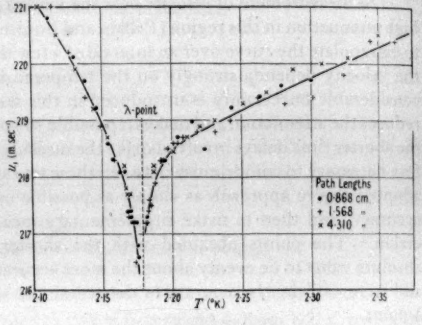

Figure 6.

Velocity of sound in liquid helium in the neighbourhood of the λ-point.

Figure 6 shows the results of measurements near the λ-point, after all corrections have been applied. For all the points on this curve the echo was large and the pulse amplitude correction discussed in § 2 was completely negligible. One of the most striking features of this curve is the sharp dip in the velocity within the last 0·02° K. above the λ-point, and a corresponding tendency for the velocity to decrease rapidly as the λ-point is approached from below. It is obviously impossible to say much about the discontinuity at the λ-point; in fact it is conceivable that both branches drop to very much lower values than have yet been observed. It should be remembered, however, that the Ehrenfest relations predict a discontinuity in the isothermal compressibility β, which is related to the velocity of sound by the formula

$$\beta = -\frac{1}{V}\left(\frac{\partial V}{\partial p}\right)_T = \frac{\gamma V}{u_1^2},$$

where γ, the ratio of the specific heats, can be expressed in terms of the coefficient of thermal expansion α: $\gamma - 1 \simeq Tu_1^2\alpha^2/C_v$, if $\gamma \simeq 1$. γ is a rapid function of temperature in the neighbourhood of the λ-point and may be entirely responsible for the peculiar behaviour of u_1 in this region. Calculations of β from u_1 using the rather inaccurate values of γ at present available suggest that β increases monotonically over the entire temperature range and has a discontinuity of at least 1% at the λ-point, but a firm decision on this issue must await more accurate measurements of the coefficient of thermal expansion α.

ACKNOWLEDGMENTS

The authors wish to thank Mr. L. R. O. Storey and Mr. T. Gold for their assistance in designing the equipment, and Dr. D. Shoenberg for his encouragement of the research. Some of the electronic units used in the work were originally built by Dr. J. M. M. Pinkerton. During the period of this research one of the authors (C.E.C.) was in receipt of a Fulbright Grant; the other (K.R.A), was the holder of an I.C.I. Fellowship in the University of Cambridge.

REFERENCES

ANDRONIKASHVILI, E. L., 1948, *J. Exp. Theor. Phys.*, **18**, 429.
ATKINS, K. R., and OSBORNE, D. V., 1950, *Phil. Mag.*, **41**, 1078.
VAN DIJK, H., and SHOENBERG, D., 1949, *Nature, Lond.*, **164**, 151.
FINDLAY, J. C., PITT, A., GRAYSON SMITH, H., and WILHELM, J. O., 1938, *Phys. Rev.*, **54**, 506; 1939, *Ibid.*, **56**, 122.
KEESOM, W. H., 1942, *Helium* (Amsterdam : Elsevier), p. 300.
LANDAU, L., 1941, *J. Phys., U.S.S.R.*, **5**, 71.
LOCK, J. M., PIPPARD, A.B., SHOENBERG, D., 1951, *Proc. Camb. Phil. Soc.*, in the press.
PELLAM, J. R., and SQUIRE, C. F., 1947, *Phys. Rev.*, **72**, 1245.
SCHMIDT, G., and KEESOM, W. H., 1937, *Physica, s' Grav.*, **4**, 971.

The Flow of Liquid Helium II through Wide Capillaries

BY K. R. ATKINS

Royal Society Mond Laboratory, Cambridge

Communicated by D. Shoenberg; *MS. received* 29*th May* 1951

ABSTRACT. A study has been made of the isothermal, pressure-induced flow of liquid helium II through glass capillaries of bore between $2{\cdot}6\times10^{-3}$ and 4×10^{-2} cm. The critical velocity is found to be less than 1 cm. sec^{-1} except, possibly, in the case of the finest capillary. The theory that there is a force of mutual friction between the normal and superfluid components predicts the correct order of magnitude for the flow velocities, but there are discrepancies which suggest the existence of some other source of friction.

§1. INTRODUCTION

WHEN liquid helium II flows through very narrow channels, or through the helium film, at velocities less than a certain critical value v_c, the frictional forces opposing the flow are very small and may even vanish (Daunt and Mendelssohn 1946, Atkins 1950 b, Bowers and Mendelssohn 1950). Above this critical velocity, however, the frictional forces increase rapidly and appreciable pressure gradients are necessary to produce even a small increase in velocity. Similar phenomena are observed when the flow is produced thermally (Kapitza 1942). Velocities up to v_c are produced by temperature differences too small to be measured, but as soon as v_c is exceeded the required temperature difference begins to increase rapidly. However, in channels of width greater than 10^{-3} cm. the situation is entirely different (Allen and Misener 1939). In such channels there is, as yet, no experimental evidence for the existence of frictionless flow and the critical velocity, if it exists, must be very small. The velocity of flow varies in a markedly non-linear manner with the pressure gradient and the frictional forces obviously have a complicated and

unprecedented character. Although superfluidity is more clearly manifested in the frictionless region below the critical velocity, the manner in which it breaks down in the imperfect region above the critical velocity may provide valuable clues concerning its nature.

One aspect of the problem, thermal conduction in capillaries, has already been extensively studied and, apart from minor discrepancies, is satisfactorily explained in terms of the two-fluid theory if one assumes that there is a mutual force between the two components varying approximately as the cube of their relative velocity (Gorter and Mellink 1949). The present paper extends the experimental evidence by a detailed study of the case of isothermal, pressure-induced flow through glass capillaries. Still further evidence is provided by the experiments of Hollis-Hallett (1950) on the damping of the motion of a disc performing large-amplitude torsional oscillations in the liquid. In a later paper these various lines of evidence will be compared in an attempt to deduce the nature of the frictional forces and to decide whether the Gorter–Mellink theory of mutual friction is adequate to explain all the results.

§ 2. DESIGN OF THE EXPERIMENTS

An experimental survey of the whole field of flow phenomena in capillaries has already been made by Allen and Misener (1939) and it is clear from this work that the situation is very complex. The present research was therefore mainly concerned with a more detailed investigation at the lowest temperature easily obtainable (about 1·2° K.), because at this temperature the normal component was only about 3% of the whole, so that one was studying the flow of practically pure superfluid and the results could be more easily interpreted. Even if the flow of the normal component had been restricted only by its own viscosity, of the order of 40 micropoises (Andronikashvili 1948), its contribution to the total flow could not have amounted to more than 1% except in the case of the widest capillary when it might have amounted to 5% at the highest pressure gradient. To obtain some idea of the variation of various quantities with temperature, the measurements were repeated at 1·5° K., which was the highest temperature at which it was reasonably certain that the flow was not being influenced by the thermal effects discussed below.

Figure 1 shows the three types of flow vessel used. The rate of flow of liquid through the capillary C was measured by taking cathetometer readings of the meniscus in the monitoring capillary M which had an internal diameter of about 0·5 mm. This procedure was preferable to making direct observations of the meniscus in the main reservoir R, because the smaller meniscus in M was more sharply defined and also the surface tension rise in M kept its meniscus clear of the bath meniscus, enabling reliable observations to be made at small pressure heads. Capillaries longer than 10 cm. were accommodated either in the form of a spiral (Figure 1 (*a*)) or as six adjacent straight portions joined together by much wider tubing (Figure 1 (*b*)). The relative advantages of these two arrangements will be discussed in § 4 (i). The constriction at F reduced transfer of liquid through the film, but, because of certain considerations discussed below in connection with the thermo-mechanical effect, it was not permissible to make this constriction so narrow that the film flow correction could be entirely neglected. Therefore, in order that this correction might be reliably estimated, it was

necessary to avoid the increased rates of flow resulting when the film is formed on a surface contaminated by solid deposits (Bowers and Mendelssohn 1949), and the experiments were therefore performed inside a cryostat specially designed to avoid such contamination (Atkins 1950a). The correction was then based on the assumption of a rate of film flow equal to 8×10^{-5} cm^3 sec^{-1} cm^{-1}, which was confirmed in the case of two of the vessels by studying the flow when the end of the capillary C was sealed off. Because the experiment was performed inside a closed chamber containing a constant amount of liquid, there was no correction to the pressure head arising from evaporation effects, and the small change in the position of the outer level accompanying a change in the inner level could be calculated accurately from purely geometrical considerations.

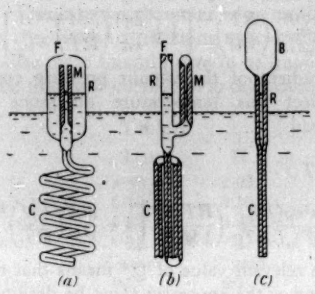

Figure 1. The vessels.

Thermal effects associated with the flow are sufficiently important to justify a detailed calculation of their magnitude. The mechano-caloric effect results in a heat input to the reservoir R of $\pi r^2 \rho v Q^*$ erg sec^{-1}, where r is the radius of the capillary C, ρ is the density of the liquid, v is the mean velocity of flow and Q^* is the amount of cold transported per unit mass of liquid, which is unknown but is certainly not greater than TS. This heat is dissipated by a distillation process in which liquid evaporates from the reservoir and is condensed again in the bath. Evaporation from the reservoir surface can take place only if there is a pressure discontinuity Δp_s between liquid and vapour and simple kinetic theory considerations show that the rate of evaporation is

$$\frac{1}{4}\left(\frac{3M}{RT}\right)^{1/2} A \Delta p_s \text{ gm.sec}^{-1}. \qquad \ldots\ldots(1)$$

M is the molecular weight, R is the gas constant, T the temperature, A the cross-sectional area of the reservoir, and we have assumed that the vaporization coefficient is unity. Equating the heat input to the required latent heat (L ergs per gm.) we obtain

$$\Delta p_s = \frac{4\pi r^2 v \rho Q^*}{LA}\left(\frac{RT}{3M}\right)^{1/2}. \qquad \ldots\ldots(2)$$

There is also a pressure drop Δp_c across the constriction F arising from the viscous flow of gas through it. If this constriction has radius a and an effective length λ and the gas has a density ρ_g and a viscosity η, then, using Poiseuille's

formula to relate the volume of gas evaporating per second to the pressure drop across the constriction,

$$\left.\begin{aligned}\frac{1}{4}\left(\frac{3M}{RT}\right)^{1/2}\frac{A}{\rho_g}\Delta p_s &= \frac{\pi a^4}{8\eta\lambda}\Delta p_c,\\ \frac{\Delta p_c}{\Delta p_s} &= \frac{2\eta\lambda}{\pi a^4}\left(\frac{3M}{RT}\right)^{1/2}\frac{A}{\rho_g}.\end{aligned}\right\} \quad \ldots\ldots(3)$$

As the cross-sectional area of the bath is so large, the pressure discontinuity there may be neglected, and so the temperature difference needed between the inner and outer levels to produce the pressure difference between them is

$$\begin{aligned}\Delta T &= (\Delta p_s + \Delta p_c)/(dp/dT)_0,\\ &= \frac{4\pi r^2 v\rho Q^*}{(dp/dT)_0 LA}\left(\frac{RT}{3M}\right)^{1/2}\left[1+\frac{2\eta\lambda}{\pi a^4}\left(\frac{3M}{RT}\right)^{1/2}\frac{A}{\rho_g}\right], \quad \ldots\ldots(4)\end{aligned}$$

$(dp/dT)_0$ being the gradient of the vapour pressure curve. Because of the thermo-mechanical effect this temperature difference is equivalent to a hydrostatic pressure head

$$\begin{aligned}\Delta h &= \frac{Q^*}{Tg}\Delta T,\\ &= \frac{4\pi r^2 v\rho Q^{*2}}{(dp/dT)_0 LATg}\left(\frac{RT}{3M}\right)^{1/2}\left[1+\frac{2\eta\lambda}{\pi a^4}\left(\frac{3M}{RT}\right)^{1/2}\frac{A}{\rho_g}\right]. \quad \ldots\ldots(5)\end{aligned}$$

The uncertainty in the relevant value of Q^* means that this correction cannot be reliably estimated, and so the apparatus must be designed in such a way that it is negligible. This was achieved by using as large a reservoir as possible (large A) and choosing the diameter of the constriction F so that the second term was no larger than the first. The investigation was in any case restricted to temperatures below 1·5° K. where the thermo-mechanical effect is small. Under these circumstances it can be shown that, even if Q^* is given its maximum value TS, the correction was entirely negligible, except at pressure heads less than 10^{-2} cm. of He, when the situation was, however, also complicated by the presence of oscillations (see Table 1).

An alternative approach to the problem would be to produce the flow thermally by deliberate supply of heat and to measure both the temperature difference and the hydrostatic pressure head, but this method was not adopted for two reasons. It is not yet certain that a temperature difference is the exact equivalent of a pressure head, and, in any case, the conversion factor between the two is not yet known. Moreover, if this conversion factor should turn out to be the one applicable to the thermo-mechanical effect in narrow slits (see equations (12) and (13)), then the smallest measurable temperature difference would correspond to a pressure head of about 5×10^{-2} cm. of helium, whereas the true hydrostatic pressure head can be measured to an accuracy of 5×10^{-3} cm. of helium and it is thought that the thermo-mechanical effect can be made as small as 4×10^{-4} cm. of helium by suitable design of the apparatus.

In the case of the very finest capillary of bore $2{\cdot}62\times10^{-3}$ cm., any permissible outlet at the top of the reservoir would have introduced an intolerably large film flow correction. Therefore, as shown in Figure 1 (*c*), the top of the reservoir was sealed off by a large thin-walled glass bulb B with a surface area of about 20 cm². Thermal contact between the inside and outside of the reservoir was

achieved by thermal conduction through the glass wall of this bulb. The figure quoted for the thermo-mechanical effect in Table 1 is based on the thermal conductivity of glass at 1·3° K. as measured by Keesom (1945).

To minimize effects due to heat entering the cryostat from outside, the vessels were illuminated by sodium light from which heat radiation had been removed by a filter of Chance ON19 glass and the efficacy of this procedure was proved by the fact that rates of emptying were equal to rates of filling to within the experimental error (see Figure 2).

§ 3. EXPERIMENTAL DETAILS

Table 1 contains a complete description of the various capillaries and their associated reservoirs. The internal diameter of a capillary was measured at various points along its length with a travelling microscope, and deviations from the mean are given in case these should prove to be important when the flow is better understood. The film flow correction is calculated on the basis of a rate

Table 1

Capillary	I	II	III	IV
Mean int. diam. (cm. $\times 10^{-2}$)	4·40	2·03	0·815	0·262
Variation of int. diam. (cm. $\times 10^{-2}$)	0·10	0·10	0·013	0·01
Cross section of reservoir (cm^2)	3·50	0·892	0·201	0·00571
Capillary lengths used (cm.)	48·6, 8·04, 1·75	46·6, 7·90	8·03, 0·83	7·76
Form of longest capillary	Zigzag	Zigzag	Straight	Straight
Diam. of film constriction (cm.)	0·2	0·1	0·09	0
Film flow corr. to velocity (cm/sec.)	0·03	0·08	0·55	0
Thermo-mech. corr. (cm $\times 10^{-4}$ of He)	3·6	2·7	2·0	~2

of film flow equal to 8×10^{-5} cm^3 sec^{-1} cm^{-1}. The thermo-mechanical correction is an upper limit obtained by putting $Q^* = TS$ in equation (5) and refers to a temperature of 1·2° K. The value at 1·5° K. is approximately four times as large. This correction is proportional to the mean velocity of flow through the capillary and the value quoted is for a mean velocity of 1 cm. sec^{-1}.

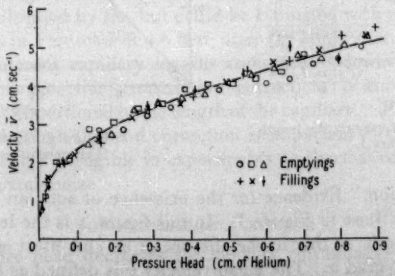

Figure 2. Mean velocity as a function of pressure head. Bore of capillary = 0·203 mm. Temperature = 1·22° K.

The experimental procedure was to raise or lower the vessel until there was a level difference of about 1 cm. and then to time the meniscus in the monitoring capillary (M in Figure 1) as it traversed the scale in the eyepiece of a cathetometer. This scale had previously been calibrated against a scale engraved on metal and

found to be linear to within 1%. The two principal sources of random error were probably fluctuations in the bath temperature and optical flaws in the walls of the Dewar flasks, and it was necessary to repeat the procedure several times in order to obtain sufficient accuracy. Figure 2 shows the size of the random error and illustrates how an accurate curve could be obtained by smoothing out the data from six runs.

§ 4. CORRECTIONS

(i) *End Corrections*

When an ideal classica. liquid with zero viscosity enters a narrow pipe in which the velocity is v, there is a pressure drop of $\frac{1}{2}\rho v^2$ at the entrance, arising from the Bernoulli effect, but there is also an equal and opposite pressure rise at the exit, so that the total end effect is zero. In the case of a viscous liquid, however, the effect of the frictional forces is to produce a non-zero total pressure drop, giving rise to the well-known Hagenbach correction (see, for example, Prandtl and Tietjens 1934). When the flow of liquid helium II is subject to frictional forces, as it is in wide capillaries, one might expect to find a similar end effect which, if comparable with the Hagenbach effect, would involve an

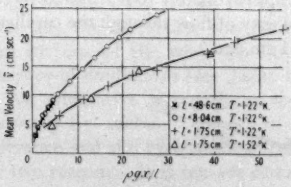

Figure 3. Effect of varying the length of capillary l.

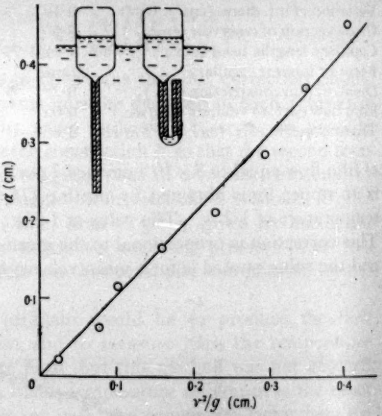

Figure 4. End effects. Temperature = 1·2° K.

important correction. Evidence for the existence of such an effect is provided by curves such as those in Figure 3. In this figure, x is the level difference and l the capillary length, so that in the absence of an end effect $\rho g x/l$ would be the pressure gradient, grad p. The mean velocity $\bar{v}$ is defined as the rate of flow in cm^3 sec^{-1} divided by the mean cross-sectional area of the capillary. The mean velocity should be a unique function of grad p, independent of capillary length, but is obviously not a unique function of $\rho g x/l$, the discrepancy going in such a direction as to indicate that $\rho g x/l$ is greater than grad p because of an end effect. To investigate the matter further and to confirm that this was really an end effect rather than, say, a thermo-mechanical effect, the vessels shown in the inset to Figure 4 were used. A capillary of internal diameter $0{\cdot}48 \pm 0{\cdot}01$ mm. and

length 8·1 cm. was attached to a reservoir of cross section 3·86 cm² with a film constriction of diameter 2 mm. The flow measurements were repeated with a bulb inserted in the middle of the capillary and the capillary length only slightly different (7·3 cm.). The bulb introduced extra end corrections and the pressure head needed to produce a given velocity of flow was considerably larger. Denoting the end correction by $\epsilon(\bar{v})$ cm. of helium and assuming that in the capillary grad $p=f(\bar{v})$ then, in the absence of the bulb,

$$\rho g x_1 = f(\bar{v}) l_1 + \epsilon(\bar{v}). \qquad \ldots\ldots(6)$$

With the bulb

$$\rho g x_2 = f(\bar{v}) l_2 + 2\epsilon(\bar{v}). \qquad \ldots\ldots(7)$$

Eliminating $f(\bar{v})$ and remembering that x_1 and x_2 then refer to the same $\bar{v}$,

$$\rho g(x_2/l_2 - x_1/l) = (2/l_2 - 1/l_1)\epsilon(\bar{v}). \qquad \ldots\ldots(8)$$

In Figure 4 $\alpha=(x_2/l_2-x_1/l_1)/(2/l_2-1/l_1)$ has been plotted against $\bar{v}^2/g$ to give a straight line of slope $1{\cdot}05 \pm 0{\cdot}05$, so the end correction is $1{\cdot}05\rho\bar{v}^2$ which includes both the entrance and exit of the capillary.

A correction of this magnitude was applied to the results at all temperatures and for all capillary sizes. Figure 3 proves that the correction is independent of temperature, because at high velocities where most of the pressure head is due to end effects, the curves at 1·2° K. and 1·5° K. coincide. There is some doubt whether the correction is the same in the finest capillaries in which the flow may be tending towards the ideal 'superfluid' character it manifests in the film, but the velocities are then small and the correction not very important. In addition to the end correction there is probably also a 'constriction correction' to be applied at every point where the bore is slightly constricted or whenever the bore tapers. It is easily seen that very slight constrictions at very few places could produce an effect comparable with the end correction and it is unfortunately impossible to make any estimate of the effect. For this reason the zigzag type of capillary shown in Figure 1 (*b*) is to be preferred to the spiral shown in 1 (*a*). When such a spiral was cut up and calibrated it was found that its bore had been appreciably distorted and this probably explains why such spirals always required anomalously high pressure heads to produce a given velocity. In the case of the zigzag capillary the end correction was multiplied by six, but could be estimated with tolerable accuracy, and it will be seen in Figures 5 and 6 that, after the application of the correction, the curves for different capillary lengths coincided. However, one must not conclude from this that the 'constriction correction' is unimportant, as this correction may be proportional to the length of the capillary. Finally, it should be mentioned that, although this end correction is important in the present experiments, it is completely negligible in experiments on thermal conduction through capillaries of comparable size.

(ii) *Acceleration Correction*

As the pressure head decreases the velocity continually decreases and the liquid always has a finite acceleration. The frictional forces are therefore not quite balanced out by the pressure head and a small correction should be applied for this. The required correction is easily shown to be

$$\Delta x = \frac{\pi\rho r^2 v}{A} \frac{\partial v}{\partial (\text{grad } p)}. \qquad \ldots\ldots(9)$$

Under all conditions in the present experiments this correction was smaller than the observational error and could be completely neglected.

§ 5. PRESENTATION AND DISCUSSION OF RESULTS

The experimental results are collected together in Figures 5 and 6, and the region of small pressure gradients is shown in greater detail in Figures 7 and 8. The previous results of Allen and Misener (1939) show a similar behaviour, but their velocities are always rather lower than the present ones. This may be a consequence of the fact that their capillaries were spiralled and therefore more susceptible to constriction effects. The use of spirals in the present research always led to lower velocities and all results obtained with them have been rejected.

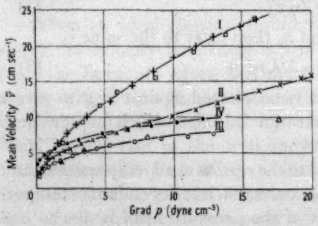

Figure 5. Mean velocity as a function of the pressure gradient for the shorter capillaries at 1·22° K.

Capillary I + l=8·04 cm. □ l=1·75 cm.
Capillary II × l=7·90 cm.

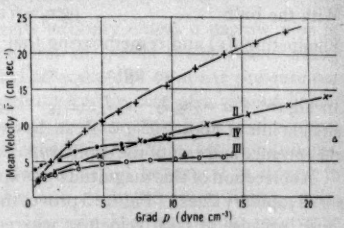

Figure 6. Mean velocity as a function of the pressure gradient for the shorter capillaries at 1·52° K.

Capillary III ○ l=8·03 cm. △ l=0·83 cm.
Capillary IV ● l=7·76 cm.

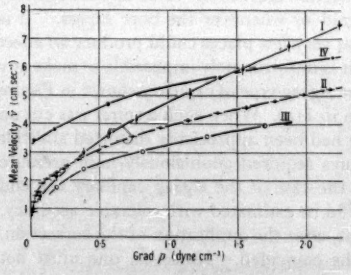

Figure 7. Variation of velocity in the region of small pressure gradients at 1·22° K.

Capillary I ◐ l=48·6 cm.
Capillary II ◒ l=46·6 cm.

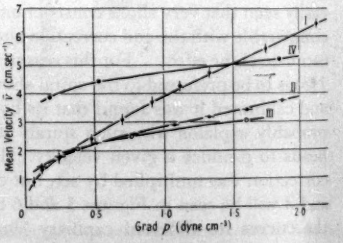

Figure 8. Variation of velocity in the region of small pressure gradients at 1·52° K.

Capillary III ○ l=8·03 cm.
Capillary IV ● l=7·76 cm.

It is important to notice that for velocities below 5 cm. sec^{-1} when the end correction is too small to influence the matter, there is good agreement between the curves for different capillary lengths. This could not be the case if the thermo-mechanical effect were important.

In an earlier paper (Atkins 1950 b) it has been suggested that flow results can be conveniently discussed on the basis of the empirical formula

$$v = v_1(r) + v_2(\text{grad}\, p) + v_3(\text{grad}\, p, r)\,. \qquad \ldots\ldots(10)$$

The critical velocity v_1 is such that the frictional forces are negligibly small until v_1 is exceeded. v_1 is believed to decrease as r increases. In Figures 5 to 8 v_1 would

appear as an intercept on the velocity axis. In the film v_1 is about 40 cm. sec^{-1}, but it is clear from Figures 5 to 8 that when r is greater than 4×10^{-3} cm. v_1 cannot be greater than 1 cm.sec^{-1}. It is noticeable, however, that the curve for the 0·0262 mm. capillary runs parallel to the curve for the 0·0815 mm. capillary but is displaced upwards from it by about 2 cm. sec^{-1}, suggesting that v_1 is greater for the finer capillary by this amount. It would be unwise to place too much reliance on the precise values of the velocities obtained with the 0·0262 mm. capillary, as this capillary was very difficult to clean and to keep free from blockages, but it is difficult to escape the conclusion that the velocity was greater in this very fine capillary, particularly as precautions were taken to eliminate film flow effects (see § 2). The product of critical velocity and radius seems to be at least 2×10^{-3} cm^2 sec^{-1}, as compared with a film transfer of 8×10^{-5} cm^2 sec^{-1}. A more detailed and careful research into capillaries of this size would probably be very fruitful, but it would be necessary to select very uniform capillaries and to develop a technique for cleaning them and measuring their bores accurately.

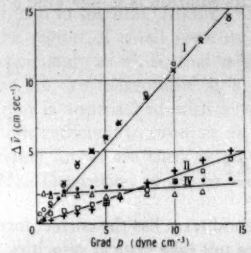

Figure 9. Difference curves.

Capillary I ⊙ 1·22° K. × 1·52° K.
Capillary II □ 1·22° K. + 1·52° K.
Capillary IV △ 1·22° K. ● 1·52° K.

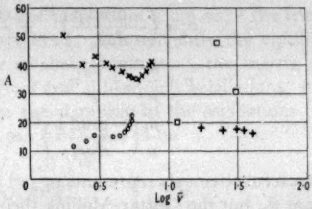

Figure 10. A as a function of velocity.

Flow through a 0·0815 mm. capillary
× 1·22° K. ○ 1·52° K.
Thermal conduction in a 0·095 mm. capillary
+ 1·31° K. □ 1·61° K.

The component v_2 of the velocity can be eliminated by subtracting curves for different radii:

$$v(r') - v(r) = v_1(r') - v_1(r) + v_2(r', \operatorname{grad} p) - v_2(r, \operatorname{grad} p). \quad \ldots\ldots (11)$$

This has been done in Figure 9 by subtracting the curve for the capillary of bore $0{\cdot}815 \times 10^{-2}$ cm. (capillary III) from all the others. It is immediately obvious that these difference curves are straight lines to within the experimental accuracy and that the curves for the two temperatures coincide. The component v_2 may therefore be represented approximately over the whole of the temperature range by the empirical formula $v_2 = \alpha(r) \operatorname{grad} p$. To evaluate v_2 exactly would require a much more extensive study of the exact form of v_1 and v_2, but it is fairly clear that for the capillary of bore $0{\cdot}815 \times 10^{-2}$ cm. (capillary III) v_1 is small (Figure 7) and v_2 is also small (Figure 9) so that the curve for this capillary may be taken to indicate the nature of v_2. It is probable that v_2 varies approximately as $(\operatorname{grad} p)^{1/3}$, but it is not possible to verify this relation more precisely.

The theory of Gorter and Mellink (1949) makes quite definite predictions concerning the velocity of flow in wide capillaries and these predictions will now be

compared with the experimental results. The fundamental equations suggested by Gorter and Mellink are

$$\rho_s \frac{dv_s}{dt} = \frac{-\rho_s}{\rho} \operatorname{grad} p + \rho_s S \operatorname{grad} T + A\rho_n\rho_s(v_n - v_s)^3, \quad \ldots\ldots(12)$$

$$\rho_n \frac{dv_n}{dt} = \frac{-\rho_n}{\rho} \operatorname{grad} p - \rho_s S \operatorname{grad} T - A\rho_n\rho_s(v_n - v_s)^3 + \eta_n \nabla^2 v_n. \quad \ldots\ldots(13)$$

Apart from the basic assumption that the two-fluid theory is still applicable at velocities exceeding the critical velocity, the novel feature of these equations is the term $A\rho_n\rho_s(v_n - v_s)^3$ which represents a force of mutual friction between the two components. For isothermal flow through capillaries these equations reduce to

$$(\rho_s/\rho) \operatorname{grad} p = A\rho_n\rho_s(v_n - v_s)^2, \quad \ldots\ldots(14)$$

$$(\rho_n/\rho) \operatorname{grad} p = -A\rho_n\rho_s(v_n - v_s)^3 + \eta_n \nabla^2 v_n. \quad \ldots\ldots(15)$$

Adding,

$$\operatorname{grad} p = \eta_n \nabla^2 v_n. \quad \ldots\ldots(16)$$

This is the usual equation for viscous flow and its solution is $v_n = (r^2 \operatorname{grad} p/8\eta_n)$, whence, from equation (14),

$$v_s = \left(\frac{-\operatorname{grad} p}{A\rho\rho_n}\right)^{1/3} + \frac{r^2 \operatorname{grad} p}{8\eta_n}, \quad \ldots\ldots(17)$$

$$\bar{v} = \frac{\rho_s}{\rho} v_s + \frac{\rho_n}{\rho} v_n \quad \ldots\ldots(18)$$

$$= \frac{\rho_s}{\rho}\left(\frac{-\operatorname{grad} p}{A\rho\rho_n}\right)^{1/3} + \frac{r^2 \operatorname{grad} p}{8\eta_n}. \quad \ldots\ldots(19)$$

The first term obviously represents v_2 and the second term has the correct form to represent v_3, but the Gorter–Mellink theory does not take critical velocities into account and so v_1 is naturally absent. For the $0{\cdot}815 \times 10^{-2}$ cm. capillary $\bar{v}$ is approximately equal to v_2 and, by equating it to $(\rho_s/\rho)[(\operatorname{grad} p)/A\rho\rho_n]^{1/3}$, A has been deduced and plotted against v in Figure 10. The same graph shows the values of A deduced by Gorter and Mellink from thermal conduction experiments. There is

Table 2

Temp. (° K.)	Diameter of capillaries r' (cm.)	Diameter of capillaries r (cm.)	Viscosity (μpoise) from Difference curves	Viscosity (μpoise) from Oscillating discs
1·22° K.	$4{\cdot}40 \times 10^{-2}$	$0{\cdot}815 \times 10^{-2}$	53	39
1·50° K.	$4{\cdot}40 \times 10^{-2}$	$0{\cdot}815 \times 10^{-2}$	53	13
1·21° K.	$2{\cdot}03 \times 10^{-2}$	$0{\cdot}815 \times 10^{-2}$	32	39
1·50° K.	$2{\cdot}03 \times 10^{-2}$	$0{\cdot}815 \times 10^{-2}$	32	13

a satisfactory order of magnitude agreement, but exact agreement is not to be expected in view of the possible errors of an experimental nature in both sets of experiments and the difficulty in eliminating contributions from v_1 and v_3.

Significant discrepancies arise, however, when v_3 is compared with $(r^2 \operatorname{grad} p/8\eta_n)$. It is immediately obvious that, whereas v_3 is practically independent of temperature in the range 1·2° K. to 1·5° K., η_n is known to vary rapidly over this temperature range. In Table 2 values of η_n deduced from the slopes of the difference curves in Figure 9 are compared with the values measured in oscillating disc experiments (Andronikashvili 1948). The disagreement appears too large to

be explained away by experimental errors. For example, if one assumes that the discrepancy is entirely due to the constriction correction discussed in § 4, this correction can be evaluated by assuming that equation (19) has to apply at 1·2° K., and one then finds that if a similar correction is applied at 1·5° K. there is still a large discrepancy at this temperature.

The possibility that the flow became turbulent should be carefully considered. Turbulence in the normal component alone can be completely discounted, as the Reynolds' number $\bar{v}r\rho_n/\eta_n$ never rose above 750. If the superfluid component is considered to be a liquid with zero viscosity, then turbulence is very likely to be set up in it, but if the fundamental equation describing its behaviour is taken to be curl $v_s=0$, then it would be very unlikely to become turbulent. The question of turbulence in the superfluid component is therefore best left in abeyance until there is strong experimental evidence in its favour.

§ 6. OSCILLATIONS

The type of oscillation observed in very narrow channels (Allen and Misener 1939) and in the film (Atkins 1950 a) was also observed in these wide capillaries. In the region of small pressure heads the frictional forces are small and vary approximately as v^3, so that when v is less than about 1 cm.sec^{-1} the frictional forces are not measurable as a pressure head. Consequently the equilibrium position is approached with a velocity of about 1 cm.sec^{-1}, the inertia of the liquid is sufficient to produce an overshoot and subsequent oscillations, and the frictional forces are then so small that the damping of the oscillations is only slight. The period of the oscillations can be shown to be

$$\tau_0=2\pi\left(\frac{\rho}{\rho_s}\frac{Al}{\pi r^2 g}\right)^{1/2}. \qquad \ldots\ldots(20)$$

In the present case there are two complications arising because (*a*) the thermo-mechanical effect cannot be ignored, and (*b*) the film is in parallel with the capillary and alters the period by a few per cent. In Table 3 the observed periods are compared with the periods calculated from equation (20). Results

Table 3

Capillary	I	IV	V	VI
Mean int. diam. (cm. $\times 10^{-2}$)	4·40	0·262	3·29	2·10
Capillary length (cm.)	48·6	7·76	76·8	93·6
Cross-sectional area of reservoir (cm^2)	3·50	0·00571	3·50	0·704
Form of capillary	Zigzag	Straight	Spiral	Spiral
Observed period (sec.) 1·2° K.	60·0	15·7	120·2	92·8
Observed period (sec.) 1·5° K.	64·3	19·2	—	100·2
Calculated period (sec.) 1·2° K.	59·5	18·4	99·7	86·3
Calculated period (sec.) 1·5° K.	62·9	19·6	—	92·0

for the spirals are included because end effects and constriction effects are not likely to be important at the small velocities involved in the oscillations. Both the thermo-mechanical effect and the film effect would decrease the period so that where the observed period is greater than the calculated period, as in some of the spiralled capillaries, this suggests that the mean radius was slightly less than the measured value because of the distortion produced when the capillary was bent. Equation (20) is based on the assumption that the velocity is constant over the cross section of the capillary, and, if this were not so, r would have to be

replaced by an effective radius. The approximate agreement between observed and calculated periods excludes such possibilities as that the flow is mainly confined to the walls of the capillary. In a more accurate experiment specifically designed to investigate oscillations and to eliminate the disturbing effects mentioned above, it might be possible to decide whether the velocity really is constant over the cross section of the capillary.

§7. CONCLUSIONS

In capillaries of diameter greater than 10^{-2} cm. the critical velocity, if it exists, is less than 1 cm. sec^{-1}, but there is evidence that it is rather greater than this in a capillary of diameter $0{\cdot}26 \times 10^{-2}$ cm. The major part of the flow in these wide capillaries is opposed by frictional forces and is not truly 'superfluid'. The Gorter–Mellink theory of mutual friction is almost adequate to explain the results, but there are discrepancies, and it seems that the results are explicable only if there is some other type of frictional force in addition to the mutual friction. This conclusion is considerably strengthened by the oscillating disc experiments of Hollis-Hallett (1950), and will be discussed in further detail in a later paper.

ACKNOWLEDGMENTS

The author wishes to thank Dr. D. V. Osborne and Mr. C. E. Chase for their assistance with the measurements. The research was made possible by the award of an I.C.I. Fellowship in the University of Cambridge.

REFERENCES

ALLEN, J. F., and MISENER, A. D., 1939, *Proc. Roy. Soc.* A, **172,** 467.
ANDRONIKASHVILI, E. L., 1948, *J. Exp. Theor. Phys.*, **18,** 429.
ATKINS, K. R., 1950 a, *Proc. Roy. Soc.* A, **203,** 119 ; 1950 b, *ibid.*, **203,** 240.
BOWERS, R., and MENDELSSOHN, K., 1949, *Nature, Lond.*, **164,** 660 ; 1950, *Proc. Phys. Soc.* A, **63,** 178.
DAUNT, J. G., and MENDELSSOHN, K., 1946, *Nature, Lond.*, **157,** 829.
GORTER, C. J., and MELLINK, J. H., 1949, *Physica*, **15,** 285.
HOLLIS-HALLETT, A. C., 1950, *Proc. Phys. Soc.* A, **63,** 1367.
KAPITZA, P. L., 1942, *J. Phys. U.S.S.R.*, **5,** 59.
KEESOM, P. H., 1945, *Physica*, **11,** 339.
PRANDTL, L., and TIETJENS, O. G., 1934, *Applied Hydro- and Aero-Mechanics* (New York : McGraw-Hill), p. 21.

LETTERS TO THE EDITOR

X-Ray Asterisms from Deformed Crystals

It has been suggested (Barrett 1940) that x-ray asterisms from deformed metal crystals originate from deformation bands, i.e. narrow regions wherein variations in lattice orientation occur. Recent work with aluminium has shown that the term deformation band embraces at least two different phenomena (Honeycombe 1951). A distinction has been made between bands of lattice curvature which have been called kink bands and bands in which local orientation differences have arisen because of slip on a second set of planes. The latter have been called bands of secondary slip. Evidence obtained by optical (Cahn 1950, 1951) and x-ray micrography (Honeycombe 1950) has suggested that the kink bands are responsible for the major part of the asterism smear in x-ray Laue photographs of aluminium single crystals deformed in tension.

Ordinary x-ray methods, using beams of 0·5 to 1 mm. diameter, cannot give direct evidence since the kink bands occur on a microscopic scale (Figure 1). They are usually about 0·01 mm. wide and between 0·02 and 0·2 mm. apart, depending on such variables as the extent of deformation, the orientation of the crystal and the purity of the metal. It appeared, however, that application of the x-ray microbeam technique (Hirsch and Kellar 1951, Gay *et al.* 1951) would provide direct evidence on this problem. The specimen examined was aluminium of 99·99% purity and of very large grain size (1–2 cm.). It was electropolished in the annealed condition, then strained in tension by about 7·5% elongation. One grain which had developed widely spaced kink bands was selected for detailed examination using an x-ray microbeam of 100μ diameter. To enable accurate location of the beam on chosen microscopic areas, a special specimen holder was used, details of which will be published elsewhere.

It was found that if the beam was directed on a region between two kink bands, the resulting Laue spots showed little asterism (Figure 2). If the width of the kink band was completely covered by the incident beam, then marked asterisms appeared in the x-ray

Figure 1. Micrograph of surface of electropolished deformed specimen of aluminium, showing kink bands (magnification ×75).

Figure 2. Section of a microbeam Laue photograph taken with the x-ray beam incident between the kink bands.

Figure 3. A similar section of a microbeam Laue photograph taken with the x-ray beam straddling a kink band. The reflections are the same as those shown in Figure 2.

photographs (Figure 3). For the cases examined, the range of orientation within the band was approximately three degrees. No marked structure was observed in the asterism streaks. In previous macrobeam experiments on lightly deformed aluminium crystals, the asterisms usually contained intensity maxima. These have been attributed to reflections from the slightly disorientated lamellae between the kink bands, the latter being responsible for the diffuse part of the asterism. This view is confirmed by the fact that in the present experiments, in which only one lamella is irradiated, the asterism streaks are continuous.

It is recognized that asterisms also arise from macroscopically bent crystals, but these experiments show that for aluminium crystals deformed by small amounts in tension the asterism is mainly caused by the kink bands, which are regions of curvature on a microscopic scale. It is relevant to note that crystals of some other metals, e.g. cadmium, which do not develop kink bands when deformed in tension, show very little asterism.

Cavendish Laboratory,
Cambridge.
23rd May 1951.

P. Gay.
R. W. K. Honeycombe.

Barrett, C. S., 1940, *Trans. Amer. Inst. Min. Metall. Engrs.*, **137**, 128.
Cahn, R. W., 1950, *Proc. Phys. Soc.* A, **63**, 323; 1951, *J. Inst. Met.*, **79**, 129.
Gay, P., Hirsch, P. B., Thorp, J. S., and Kellar, J. N., 1951, *Proc. Phys. Soc.* B, **64**, 374.
Hirsch, P. B., and Kellar, J. N., 1951, *Proc. Phys. Soc.* B, **64**, 369.
Honeycombe, R. W. K., 1950, *Proc. Phys. Soc.* A, **63**, 673; 1951, *J. Inst. Met.*, in the press.

On the Identity of β-Rays with Electrons

Goldhaber and Goldhaber (1948) have pointed out that if the identity of negative β-rays with atomic electrons were not complete, then, in accordance with the Pauli principle, β-rays might be expected to undergo capture into bound orbits which are already filled with atomic electrons. Such a process must occur as a prelude to the capture of negative mesons by nuclei (Fermi, Teller and Weisskopf 1947). If this effect exists one should detect characteristic x-radiation from the capturing atom, modified by screening and the possible differences in mass or spin between the β-particle and an atomic electron. Goldhaber and Goldhaber (1948) gave an experimental upper limit of 3% to the number of β-rays from a ^{14}C source which could have been captured into the K shell of a lead absorber.

A more suitable source and more efficient detection have allowed us to improve on this figure.

We have examined the bremsstrahlung from the β-rays emitted by a source of ^{3}H absorbed in a thin layer of zirconium (approximately 0·2 mm. thick) in which sensibly all the β-rays were stopped. A NaI (Tl) crystal (Harshaw Chemical Co.) and a photomultiplier (E.M.I. type VX5032) were used to analyse the x-radiation in the manner described by West, Meyherhof and Hofstadter (1951).

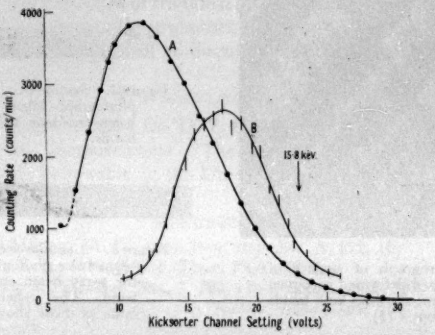

Pulse height distributions for bremsstrahlung due to tritium β-rays stopped in zirconium (curve A) and L x-rays (mean energy 11·8 kev.) of bismuth (curve B).

In the Figure is shown the pulse height distribution from the tritium source; on the same Figure is plotted, as an indication of the resolution and the calibration, the distribution for the bismuth L x-rays.

Tests showed that over the energy range 10–100 kev. the pulse height varied linearly with quantum energy.

The general form of the spectrum can be explained as bremsstrahlung from the tritium β-rays modified by the spread in pulse height and the heavy absorption in the Zr below about 6 kev. (corresponding to 12 volt pulses).

From our results we may set an upper limit to the number of β-rays of ^{3}H which could have been captured into a K shell of Zr. Since the mass of a β-particle of ^{3}H can differ from that of an electron by at most about 4%, we should expect to find the radiation from its capture into a K orbit of Zr close to the normal K line, i.e. at approximately 16 kev.

The pulse height distribution fails to reveal any trace of an x-ray line in this region; we may set an upper limit to the intensity of such a line by attributing to it all pulses of height exceeding 23 volts (corresponding to $h\nu = 15{\cdot}8$ kev.). The resulting counting rate is 10^{4} per second or, when corrected for self absorption, $2{\cdot}5 \times 10^{4}$ per sec. Since the crystal was sufficiently thick to stop all the x-rays reaching it from the source we have assumed that the detection efficiency was close to 100%.

The number of β-rays per second from the source of ^{3}H was estimated as 10^{10} from the known volume of tritium occluded in the zirconium. Hence not more than 2·5 in 10^{6} β-rays of tritium can have been captured into a K shell of zirconium.

In recent notes Charpak and Suzor (1950, 1951) explain certain details of their experiments on the back scattering of positive and negative β-rays (as compared with internal conversion electrons) by the assumption that β-rays are emitted as charged particles differing from electrons, into which they are subsequently transformed by some unspecified mechanism. Irrespective of whether this suggestion can be substantiated or disproved, it raises the question as to how soon after the instant of disintegration a β-particle may be identified with an atomic electron.

For the β-rays of tritium we can set a limit to this interval if we can estimate the time for their slowing down and supposed capture into a K orbit in zirconium. The time to reduce them to thermal velocities will be of the order 10^{-14} sec.; the time for capture of a meson of electronic mass into a K orbit has not been calculated, but if we assume that it is of the order of the lifetime of an X-ray transition (i.e. 10^{-16} sec. in zirconium) then the predominant factor will be the slowing-down time.

Thus we may conclude that in the case of the β-rays of ^{3}H not more than a few in a million can be other than electrons at a time of the order 10^{-14} sec. after disintegration.

The Clarendon Laboratory, Oxford.
31st May 1951.

W. T. Davies.
M. A. Grace.

Charpak, G., and Suzor, F., 1950, *C. R. Acad. Sci., Paris*, **231**, 1471; 1951, *Ibid.*, **232**, 322, 720.
Fermi, E., Teller, E., and Weisskopf, V., 1947, *Phys. Rev.*, **71**, 314.
Goldhaber, M., and Scharff-Goldhaber, G., 1948, *Phys. Rev.*, **73**, 1472.
West, H. I., Meyerhof, W. E., and Hofstadter, R. H., 1951, *Phys. Rev.*, **81**, 141.

Measurement of Fast Neutron Velocities by Delayed Coincidence

In a nuclear reaction in which neutron emission is followed by a gamma-ray from an excited nucleus, a study of the angular correlation between these particles may enable one to infer properties of compound and residual nuclei. In such an experiment (Thirion and Muller 1951) there are in general many neutron groups, and the interpretation of results may be difficult. By means of a delayed-coincidence method we have found it possible to measure the velocity of a neutron that is followed by a gamma-ray in a nuclear reaction. Although no conclusive results have yet been obtained, we feel that our method is of sufficient interest to justify a short description.

Photo-multipliers with liquid scintillators are used for detection of both neutron and gamma-ray. The multipliers are E.M.I. type end-window 14 stage tubes, with gains about 10^9. The scintillators consist of terphenyl in toluene (0·25 gm. per 100 cm^3) and are contained in glass flasks coated on the outside with magnesium oxide. One phosphor (the 'gamma detector') is one litre in volume, and situated close to the target. The 'neutron detector', five litres in volume, is placed one metre from the target.

The principle is to measure the time of flight of the neutron to the large phosphor. This is done by using a fast coincidence arrangement and producing a delay between gamma counter and coincidence unit. Thus a 2 Mev. neutron that travels one metre from the target arrives $5{\cdot}1 \times 10^{-8}$ sec. later than the gamma-ray following it (corresponding to a length of 10·2 metres of Uniradio 32 coaxial cable). In order to produce rectangular pulses of short duration, the output from each multiplier is fed to the grid of an E.M.I. type E.2133 secondary-emitting pentode, whose twofold purpose is to transform the high output impedance of the multiplier and produce pulses of uniform height. The pulses are 'clipped' by means of a shorted delay line (Bell and Petch 1949). A plot of coincidence rate against delay time using a ^{60}Co source showed a half-width of $2{\cdot}2 \times 10^{-8}$ sec., which for a 2 Mev. neutron corresponds to an energy spread from 1·4 to 3·2 Mev.

As an example of what can be obtained under these conditions, the Figure shows the delay spectrum for coincidences from the ^{9}Be(d, nγ)^{10}B reaction at 0·48 Mev. bombarding energy. The large peak corresponds to gamma–gamma coincidences and to 'reversed' neutron–gamma coincidences (neutrons recorded by the 'gamma-counter' and vice versa).

The small peak corresponds to a mean neutron energy of 2·5 MeV. In order to detect the angular correlation between this neutron group and its associated gamma-ray the neutron counter was kept fixed and the gamma counter rotated with respect to it, in the plane normal to the deuteron beam. This experiment gave isotropy to within 3%.

Since this work was started the neutron spectrum from this reaction has been studied in detail (Ajzenberg 1951), and it seems likely that the ' group ' is in fact a mixture of three groups, too close in energy to be resolved in our experiment. Hence the lack of correlation

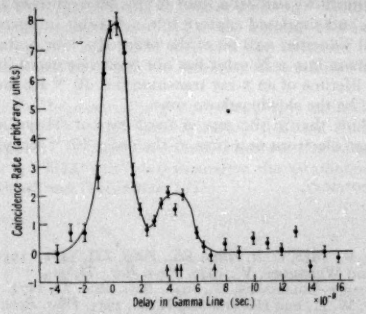

Delay spectrum of coincidences from ^{9}Be (d, nγ) ^{10}B. Arrows indicate delays corresponding to known neutron groups (Ajzenberg 1951).

means little or nothing. In principle the energy resolution can be improved to any desired accuracy by moving the neutron counter further from the target, but a limit is set by the drop in counting rate; the background rate does not however decrease proportionately, since it is due partly to slow neutrons entering the counters from random directions.

The method described can be used to measure velocities of other types of particles in coincidence with gamma-rays, and it is hoped to apply it to a study of alpha–gamma coincidences resulting from nuclear reactions.

Cavendish Laboratory, Cambridge.
15th June 1951.

D. B. James.
P. B. Treacy.

Ajzenberg, F., 1951, *Phys. Rev.*, **82**, 43.
Bell, R. E., and Petch, H. E., 1949, *Phys. Rev.*, **76**, 1409.
Thirion, J., and Muller, T., 1951, *C.R. Acad. Sci., Paris*, **232**, 1093.

An Investigation of the Reaction ^{9}Be (d, p)

Thin evaporated targets of beryllium have been bombarded with an unanalysed deuteron beam accelerated by an electrostatic generator. The deuteron content of the beam was determined, by magnetic analysis, to be (92 ± 2)%. The particles emitted from the resultant reactions were detected in Ilford C2 nuclear emulsions. The voltmeter measuring the generator voltage was calibrated by means of the ^{7}Li (p, γ) reaction, and was known to be linear in the voltage range used.

In some of the experiments the emulsions were placed in a small magnetic spectrograph. The intensity of each group detected was plotted as a function of distance along the emulsion from a fixed and known reference line. The spectrograph was calibrated by means of the direct deuteron beam which was arranged to pass into the spectrograph at known and constant energies.

Although the proton content of the beam was small, sufficient protons were present to produce a particle group from the ^{9}Be(p, d)^{8}Be reaction. By taking the position of this group as the position of half-maximum intensity, on the high energy side of the group, the

Q-value for this reaction was found to be (560 ± 13) kev., in agreement with previous values, see Hornyak *et al.* (1950). The position of half-maximum intensity of each group observed was therefore taken empirically as the position of that group, following the method described by Buechner *et al.* (1949).

The group emitted from the reaction $^{9}Be(d, p)^{10}Be^{*}$ was observed and the Q-value of the reaction determined from the measured momentum of the group. This gave $Q=(1{,}214 \pm 13)$ kev.

The Q-value determined from the range of the particles in the emulsion was $Q=1{,}204$ kev.; this is the mean of three measurements each having a standard deviation of 45 kev. These Q-values are in agreement with that of $(1{,}201 \pm 7)$ kev. obtained by Buechner and Strait (1949).

From a knowledge of the acceptance of the spectrograph, determined from the geometry, an estimate was made of the cross section of this reaction at two energies. The results are:

$$\sigma(90°) = (0{\cdot}43 \pm 0{\cdot}09) \times 10^{-28} \text{ cm}^2 \text{ sterad}^{-1} \text{ at } 301 \text{ kev.},$$
$$\sigma(90°) = (2{\cdot}96 \pm 0{\cdot}59) \times 10^{-28} \text{ cm}^2 \text{ sterad}^{-1} \text{ at } 440 \text{ kev.}$$

The thickness of each target was calculated from the known weight of beryllium evaporated on to each backing. The error in the calculated thickness is estimated at $\pm 20\%$. The pressure at the bottom of the accelerator tube and above the target was 10^{-5} mm. Hg or less, the scattering of protons out of the true image was about 2%. The intensity of contamination products from the $^{16}O(d, p)^{17}O^{*}$ reaction was less than 3% of the intensity of the $^{9}Be(d, p)^{10}Be^{*}$ groups. This was determined by blank target exposures, and by evaporating emulsions in an auxiliary camera to all the reaction products so that the group from the $^{16}O(d, p)^{17}O$ reaction also could be observed. The angle of dip of the tracks in the emulsion in the spectrograph was about 15°.

The Q-value for the reaction $^{9}Be(d, p)^{10}Be$ was determined from the range of the particles in emulsions exposed in the auxiliary camera, which is similar to that used by Rubin (1947). For this reaction $Q=(4{\cdot}55 \pm 0{\cdot}03)$ Mev.

The energy measurements were based on the range–energy relationship due to Rotblat (1950). In all the measurements made this relationship gave better agreement with Q-values than did the relationship due to Lattes and others.

I am indebted to Mr. D. R. Petrie who designed the spectrograph.

A. J. Salmon.

Research Laboratory,
Associated Electrical Industries Ltd.,
Aldermaston, Berks.,
2nd July 1951.

Buechner, W. W., and Strait, E. N., 1949, *Phys. Rev.*, **76**, 1547.
Buechner, W. W., *et al.*, 1949, *Phys. Rev.*, **76**, 1543.
Hornyak, W. F., *et al.*, 1950, *Rev. Mod. Phys.*, **22**, 312.
Rotblat, J., 1950, *Nature, Lond.*, **165**, 387.
Rubin, S., 1947, *Phys. Rev.*, **72**, 1176.

Note on Experimental Determination of the Half-Life of ^{8}Be

$^{16}O(\gamma, 4\alpha)$ photodisintegration stars frequently involve a ground-state ^{8}Be nucleus as an intermediary product (Goward and Wilkins 1950). In recent studies of such stars with Ilford E1 nuclear emulsions (Millar and Cameron 1951), the observation of single tracks produced by ^{8}Be nuclei, prior to splitting into two alpha-particles, has been reported and a half-life of $(5{\cdot}3 \pm 1{\cdot}1) \times 10^{-14}$ sec. deduced. This long half-life has been advanced (Stearns and McDaniell 1951) as evidence for $J=2$ for the ground-state of ^{8}Be. The observations in the present note on 280 similarly formed ^{8}Be nuclei do not support the possibility of such a definite deduction of the half-life.

Examination of the narrow V-shaped alpha-particle tracks from the above-mentioned 280 $^{16}O(\gamma, 4\alpha)$ stars leads to the following conclusions. Firstly, closely neighbouring tracks of this kind can only be resolved sufficiently to allow an upper limit (not an actual value) of about 5×10^{-14} sec. to be obtained for the half-life of ^{8}Be. Secondly, the degree

of scattering evident in the tracks is sufficient to produce an occasional illusion of a single ^{8}Be track. The importance of these factors may be estimated from photographs already published (Wilkins and Goward 1950). Processing techniques directed especially towards studying the ^{8}Be half-life may give a limited improvement in resolution, but the use of grain gradation development is more likely to increase the illusion of a single ^{8}Be track by thickening the unresolved part of the V-tracks.

The above qualitative remarks may be supported by simple numerical considerations, complications such as scattering being neglected. Assume that a separation of about 0·3 micron (the grain diameter) is sufficient to give clear resolution between tracks, whatever their orientation relative to the observer, and further that the ^{8}Be nuclei are ejected with 2·5 MEV. kinetic energy and disintegrate immediately and isotropically. Then about 35% of the resulting V-tracks have the first micron or more unresolved, and an upper limit of 9×10^{-14} sec. might be deduced for the half-life. Extrapolation of the tracks backwards would reduce this upper limit estimate, but hardly by a factor of more than two.

The resolution of the method might be improved with considerably higher ^{8}Be kinetic energies, although the advantage of a higher initial velocity is almost exactly offset by a narrower V angle. It is significant, however, that a report on some observations of ^{8}Be nuclei in cosmic-ray stars by Crussard (1950) makes no mention of single ^{8}Be tracks in 16 events (see also Perkins 1950). A specific attempt by Hodgson (private communication) to extend the present results by measurement on such stars places an upper limit of about 2×10^{-14} sec. on the ^{8}Be half-life.

Atomic Energy Research Establishment,
Harwell, Didcot, Berks.
2nd July 1951.

J. J. WILKINS.
F. K. GOWARD.

CRUSSARD, J., 1950, *C. R. Acad. Sci. Paris*, **231**, 141; *Nature, Lond.*, **166**, 825.
GOWARD, F. K., and WILKINS, J. J., 1950, *Proc. Phys. Soc.* A, **63**, 1171.
MILLAR, C. H., and CAMERON, A. G. W., 1951, *Phys. Rev.*, **81**, 316.
PERKINS, D. H., 1950, *Proc. Roy. Soc.* A, **203**, 399.
STEARNS, M. B., and MCDANIELL, B. D., 1951, *Phys. Rev.*, **82**, 451.
WILKINS, J. J., and GOWARD, F. K., 1950, *Proc. Phys. Soc.* A, **63**, 1173.

On the Supplementary Condition in Quantum Electrodynamics

It has been shown by Koba, Tati and Tomonaga (1947) and Schwinger (1948) that when we pass over from the Heisenberg representation to the interaction representation, the supplementary condition for the electromagnetic field has to be modified by adding a 'charge-term'. Since the treatment by these authors is fairly complicated, it is not easy to see why the additional charge-term should appear in the interaction representation. It will, therefore, be of interest to show that the supplementary condition in the interaction representation may be obtained in a very straightforward way by the general method of passing over from the Heisenberg representation to the interaction representation. The treatment, to be described here, also proves very convenient for obtaining the supplementary conditions (or the coordinate conditions) for Einstein's gravitational field in the interaction representation (Gupta, to be published).

Fermi's supplementary condition. According to Fermi the supplementary condition for the electromagnetic field in the Heisenberg representation is given by

$$\frac{\partial A_\mu'}{\partial x_\mu}\,\Psi'=0, \qquad \ldots\ldots(1)$$

where we use primed quantities for the Heisenberg representation. The condition (1), which is required to hold at all times, is equivalent to the initial conditions

$$\frac{\partial A_\mu'}{\partial x_\mu}\Psi'=0, \qquad \frac{\partial}{\partial t}\frac{\partial A_\mu'}{\partial x_\mu}\Psi'=0. \qquad \ldots\ldots(2)$$

In order to pass over to the interaction representation, we can use the following general method for any field quantity. First, remove all explicit time derivatives from the field quantity in the Heisenberg representation by expressing it in terms of the field variables and their canonical conjugates. Then, replace these field variables and their canonical conjugates by the corresponding variables for free fields. This gives the required field quantity in the interaction representation.

If we use the Lagrangian density, given by Schwinger (1948), for a system of photons and electrons, the canonical conjugates of A_μ will be given by

$$\pi_\mu' = \partial A_\mu'/\partial t. \qquad \ldots\ldots (3)$$

Using (3), and the field equation $\Box^2 A_\mu' = -j_\mu'$, we get

$$\frac{\partial A_\mu'}{\partial x_\mu} = \frac{\partial A_i'}{\partial x_i} + \pi_0'; \quad \frac{\partial}{\partial t}\frac{\partial A_\mu'}{\partial x_\mu} = \frac{\partial \pi_i'}{\partial x_i} + \frac{\partial^2 A_0'}{\partial x_i^2} + j_0'. \qquad \ldots\ldots (4)$$

Therefore, corresponding to (2), we have in the interaction representation

$$\left(\frac{\partial A_i}{\partial x_i} + \pi_0\right)\Psi = 0, \qquad \left(\frac{\partial \pi_i}{\partial x_i} + \frac{\partial^2 A_0}{\partial x_i^2} + j_0\right)\Psi = 0, \qquad \ldots\ldots (5)$$

where the operators A_μ, π_μ and j_0 refer to free fields. Thus, on expressing π_μ in terms of A_μ, (5) gives

$$\frac{\partial A_\mu}{\partial x_\mu}\Psi = 0, \qquad \left(\frac{\partial}{\partial t}\frac{\partial A_\mu}{\partial x_\mu} + j_0\right)\Psi = 0. \qquad \ldots\ldots (6)$$

The above equations may be written in a more elegant form as

$$\Omega(x)\Psi(t) = 0, \qquad \frac{\partial \Omega(x)}{\partial t}\Psi(t) = 0, \qquad \ldots\ldots (7)$$

with

$$\Omega(x) = \frac{\partial A_\mu(x)}{\partial x_\mu} - \int_{t'=t} D(x-x')j_0(x')dv', \qquad \ldots\ldots (8)$$

the equivalence of (6) and (7) being obvious from the fact that

$$[D(x-x')]_{t=t'} = 0, \qquad \left[\frac{\partial D(x-x')}{\partial t}\right]_{t=t'} = -\delta(x-x').$$

It is interesting to note that it is the second relation in (2), and not the first, which gives rise to the charge-term. The initial conditions (7) are, of course, equivalent to requiring that the supplementary condition

$$\Omega(x)\Psi(t) = 0. \qquad \ldots\ldots (9)$$

should hold at all times.

Modified supplementary condition. Fermi's supplementary condition, discussed above, involves the difficulty that there is no normalized state which satisfies it (Ma 1949, Belinfante 1949). Therefore, the present writer (Gupta 1950) has given a new treatment for the longitudinal part of the radiation field, in which an indefinite metric is used for the scalar photons and (1) is replaced by a modified supplementary condition

$$\left[\frac{\partial A_\mu'}{\partial x_\mu}\right]^+ \Psi' = 0, \qquad \ldots\ldots (10)$$

$[\partial A_\mu'/\partial x_\mu]^+$ being the positive frequency part of $\partial A_\mu'/\partial x_\mu$. In the absence of interaction (10) may also be written as $(\partial A_\mu'^{(+)}/\partial x_\mu)\Psi' = 0$, where $A_\mu'^{(+)}$ is the positive frequency part of A_μ'. But, in general one has to use the form (10), because in the presence of interaction A_μ' cannot be split into the positive and the negative frequency parts. However, such a splitting is still possible for $\partial A_\mu'/\partial x_\mu$, which always satisfies the wave equation for plane waves: $\Box^2(\partial A_\mu'/\partial x_\mu) = -\partial j_\mu'/\partial x_\mu = 0$.

If we now pass over to the interaction representation, then, as Bleuler (1950) has already done, we ought to replace (9) by

$$\Omega^{(+)}(x)\Psi(t) = 0, \qquad \ldots\ldots (11)$$

where $\Omega^{(+)}$ is the positive frequency part of Ω, which satisfies the wave equation $\Box^2\Omega=0$. Thus, we have from (8) :

$$\Omega^{(+)}(x)=\frac{\partial A_\mu{}^{(+)}(x)}{\partial x_\mu}-\int_{t'=t} D^{(+)}(x-x')j_0(x')\,dv', \qquad \ldots\ldots (12)$$

$A_\mu{}^{(+)}$ and $D^{(+)}(x)$ being the positive frequency parts of A_μ and $D(x)$.

Cavendish Laboratory, Cambridge.
3rd July 1951.

SURAJ N. GUPTA.*

* State Scholar of the Government of India.

BELINFANTE, F. J., 1949, *Phys. Rev.*, **76**, 226.
BLEULER, K., 1950, *Helv. phys. Acta*, **23**, 567.
GUPTA, S. N., 1950, *Proc. Phys. Soc.* A, **63**, 681.
KOBA, Z., TATI, T., and TOMONAGA, S., 1947, *Progr. Theor. Phys.*, **2**, 101.
MA, S. T., 1949, *Phys. Rev.*, **75**, 535.
SCHWINGER, J., 1948, *Phys. Rev.*, **74**, 1439.

The Band Systems of Thorium Oxide and Hafnium Oxide

In continuation of the work in this laboratory on the band systems of titanium oxide the systems of thorium oxide and hafnium oxide have been investigated. Both spectra were developed in arcs between graphite rods, the lower positive of which was filled with the oxide in question. Glass and quartz Littrow spectrographs were used to photograph the hafnium oxide spectrum, while a 21-ft. grating could also be used for the less expensive thorium oxide from λ 8500 to λ 3800.

The spectra were very rich in red degraded systems throughout the whole region photographed and a number of sequences could be recognized. Extrapolation of the vibration frequencies of the other elements of the group of the periodic table suggested the corresponding frequencies in thorium oxide and hafnium oxide as about 740 cm^{-1} and 865 cm^{-1} respectively for the ground states.

About fifteen systems in ThO and eight in HfO could be distinguished. The energy level diagrams of the two molecules showed three important lower levels at values of ν: 0, 2721 and 4177 for ThO and 0, 2084 and (4003) for HfO. These levels are probably $^3\Pi$ levels, and the $^3\Pi_0-{}^3\Pi_1$ intervals 2721 and 2084 of ThO and HfO are comparable with the $^3F_2-{}^3F_3$ intervals 2869 and 2320 of the arc spectra of thorium and hafnium. It is hoped that full details will be published shortly.

Spectroscopy Laboratory,
Imperial College, London.
12th July 1951.

S. G. KRISHNAMURTY.

REVIEWS OF BOOKS

Weltsystem, Weltäther und die Relativitätstheorie, by K. JELLINEK. Pp. xv+450. (Basle: Wepf, 1949.) Sfr. 45.

This is a book the like of which one would not, during the past thirty or forty years, have expected ever again to see published: for it is no less than an attempt to retain a universal aether and a universal absolute frame of reference while seeking to reconcile with these many of the notions and results of relativity theory.

One must hasten to admit that, in view of recent trends in cosmological theory, the attempt must not be condemned out of hand as being entirely misdirected, as it almost certainly would have been not many years ago. It is in fact well known that almost all current theories of the expanding universe introduce what is usually called ' cosmic time ', which may seem very like the universal time of pre-relativity physics. This feature has been particularly

emphasized during the past couple of years in the writings of Bondi and Gold, and of Hoyle, on the possibility of continuous creation; for if newly created matter does appear throughout the universe it must apparently serve to define an absolute standard of rest at every point of space (i.e. a preferred time-direction at every event in space–time).

Nevertheless, science is never known to go back completely on its tracks. If it reverts to a position something like one it has held prior to what has been regarded as a major advance, the likeness is found to be superficial or even illusory. The photons of modern physics are not really much like Newton's light corpuscles. Similarly, any preferential frame of reference in modern cosmology is conceptually far removed from a frame at rest in a pre-relativity aether.

As far as I can understand him, Professor Jellinek wants to keep the nineteenth century aether and to make the best job he can of accommodating relativity in it. The job is a difficult one, and Professor Jellinek's intellectual candour is such that he conceals none of the difficulties. Indeed, reading his book one repeatedly expects him to produce the standard arguments which originally showed how much simpler it is to do away with the aether and to accept the orthodox formulation of relativity theory. But he never surrenders.

Professor Jellinek's purpose is to provide a serious treatise of not too mathematical a character on special and general relativity for the use of experimental physicists and others who are not professional mathematicians. He is justified in his belief that no such book exists which includes general relativity. The reason is that hitherto the latter has been of very little interest to experimental physicists as such. Quite recently it has gained some interest for them on account of the possible connections between cosmological theory and the theory of the relative abundances of the elements. Owing to Professor Jellinek's unusual presentation, and the extremely involved discussions of particular points to which it leads him, his book, unfortunately, seems scarcely to meet the need.

Here is not the place to attempt a lengthy criticism of Professor Jellinek's treatment. It would be largely a repetition of arguments that were familiar in the early days of relativity theory. But it would also demand the admission that much of what he says in criticism of other treatments is in itself very pertinent, though I think it can be countered in more simple ways than he allows. Two general points may be made. First, a great merit of general relativity theory is that it is a 'differential' theory, i.e. it can be formulated in terms of the properties of space–time in an observer's neighbourhood. Even if it ultimately leads to the recognition of a preferential universal frame of reference in a cosmological model, it does not, as Professor Jellinek seems to assert, require to *assume* the existence of such a frame at the outset. The second point is that it is primarily only in the theoretical models of a 'smoothed-out' universe that general relativity recognizes a preferential frame of reference. If we liken such models to simple surfaces of revolution, as we can, the preferred frame of reference corresponds to the meridian sections and circular sections, and it is obvious that these are to be recognized as a preferred system. But on this analogy we should liken the actual universe to the surface of, say, a very rough tree-trunk. Though we might again find a preferred coordinate system suitable for describing its general features, such a system would play no special part in the description of minute local configurations in the surface. Similarly, I think that concepts such as 'cosmic time' have very little to do with applications of relativity theory to anything but the very large-scale features of the universe. These concepts do not seem to me to offer any justification for thinking that relativity theory requires anything that corresponds to a universal aether in Professor Jellinek's sense.

Anyone who does want an 'aether' in relativity theory can, however, have it for the asking. The theory deals exclusively with the entity it calls 'space–time'. Where space–time possesses such a curvature that the Einstein tensor is non-zero, it asserts that 'matter' is present. Where the curvature is such that this tensor vanishes, it says that space–time is 'empty'. That is, it does not regard matter as something immersed in space–time, but as being a property of space–time. Where space–time does not possess this particular property, general relativity still treats it as being by no means featureless. Therefore, to give it a name like the 'aether' might well be more appropriate than to call it 'empty' space. This, though not in the context of orthodox general relativity, seems to be the point made by Eddington (*Fundamental Theory*, 1946, p. 172). But to retain the term 'aether' in this way would be to run the risk of retaining also those properties of the classical aether which relativity has abandoned. It seems to the reviewer that these are just the properties that Professor Jellinek does desire to retain.

Nevertheless, it is abundantly evident that Professor Jellinek has pondered long and deeply upon the subjects of which he writes, and what he has written commands one's respectful attention. If it cannot be deemed wholly suitable for the requirements of the experimental physicist making his first acquaintance with relativity theory, it will probably be found of much value to other relativists who may themselves be called upon to supply these requirements. It will stimulate them to think of their subject from fresh points of view and will be a challenge to them to re-examine the foundations of their own presentations.

W. H. MCCREA.

Sourcebook on Atomic Energy, by S. GLASSTONE. Pp. 546. (London: Macmillan, 1950.) 24*s*.

The book under review is of the type perhaps more common in the United States than in Great Britain. It was apparently originally requested as a comprehensive sourcebook on atomic energy for the use of textbook authors and editors. It stands somewhere between an elementary textbook and an encyclopaedia. As stated in the foreword, Dr. Glasstone has written a book which is of far broader usefulness and which provides a source of basic atomic energy information for everyone interested in this field.

Beginning with the earliest theories of the atom and its structure, it describes the growth of thought and knowledge in the field—the development of the theories of the nature of electricity, energy and matter, the discovery of the phenomena of radioactivity—and so leads to problems of modern developments. The following chapters deal with the acceleration of charged particles, nuclear transmutation and artificial radioactivity, the neutron, nuclear structure and nuclear forces, nuclear fission, utilization of nuclear energy, new elements, the uses of isotopes, and finally cosmic rays and mesons. It concludes with a chapter giving an outline of radiation protection and 'health physics'.

It is certainly an amazing concentration of information which, in view of its nature, is surprisingly readable, though it is certainly not a book to be read through at one sitting. The chapters are divided into a large number of paragraphs each of which is clearly labelled, thus making cross reference much easier and more satisfactory. Each of the subjects is dealt with largely historically. Only a rudimentary knowledge of science or mathematics is required to follow the narrative, which will doubtless be of interest to a very large number of readers without much scientific training.

Atomic energy is of great importance in medicine, biology, astronomy, physics, and other branches of knowledge. This miniature encyclopaedia, arranged nevertheless on a logical system, will probably be of great interest and use to the type of reader for whom it was intended. It will be the basis of a good many popular articles in newspapers even if not, as it is surely not intended to be, useful as a basis for further advances. It is a well written and a skilfully organized account of the fundamentals of 'atomic energy' and its applications.

W. V. MAYNEORD.

Introductory Nuclear Physics, by DAVID HALLIDAY. Pp. 558. (New York: Wiley and Sons; London: Chapman and Hall, 1950.) 52*s*.

Professor Halliday has written a remarkable and interesting book which is intended for post-graduate students about to start experimental work in nuclear physics. It is a typically American book with plenty of facts well displayed in convenient tables, plenty of references to modern work and plenty of diagrams of apparatus which has been in use in the last five years. The student is early introduced to the idea that one should consult the literature, and above all reminded that the best way to find out whether you understand the meaning of an expression is to work out a few elementary numerical examples. These are amply provided at the end of each chapter; on the whole they are well graded and match the easy descriptive standard of the text better than is usual in American books, in which a hard text is so often combined with trivial examples.

Clearly an author who sets out to cover at an advanced level the whole of nuclear physics in 500 pages has to jettison much traditional material.

History is the first to go. The opening sentence baldly states that "Nuclear physics began in 1896 when Henri Becquerel discovered radioactivity", and leaves it at that.

Its further progress is summarized in a table giving the author, date and country of origin of the chief subsequent discoveries. The only ghost from the past which is allowed on the stage is the familiar diagram of Geiger and Marsden's apparatus for measuring Rutherford scattering. It is, however, rapidly exorcized by a footnote which remarks that "with modern techniques this pioneer experiment can be done as a three-hour student exercise". I wonder how many students do it on this side of the Atlantic.

Secondly, no attempt is made to derive, where possible, well known and important results by relatively elementary methods. Although a fairly extensive general knowledge of wave mechanics is assumed, the book contains practically no mathematics.

The author is an ardent, logical positivist, and one gains the impression that he thoroughly enjoyed throwing overboard the dusty treasure of the past. The merits of this course of action, when pursued with Professor Halliday's vigour and enthusiasm, depend very much on the graduate training of the student. The differences in this respect between English and American students may somewhat reduce the value of the book to English students, who on the whole are probably better grounded in classical physics and less immediately aware of the elementary properties of neutrons and high energy particles. For example, the book has passages in small print judged too hard for inclusion in a graduate course; in what British University would one find students to whom the statement that "Mott and Massey give the differential cross section for neutron–proton scattering as

$$d\sigma=(\lambda^2/16\pi^2)\,|\Sigma(2l+1)P_l\cos\theta(e^{2i\delta_l}-1)|^2\,d\Omega\ "$$

would be reasonably intelligible and for whom the proof of the formula $\Delta E/E\simeq 4m/M$, for the head-on collision of elastic spheres, is considered so hard as to be relegated to small print? This is only one of many similar anomalies.

Nevertheless the amount of new material included is stimulating and surprising, and there can be few who will not find in these pages some aspect of nuclear physics of which they were only dimly aware.

On the whole the author's philosophical position is not unduly in evidence, though in some instances it has led him to omit material which should have been included. For example, the discussion of the specific ionization of charged particles omits much important material. The index has no entry under Bragg (in this connection), although the term 'Bragg curve' is still in common use in American journals; no mention is made of the different mechanisms of ionization which account for the falling and rising parts of the curve. Furthermore, no mention is made of the convenient and empirical Geiger law, although the standard measurements in this field are still tabulated as deviations from this law.

In spite of these minor criticisms the book can be confidently recommended. The research student provided with this vade-mecum will find that he can rapidly run down a list of references and advanced texts dealing with the problems facing him in the laboratory on starting work in nuclear physics. What use he makes of them is up to him. Well, so it is; life is like that!

I imagine that lecturers who have to give an advanced course in nuclear physics will find this volume most useful because it supplies just what is needed in the way of references and tabulated data to form the coping-stone of a more traditional treatment.

The standard of paper, printing and diagrams is excellent, and the price no more than holders of a devalued currency can expect.

C. H. C.

Superfluids, Vol. I: Macroscopic Theory of Superconductivity, by F. LONDON. Pp. viii+161. (New York: Wiley and Sons; London: Chapman and Hall, 1950.) 40*s*.

In 1937 Professor F. London expounded, in *Une Conception Nouvelle de la Supraconductibilité*, the views of the nature of the superconducting state which he and his brother had introduced some two years before. Now, in the first volume of a projected series under the general title *Superfluids*, he sets out the same views once more, in a considerably expanded form. The fact that in fifteen years he has not seen fit to make any substantial alterations to the fundamental framework of his theory is to be regarded not as evidence of a conservative nature, but as testimony to the logical beauty of the theory in its original form. It

must be admitted, however, that there would in any case be strong justification for a passively conservative attitude, since a rigorous experimental test of the theory has so far not been undertaken on account of the technical obstacles to such an investigation.

The book is divided into five sections. The first, a brief development of the concept of the ' ideal superconductor ', with an account of its thermodynamical properties, is followed by a long discussion of the electrodynamics of superconductivity. This section, which occupies nearly half the book, is perhaps the most satisfactory, and is a real pleasure to read. The basic idea, that the supercurrent is linked to the magnetic rather than to the electric field, is introduced as a postulate in the form of the well-known ' London equations ', and the implications of these equations are then examined in detail. It is proved very elegantly that they lead to a unique field distribution if the sources and ' fluxoids ' are prescribed and to perfect diamagnetism of macroscopic superconductors of any shape. Among other passages of great value may be mentioned especially the lucid discussion of the difference between perfect conductivity and superconductivity.

It is perhaps because the disturbing shadow of experimental facts has not fallen upon this section that it seems more complete than the two which follow. Here the intermediate state and the properties of thin films are discussed, and it becomes only too plain that the ideal superconductor is too remote a conception. Much as we may admire the mathematical structure which Professor London has erected, we feel that the security of the experimental foundations is still open to question, and it is quite certain that the last word on these subjects is still to be said.

Finally Professor London examines the relation between the macroscopic electrodynamics and the quantum mechanics of an assembly of electrons, in order to formulate the conditions under which, in his view, the superconducting state may exist. The major requirement, that the wave functions of the electrons shall be rigid, in the sense that they are not readily perturbed by an applied magnetic field, is one which has not in the past been accepted by all who have attempted to construct theories of superconductivity, but it is significant that the most recent attempts have been along these lines, and show in other respects a considerable improvement on their forerunners. Though short, this section contains much weighty matter, and is certainly one of the most important.

The general impression which the book leaves is that it is not a balanced textbook on superconductivity—it is not even a balanced textbook on the theory of superconductivity; rather is it a personal account of an important aspect of the theory written by one who has contributed perhaps more than anyone else to our understanding of the phenomenon. It can hardly be recommended as an introduction to the subject for the general physicist, for whom a fuller account of the experimental facts would be desirable, but to the theoretical physicist, and above all to the low-temperature physicist, it represents an extremely valuable addition to the small body of literature in this field.

A. B. PIPPARD.

Process Heat Transfer, by D. Q. KERN. Pp. xii + 871. 1st Edition. (New York and London: McGraw-Hill, 1950.) 68*s*.

The justification for an addition to the already extensive literature on heat transfer must lie in a new or novel approach to the subject, and in this respect Professor D. Q. Kern's book has serious claims to consideration. Whilst we do not consider his aim of providing fundamental instruction in heat transfer " using the methods and language of industry " as being fully capable of realization or even as being altogether desirable, the endeavour to adhere to it has resulted in a book containing much practical data of direct value to the designer. An admirable feature of the book is the linking up of theory and practice by means of well chosen practical examples worked out in full and illustrated by clear line drawings of plant and equipment.

According to the author's definition, *Process Heat Transfer* deals with the rates of heat exchange as they occur in the heat transfer equipment of the engineering and chemical processes. A typical problem of process heat transfer is one concerned with the quantities of heat to be transferred, the rates at which they may be transfered because of the nature of the bodies, the driving potential, the extent and arrangement of the surface separating the source and receiver, and the amount of mechanical energy which may be expended to facilitate the transfer.

The first five chapters of the book deal on orthodox lines with the mechanism of heat transfer by conduction, convection and radiation, with fundamental definitions of heat transfer coefficients and with the relation between parallel flow and counter flow.

The main body of the book then treats in detail the more important classes of heat-transfer equipment, including all common commercial types of exchangers, heaters, coolers, condensers, evaporators, reboilers, and distillation columns. In view of recent developments, the reader will find a useful summary of the methods of deriving the efficiencies of various forms of extended surfaces such as finned tubes.

Other sections of interest relate to unsteady-state processes as exemplified by the regenerator and the reversing exchanger which is now coming into extensive use in gas separation plant, and to furnace calculations based upon empirical and semi-empirical methods. The final chapter of the book deals with the control of process variables.

The book is well illustrated and, although the bibliographies are by no means complete, adequate references are given to most of the significant work of the past twenty years.

D. M. N.

CONTENTS FOR SECTION B

PAGE

Prof. N. F. MOTT. The Mechanical Properties of Metals. (35th Guthrie Lecture.) 729

Dr. E. O. HALL. The Deformation and Ageing of Mild Steel: II—Characteristics of the Lüders Deformation 742

Dr. E. O. HALL. The Deformation and Ageing of Mild Steel: III—Discussion of Results 747

Dr. R. S. TEBBLE, Dr. W. D. CORNER and Mr. J. E. WOOD. Reversible Effects in the Magnetization of Nickel 753

Dr. C. DODD. The Surface Tension of Supercooled Phenyl Ether 761

Dr. A. W. BREWER and Mr. H. P. PALMER. Freezing of Supercooled Water . 765

Dr. B. J. MASON. Spontaneous Condensation of Water Vapour in Expansion Chamber Experiments 773

Dr. L. A. WOODWARD and Mr. J. H. B. GEORGE. Light Flux received by a Spectrograph from a Spatially Extended Refracting Source 780

Mr. J. J. DOWD. Optical Properties of Selenium 783

Dr. O. KLEMPERER. On a New Test Method for Spherical Aberration of Electron Lenses 790

Dr. R. L. F. BOYD. The Mechanism of Positive Ion Collection by a Spherical Probe in a Dense Gas 795

Prof. D. R. BATES. The Temperature of the Upper Atmosphere 805

Letters to the Editor:

Mr. E. SCHWARZ. Photoconductive Cells of Cadmium Selenide . . . 821

Dr. C. A. HOGARTH. Crystal Diode and Triode Action in Lead Selenide . 822

Reviews of Books 823

Contents for Section A 830

Abstracts for Section A 831

ABSTRACTS FOR SECTION B

The Mechanical Properties of Metals, by N. F. MOTT. (*35th Guthrie Lecture.*)

ABSTRACT. A description is given of edge and screw dislocations in a close-packed cubic lattice, which leads up to an account of the theory of Frank and Read of the origin of slip bands. Consideration is then given to a crystalline grain containing Frank–Read sources; it is shown that one has to expect cross-slip and the formation of deformation bands. It is shown moreover that the formation of vacancies by moving dislocations plays an essential role in these processes. Some speculations on the stability of deformation bands are given. It is suggested that the movement of vacancies (self-diffusion) plays an essential part in polygonization, recovery and steady-state creep, enabling dislocations in deformation bands to move out of their slip planes and so relieve stress. It is probable moreover that in these bands the stresses are several hundred times greater than the applied stress, and that this enables diffusion to occur at temperatures at which it would not be possible otherwise. Finally an account is given of low temperature creep of the type which does not involve recovery.

The Deformation and Ageing of Mild Steel: II—Characteristics of the Lüders Deformation, by E. O. HALL.

ABSTRACT. In this paper, some of the factors which influence the appearance of Lüders bands in mild steel are studied. It is shown that the Lüders band is adequately described by a uniform shear front, spreading over the specimen. In coarse-grained specimens, experiments indicate that this front becomes diffuse; diffuse bands are also present in strain-aged material, but here the diffuse fronts become sharper as the ageing becomes progressively longer.

The Deformation and Ageing of Mild Steel: III—Discussion of Results, by E. O. HALL.

ABSTRACT. An attempt is made here to explain the observed phenomena in the yielding and ageing of mild steel, described in two previous papers, in the general terms of a grain-boundary theory. On this hypothesis, a satisfactory explanation of the variation of the lower yield point with grain size may be developed. It is shown that strain-ageing must involve two processes: a healing of the grain-boundary films, coupled with a hardening in the grains themselves. A discussion of the possible nature of the grain-boundary film is also undertaken.

Reversible Effects in the Magnetization of Nickel, by R. S. TEBBLE, W. D. CORNER and J. E. WOOD.

ABSTRACT. An account is given of investigations on the temperature dependence of the contribution from reversible processes to the magnetization of annealed and strained nickel wires. This involves the measurement of reversible susceptibility κ_r over a range of field, and of temperature ($-50°$ C. to $+200°$ C.), and a rapid automatic method of recording (κ_r, H) curves has been developed. The effect of temperature on κ_r is discussed in relation to Becker's strain theory and reasons for the discrepancies are suggested. It is shown that the contribution of reversible processes to the total change in magnetization, integrated over the hysteresis cycle, increases with temperature and strain, from 15% for an annealed specimen at $-50°$ C. to 85% for a strained specimen (17·1 kg. mm^{-2}) at 150° C. The effect is not uniform over the whole cycle and in the region of the coercive field a considerable part of the change in magnetization must be attributed to irreversible processes.

The Surface Tension of Supercooled Phenyl Ether, by C. DODD.

ABSTRACT. Determinations of the surface tension of phenyl ether have been made, using Jaeger's method, for the liquid in both the ordinary and the supercooled state.

No abnormal change with temperature, of the type already found for viscosity and dielectric constant, has been detected for surface tension as the liquid enters the supercooled region.

Freezing of Supercooled Water, by A. W. BREWER and H. P. PALMER.

ABSTRACT. Rau has claimed that, by repeated freezing and thawing, the temperature to which a drop of water supercools before freezing can be lowered and, with special care, the freezing temperature can be reduced to $-72°$ C. This is claimed to be the temperature of spontaneous nucleation of ice. At that temperature the ice forms in rectangular crystals which also melt at $-72°$ C. This note describes a careful attempt to repeat Rau's work. Like Cwilong, we have been unable to do so except by deliberate contamination, and it is presumed that Rau's apparatus was faulty and his drops were contaminated by his cooling fluid. Information is given concerning the reproducibility of the freezing temperature of individual drops when repeatedly frozen and thawed. Rau's rectangular crystals have been observed in strong alcohol solutions but no information concerning their nature has been obtained.

Spontaneous Condensation of Water Vapour in Expansion Chamber Experiments, by B. J. MASON.

ABSTRACT. When clean, saturated air is subjected to a sufficiently large adiabatic expansion, small water droplets arise spontaneously from the vapour. An equation is derived for the growth rate of a droplet in an atmosphere of given supersaturation and temperature. This is used in conjunction with the Becker–Döring theory of nucleation to calculate the supersaturation and the concentration of droplets at successive time intervals during a cloud-chamber expansion, allowance being made for warming of the air by liberation of the latent heat of condensation. For large expansion ratios, the supersaturation attains a maximum and the droplet concentration a sensibly constant value *before* the end of the expansion. The computed value of this maximum droplet concentration is in acceptable agreement with the recent observations of Frey. The experimental results appear incompatible with Tolman's recent theory concerning the variation of surface tension with droplet radius. The predicted rates of droplet growth agree well with recent measurements made by Hazen.

Light Flux received by a Spectrograph from a Spatially Extended Refracting Source, by L. A. WOODWARD and J. H. B. GEORGE.

ABSTRACT. The geometrical-optical treatment of Nielsen, which referred to a spatially extended source of refractive index unity, is extended to sources of any refractive index. Provided that the direction of emergence of the light from the source is nearly normal, it is shown that a change of refractive index from 1 to n modifies the light flux by the factor $1/n^2$. This result is independent of whether or not a condensing lens is used between source and spectrograph. Its relevance in connection with observed intensities in Raman spectra is discussed.

Optical Properties of Selenium, by J. J. DOWD.

ABSTRACT. Measurements have been made of the refractive index of amorphous selenium in the red and near infra-red spectral region. The absorption coefficient of amorphous selenium has been measured in the ultra-violet visible and near infra-red spectral regions. The transmission coefficients of several single crystals of selenium have been measured and an estimate made of the absorption coefficient in the wavelength range 0·68 to 2·0 μ. The results show that the absorption edge of the crystalline material occurs at about the same wavelength as that for the amorphous form. A discrepancy between the value of the near infra-red refractive index and the dielectric constant of amorphous selenium indicates a further absorption band in the infra-red.

On a New Test Method for Spherical Aberration of Electron Lenses, by O. KLEMPERER.

ABSTRACT. The focus of rays from a lens with spherical aberration appears as a spot surrounded by a discrete halo ring if a diaphragm with fine circular aperture is placed across the beam in front of the focus. The diameter of the halo allows an estimate of the magnitude of the aberration involved. The geometry of rays forming the halo is explained here by schematic drawings. The practical application of the halo test is illustrated by some examples. In particular, the negative spherical aberration produced by an electronic space charge in a saddle field lens is demonstrated.

The Mechanism of Positive Ion Collection by a Spherical Probe in a Dense Gas, by R. L. F. BOYD.

ABSTRACT. The Langmuir probe technique is not suitable for measuring ion densities above 1 mm. Hg pressure because the probe dimensions approach those of the ionic and electronic mean free paths. In addition to the invalidity of the Langmuir theory for this case, such a probe also causes a great disturbance of the discharge.

In this paper a detailed examination is made of the possibility of using a probe collecting positive ions as a means of finding ion densities.

It has been found possible to calculate the potential distribution, outside a space-charge sheath around a spherical probe, if the radius of the sheath is known. From this the current of positive ions to the probe may be found. Curves are given to facilitate this calculation.

It is found that, depending on the ion concentration and pressure, there are two rather different sets of conditions around the probe. If the ion density is high (greater than about 10^6/mean free path (in cm.)) a thin sheath will form on the probe and a complete solution of the problem is possible. Under such conditions the energies of the diffusing ions in the neighbourhood of the probe greatly exceed the thermal energies of the gas particles. At the lower ion densities normally encountered, a thick 'diffusion' sheath occurs and the problem can now only be solved if the sheath thickness is known. The ion energies may or may not greatly exceed the thermal energies, depending on conditions.

These results contradict one of the basic assumptions made by Davydov and Zmanovskaja in their approach to the same problem. They assume a thin sheath with the ions in thermal equilibrium with the surrounding gas. As a result their conclusion is in conflict with the conclusion of this paper, that in most circumstances it is not possible to use a negative probe to measure ion densities unless an additional means of determining the sheath thickness is available.

The Temperature of the Upper Atmosphere, by D. R. BATES.

ABSTRACT. The properties of a number of simple models of the upper atmosphere are tabulated. A study is made of the thermal equilibrium in the region of the F layers. The rate at which energy is gained from ionizing photons is estimated. Various loss processes are examined. It is found that the most important is conduction, and the next most important is probably emission by the magnetic dipole connecting the two low levels of the ground term of atomic oxygen. These are so effective indeed, that the energy source first considered appears inadequate to maintain the high temperature the upper atmosphere is generally supposed to possess. Alternatives are investigated. Sufficient energy might conceivably be supplied either by band absorption by nitric oxide, or by incoming interstellar matter: but neither source is attractive. Attention is drawn to the possibility that the original estimate of the contribution from ionizing photons may be much too small. This estimate is based on radio measurements. It is shown that these only give a *lower limit* to the electron production rate: for certain ions may be removed so rapidly by recombination that they would escape detection even if their formation rate were greater than that of the dominant ions in the layers. The suggestion is tentatively made that heat is supplied to the upper atmosphere mainly by non-observed ionization. It is pointed out that owing to the possible existence of such ionization, the measurements of the radio scientists cannot be assumed to give the intensity of the solar emission beyond the Lyman limit. The temporal variation of the temperature is briefly discussed.